

Partitioning the phenotypic variance of reaction norms

Pierre de Villemereuil^{1,2} and Luis-Miguel Chevin³

¹*Institut de Systématique, Évolution, Biodiversité (ISYEB), École Pratique des Hautes Études PSL, MNHN, CNRS, SU, UA, Paris, France*

²*Institut Universitaire de France (IUF)*

³*CEFE, CNRS, Université de Montpellier, Université Paul Valéry Montpellier 3, EPHE, IRD, Montpellier, France*

Keywords: phenotypic plasticity, quantitative genetics, character-state approach, polynomial approach, non-linear modelling

Corresponding author: Pierre de Villemereuil, E-mail: pierre.^[..¹]de-villemereuil@[..^[..²]]mnhn.fr

Abstract

Many phenotypic traits vary in a predictable way across environments, as captured by their norms of reaction. These reaction norms may be discrete or continuous, and can substantially vary in shape across organisms and traits, making it difficult to compare amounts and types of plasticity among (and sometimes even within) studies. In addition, ^[..³]the evolutionary potential of phenotypic traits in heterogeneous environments critically depends on how reaction norms vary genetically, but there is no consensus on how this should be quantified. Here, we propose a partitioning of phenotypic variance across genotypes and environments that jointly address these challenges. We ^[..⁴]start by distinguishing the components of phenotypic variance arising from the average reaction norm across genotypes, (additive) genetic variation in reaction norms^[..⁵], and a residual that cannot be predicted ^[..⁶]from the genotype and the environment. We then further partition the ^[..⁷](additive) genetic variance of the trait into a component related the marginal (additive) genetic variance in the trait and a component due to (additive) genetic variance in plasticity, including for complex, non-linear reaction norms. The last step involves estimating contributions from different parameters of reaction norm shape ^[..⁸]to these variance components. This decomposition is general and we show how to ^[..⁹]apply it to various modelling approaches, from the character-state ^[..¹⁰]to curve-parameter

¹removed: devillemereuil

²removed: ephe.psl.eu

³removed: genetic variation and evolutionary potential

⁴removed: first derive

⁵removed: (including additive genetic variance)

⁶removed: by reaction norms

⁷removed: first two terms into contributions from

⁸removed: , such as the mean and variance of reaction norm slope and curvature. We

⁹removed: implement this approach in practice in various contexts, including

¹⁰removed: approach,

17 approaches, including polynomial functions, or arbitrary non-linear models. [¹¹] To facilitate the
18 use of this variance decomposition, we provide the Reacnorm R package, including a practical tutorial.
19 Overall the toolbox we develop [¹²] should serve as a base for an unifying and deeper understanding
20 of the variation and genetics of reaction norms and plasticity, as well as more robust comparative
21 studies of plasticity across organisms and traits.

22 Introduction

23 The phenotype of a given genotype can vary in response to its environment of development or ex-
24 pression, [¹³] through a phenomenon broadly described as phenotypic plasticity (Schlichting & Pigliucci
25 1998; Bradshaw 1965). Phenotypic plasticity is currently attracting considerable interest in the context
26 of rapidly changing natural environments (Gienapp et al. 2008; Chevin et al. 2010; Merilä & Hendry
27 2014). While the mere existence (and even prevalence) of phenotypic plasticity is uncontroversial, its
28 relative contribution to observed or predicted phenotypic change in the wild (Teplitsky et al. 2008;
29 Gienapp et al. 2008; Merilä & Hendry 2014; Bonamour et al. 2019), as well as the extent of its interplay
30 with population-level processes such as natural selection and population dynamics (Reed et al. 2010;
31 Vedder et al. 2013; Schaum & Collins 2014; de Villemereuil et al. 2020), are very active research areas.
32 Answering these questions requires [¹⁴] for biologists to be able to dissect and compare phenotypic plas-
33 ticity in detail in a wide range of traits, environmental contexts and species. This requires a methodology
34 that is appropriate for each context, while being general enough to be comparable across context.

35 The relationship between the phenotype and the environment is captured by the reaction norm (or
36 norm of reaction), which is defined at the level of genotypes (Woltereck 1909; Schlichting & Pigliucci
37 1998). Reaction norms encompass phenotypic responses to both continuous environments (such as
38 temperature, salinity, etc.) and categorical/discrete ones (such as host plant for a phytophagous
39 insect). Within a simple model of reaction norm, quantifying plasticity may be straightforward. For
40 instance [¹⁵], both empirical (Charmantier et al. 2008; Nussey et al. 2005) and theoretical (Gavrilets
41 & Scheiner 1993b; Lande 2009) work have extensively relied on the assumption of a linear reaction
42 norm [¹⁶], whose slope is used as a metric of plasticity [¹⁷] [¹⁸] [¹⁹], since it quantifies how

¹¹removed: We also show how the combination of character-state and curve-parameter approaches can provide a metric of goodness of fit of a given model of reaction norm shape

¹²removed: , summarized in an online tutorial,

¹³removed: and such phenotypic plasticity

¹⁴removed: being able to quantify phenotypic plasticity at broad taxonomic, ecological, and phenotypic scales.

¹⁵removed: when

¹⁶removed: is assumed, the reaction norm slope is generally

¹⁷removed: in both empirical

¹⁸removed: and theoretical

¹⁹removed: work

43 much phenotypic change is induced per unit environmental change. However, regression slopes are
44 signed and have units of trait per environment, so even in this simple case some standardization is
45 needed in order to compare the magnitude of plasticity among studies. Beyond this simple scenario,
46 drawing robust conclusions about phenotypic plasticity requires being able to quantify and compare
47 its magnitude across organisms, traits and environments, in a way that [..²⁰] is applicable across the
48 statistical frameworks used to study plasticity.

49 Beyond [..²¹] how much phenotypes change with the environment, how they change can also
50 be of importance [..²²]. First, different reaction norm shapes may come with different biological
51 interpretations. For instance, a bell-shaped (eg quadratic, Gaussian) reaction norm may indicate
52 that some mechanism underlying a measured trait is maximized at an intermediate value of the
53 environment. This is often expected for traits that are direct components of fitness, or that can
54 be interpreted as proxies for performance, for which the reaction norms are generally [..²³] termed
55 tolerance or performance curves (Lynch & Gabriel 1987; Deutsch et al. 2008; Angilletta 2009). A
56 sigmoid shape, on the other hand, may indicate that plasticity is directional but that the range of
57 possible phenotypes is constrained, or that selection favors discrete-like variation (Moczek & Emlen
58 1999; Suzuki & Nijhout 2006; Hammill et al. 2008; Chevin et al. 2013). Second, most theoretical
59 models on the evolution of plasticity, especially those based on quantitative genetics [..²⁴] which are
60 most directly comparable to [..²⁵] empirical data, assume a given reaction norm shape - often linear
61 for simplicity (Scheiner 1993b; Tufto 2000; Lande 2009). The extent to which theoretical predictions
62 on the evolution of plasticity apply to any particular empirical system thus depends on how well the
63 reaction norm shape assumed in the models conforms to observations in this system. In other words,
64 we need some metric for whether a reaction norm is "mostly linear" or "mostly curved", for instance.
65 In addition, when fitting a particular model of reaction norm shape to an empirical dataset, we would
66 like to know how well this model captures the overall plastic variation of the trait across environments.

67 A third crucial question regarding reaction norms is how (and how much) they vary genetically.
68 It has long been recognized that plasticity can evolve if reaction norms vary genetically (Bradshaw
69 1965), and theory has predicted how different aspects of reaction norm shape are expected to respond
70 to selection in a variable environment (de Jong 1990; Gomulkiewicz & Kirkpatrick 1992; Gavrillets &
71 Scheiner 1993b). However this theory has been little applied empirically, except for predictions about

²⁰removed: does not depend on reaction norm shape, and can be applied even when shape cannot be simply defined (for instance because environments have no intrinsic order). Such unified measure of plasticity seems to be currently lacking

²¹removed: How

²²removed: , beyond *how much* they change

²³removed: described as

²⁴removed: ,

²⁵removed: data on phenotypic plasticity

72 the slope of linear reaction norms (or ²⁶phenotypic differences between two environments)²⁷
73]. But beyond this, it should also be of interest to ²⁸identify which aspects of reaction norm
74 shape are more likely to evolve, based on how they vary genetically. For instance, a reaction norm
75 may be highly curved (e.g. quadratic) but have little genetic variability in curvature, instead mostly
76 varying in position, height, or local slope. **Distinguishing between the genetic variance of the trait,
77 marginalised across environments, and the genetic variance of plasticity itself, can also be a conceptual and
78 methodological challenge.** There is thus a need to compare genetic variation in different components
79 of reaction norm²⁹], but previous attempts to do so (in a meta-analysis³⁰]) were limited by
80 **methodological obstacles** (Murren et al. 2014, see Appendix G). **In fact**, comparing genetic variation in
81 the slope versus curvature of a reaction norm, for instance, is not straightforward, as these parameters
82 have different scales and even units (trait per environment, vs trait per squared environment). **More,
83 even the notion of average slope and curvature can have different meanings depending on the assumed
84 distribution for the environment.** Genetic variation in reaction reaction norm shape can be analyzed
85 by estimating variation in the parameters of a continuous function of the environment³¹], as done
86 by the flexible framework of function-valued traits (Kirkpatrick & Heckman 1989; Gomulkiewicz &
87 Kirkpatrick 1992; Stinchcombe et al. 2012). ³² ³³ In addition, it would be useful to be able
88 to compare the relative contributions of variation in different aspects of reaction norm shape to the
89 overall variance in plasticity of a trait.

90 We herein propose a ³⁴theoretically justified and generally applicable framework to estimate and
91 partition the phenotypic variance of reaction norms, towards three main goals: (i) quantify ³⁵the
92 **contribution of plasticity to the total phenotypic variance in reaction norms**; (ii) evaluate the contribution
93 of different aspects of reaction norm shape, and of the full assumed reaction norm model, to overall
94 plastic phenotypic variation; and (iii) quantify heritable variation in **the trait and its plasticity, due
95 to the** different aspects of ³⁶the reaction norm. **We provide this framework as a new R package
96 Reacnorm, including a tutorial to guide users in applying it.** Our hope is that this ³⁷will stimulate
97 more quantitative investigations of the ways in which phenotypic plasticity contributes to phenotypic

²⁶removed: equivalently,

²⁷removed: , which directly quantifies the degree of plasticity

²⁸removed: find out

²⁹removed: slope, as previously done

³⁰removed: . However

³¹removed: (e.g. polynomial), possibly using

³²removed: But even this flexible approach generally "makes the restrictive assumption that all individuals or genotypes are fully characterized by the chosen parametric model"

³³removed: , and the degree to which the overall plastic variance in the trait is explained by this model is rarely evaluated.

³⁴removed: simple

³⁵removed: plasticity across reaction norm shapes and types

³⁶removed: reaction norm shape.

³⁷removed: study

98 variation and evolutionary change.

99 **[..³⁸]Reaction norm models[..³⁹]**

100 In the broadest sense, a reaction norm is a decomposition of phenotypic variation among known
101 (often controlled) versus unknown sources of environmental variation. **[..⁴⁰]In this sense, we can start**
102 **by decomposing the** phenotypic trait z **[..⁴¹]into two components:**

$$z[..⁴²] = \hat{z}[..⁴³] + \tilde{z}[..⁴⁴]. \tag{1}$$

103 The first term **[..⁴⁵]** \hat{z} is the reaction norm, that is, the component of phenotypic variation that can be
104 predicted (hence the hat notation) from knowing both the genotype **(which we will note g throughout)**
105 of an individual and the environment **(which we will note ε throughout)** in which it developed. **Note**
106 **that by “environment”, we mean either an experimentally controlled environmental variable, or a focal**
107 **variable (e.g. temperature) within a naturally occurring environmental context.** The second term **[..⁴⁶]** \tilde{z}
108 is the component of the measured phenotype that cannot be predicted from genotype and environment,
109 and arises from unknown environmental factors (usually described as micro-environmental variation),
110 developmental noise, and measurement error.

111 **[..⁴⁷]Types of reaction norms \hat{z}** can be further **[..⁴⁸]categorised** according to the type of envi-
112 ronmental variation. The environment may be inherently categorical and unordered, such as host
113 plant for a herbivore insect. It may be ordered but with no (or unknown) quantitative value, such as
114 low, medium, and high treatments. Or it may be ordered quantitatively, with values that are either
115 intrinsically discrete**[..⁴⁹], such as habitat quality**, or continuous**[..⁵⁰], such as temperature or salinity.**

116 When environments are **[..⁵¹]categorical**, the reaction norm can be studied by treating phenotypic
117 values in different environments as alternative ‘character states’, considered as different traits in a
118 multivariate framework (Via & Lande 1985; Falconer 1952). The mean character state may differ
119 among environment if the trait is plastic; phenotypic and genetic variation may be larger in some
120 environments; and phenotypes may be more or less correlated across environments (Via & Lande 1985;

³⁹removed: of reaction norms

⁴⁰removed: We can write the measure i of

⁴¹removed: for genotype g developing in environment k as

⁴⁵removed: \hat{z}_{gk}

⁴⁶removed: \tilde{z}_i

⁴⁷removed: The reaction norm \hat{z}_{gk}

⁴⁸removed: categorized

⁴⁹removed: (such as number of resource items)

⁵⁰removed: (even if sampled at discrete intervals)

⁵¹removed: purely

121 Falconer 1952). Such a modelling framework is readily described by Equation 1 for a ^[.52] genotype
 122 g and environment ε_k (where the index k is used to reflect the discrete aspect of the environmental
 123 variable). In practice, such an approach would correspond to an ANOVA (or a mixed model) with
 124 discrete environment and genotype-within-environment as (random) effects of the model. In its most
 125 compact form, such a statistical model can be framed as a multivariate Gaussian distribution, with a
 126 number of dimensions corresponding to the number of categories in the environment,

$$\hat{z} \sim \mathcal{N}(\boldsymbol{\mu}, \mathbf{G}_z), \quad (2)$$

127 where $\boldsymbol{\mu}$ is the vector of expected phenotypic values (across genotypes) within each environment,
 128 and \mathbf{G}_z is the genetic variance-covariance matrix of ^[.53] trait values within and across environments.
 129 Note that when the environment is quantitative but discrete, one may still use the ^[.54] character-
 130 state approach, but structuring correlations in \mathbf{G}_z by environmental distance, in effect treating the
 131 phenotype as a stochastic process characterized by its autocovariance function across environments
 132 (Pletcher & Geyer 1999).

133 For quantitative environments (both discrete and continuous), the most common approach is to
 134 ^[.55] model the reaction norm ^[.56] as a function of environment and genotype:

$$\hat{z}^{[.57]} = f(\varepsilon^{[.58]}, \boldsymbol{\theta}_g), \quad (3)$$

135 where ε is the environmental value, and $\boldsymbol{\theta}_g$ is a vector that contains the parameters of the function (e.g.
 136 coefficients associated to each exponent for a polynomial) for each genotype g ; these parameters are
 137 thus genetically variable. ^[.59] ^[.60] The parameters $\boldsymbol{\theta}_g$ are generally assumed to be polygenic and
 138 thus follow a multivariate Gaussian distribution,

$$\boldsymbol{\theta}_g \sim \mathcal{N}(\bar{\boldsymbol{\theta}}, \mathbf{G}_\theta), \quad (4)$$

139 where $\bar{\boldsymbol{\theta}}$ is the vector of average parameter values across genotypes and ^[.62] \mathbf{G}_θ is the additive genetic
 140 variance-covariance matrix of the parameters ^[.63] $\boldsymbol{\theta}_g$. This approach has been described alternatively

⁵²removed: discrete

⁵³removed: the phenotype

⁵⁴removed: character state

⁵⁵removed: use a function f to

⁵⁶removed: ,

⁵⁹removed: In practice, such approach is implemented through (possibly non-linear) mixed models

⁶⁰removed: , in which genetic variation in f is modelled through random effects on its parameters $\boldsymbol{\theta}$ (omitting the subscript g for simplicity). The $\boldsymbol{\theta}$

⁶²removed: Θ

⁶³removed: $\boldsymbol{\theta}$

141 as the “reaction norm” approach, the “polynomial approach”, or a parametric version of [..⁶⁴]function-
142 valued traits. To keep it general here and avoid confusion with the general concept of reaction norm as
143 defined in Equation 1 (which applies even to categorical environments), we will describe it as the “[..⁶⁵
144]curve-parameter” approach. [..⁶⁶][..⁶⁷]

145 [..⁶⁸]It can be shown that the character-state and curve-parameter approaches are equivalent, following
146 the spirit of de Jong (1995)[..⁶⁹], who showed that a polynomial curve of sufficient order is exactly
147 equivalent to a character-state model. In particular, the character-state in Equation 2 can be expressed
148 using Equation 3 and [..⁷⁰]Equation 4 by letting $\bar{\theta} = \mu$, $\mathbf{G}_\theta = \mathbf{G}_z$ and f a function that outputs the k th
149 value of θ_g when evaluated at ε_k environment (see Appendix A). In the following, we will derive general
150 results using the more general formalism of Equation 3 and Equation 4, and then express them for the
151 particular case of the character-state [..⁷¹]approach when relevant.

152 Partitioning variation in reaction norms

153 [..⁷²]

154 Complete partition of the variation in reaction norms

155 The total phenotypic variance in the reaction norm can be partitioned by isolating independent components
156 of variation. The main reasoning will be summarised here, with more mathematical details provided in the
157 Appendix A to Appendix D. For a start, the terms in Equation 1 are assumed to be independent, such
158 that the total phenotypic variance $V(z)$ (usually noted [..⁷³] V_P) is the sum of the variance predicted
159 by the genotype and the environment $V(\hat{z})$, plus a residual component of variance $V(\tilde{z}_i)$, which we
160 will note V_{Res} . [..⁷⁴]

[..⁷⁵]

⁶⁴removed: function-values

⁶⁵removed: curve parameter

⁶⁶removed: Note that, for a given reaction norm, some parameters in θ (and/or their genetic variation) may depend on how ε was defined (e.g. whether it was mean-centered or not). For instance, changing what environment is chosen as the reference (where $\varepsilon = 0$) will change the intercept of a linear reaction norm and its genetic variance

⁶⁷removed: .

⁶⁸removed: We show below that these modelling choices can be unified under a common framework

⁶⁹removed: . More specifically, common metrics of variance partitioning can be computed regardless of the approach used,

⁷⁰removed: translated from one approach to another, allowing for broad comparison of plasticity across organisms, traits, and environments. This also allows highlighting complementary strengths and weaknesses of

⁷¹removed: and curve parameter approaches, when both are available

⁷²removed: The

⁷³removed: V_P

⁷⁴removed: The predicted variance component $V(\hat{z})$ can be furthered partitioned using the law of total variance across genotypes and environments, leading to

161 [..⁷⁶] Then, a second distinction can be made between the general, average shape of the reaction norm,
 162 and the genotype-specific variation surrounding such average, as illustrated in Figure 1 [..⁷⁷] using a
 163 quadratic reaction norm. The [..⁷⁸] component of phenotypic variance arising from plastic responses to
 164 the environment by the mean reaction norm [..⁷⁹], i.e. after averaging across all genotypes (Figure 1),
 165 [..⁸⁰] will be denoted V_{Plas} . [..⁸¹] This variance can be considered as fully ascribed to the environmental
 166 component of phenotypic variation. The component of phenotypic variation attributable to genetic variation
 167 in the reaction norm Figure 1 [..⁸²] will be denoted V_{Gen} . [..⁸³] As these two components are independent
 168 by construction, denoting as $E_{g|\varepsilon}(\hat{z})$ the expected value of the reaction norm across genotypes at a given
 169 environmental value ε , we have

$$[..⁸⁴] V(\hat{z}) = V(E_{g|\varepsilon}(\hat{z})) + V(\hat{z} - E_{g|\varepsilon}(\hat{z})) = V_{\text{Plas}} + V_{\text{Gen}} [..⁸⁵], \quad (5)$$

170 [..⁸⁶] [..⁸⁷] such that

$$V_{\text{P}} = V_{\text{Plas}} + V_{\text{Gen}} + V_{\text{Res}}. \quad (6)$$

171 Compared to the classical equation $V_{\text{P}} = V_{\text{G}} + V_{\text{E}} + V_{\text{G} \times \text{E}}$ (Falconer & Mackay 1996; Lynch & Walsh 1998;
 172 Des Marais et al. 2013), the correspondence is that $V_{\text{E}} = V_{\text{Plas}} + V_{\text{Res}}$ and $V_{\text{Gen}} = V_{\text{G}} + V_{\text{G} \times \text{E}}$. We have
 173 thus decomposed the environmental variance into a component due to phenotypic plasticity in response to
 174 ε (V_{Plas} [..⁸⁸]) on the one hand, and any other residual source of phenotypic variation (V_{Res} [..⁸⁹]) on the
 175 other hand, as commonly done in theory (Via & Lande 1985; Gavrillets & Scheiner 1993b) as well as in
 176 practice.

177 The genotypic variance V_{Gen} [..⁹⁰] accounts for all sources of genetic variation, including the genotype-
 178 by-environment [..⁹¹] interaction. Note that this [..⁹²] contrasts with a view where the genotype-
 179 by-environment interaction is instead associated with the environmental component, e.g. as *plastic*
 180 *variance* (Scheiner & Lyman 1989; Scheiner 1993a; Falconer & Mackay 1996; Lynch & Walsh 1998).

⁷⁶removed: where E_x and V_x denote expectation and variance along variable x (either the environment ε , or the genotype-within-environment $g|\varepsilon$).

⁷⁷removed: illustrates this variance partitioning for

⁷⁸removed: first term captures how much phenotypic variance across environments results from plasticity in the

⁷⁹removed: averaged over genotypes (see

⁸⁰removed: so we denote it as

⁸¹removed: The second term is the phenotypic variance among genotypes within environment averaged across environments, *i.e.* the variance arising from genetic variation around the average reaction norm (

⁸²removed:), so we denote as

⁸³removed: Overall, we thus have for the total phenotypic variance

⁸⁶removed: This differs from the classical partitioning into genetic, environmental, and genotype-by-environment interaction effects in quantitative genetics

⁸⁷removed: . The environmental component from this classical partitioning is here split between the

⁸⁸removed: and

⁸⁹removed: component, while our

⁹⁰removed: component accounts for both the genetic and

⁹¹removed: effects

⁹²removed: is in contrast to another view ,

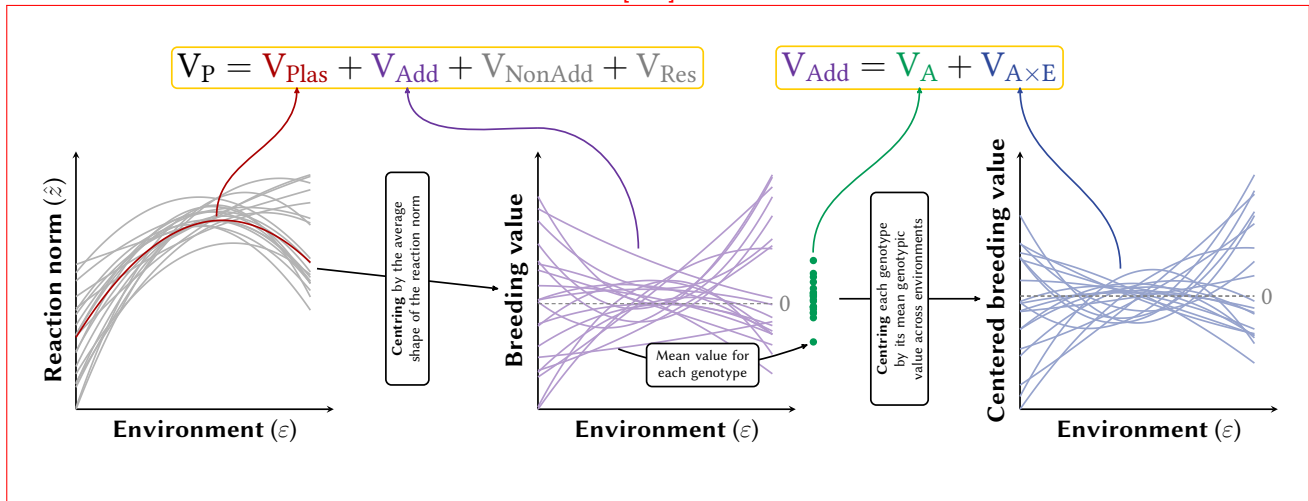


Figure 1: Illustration of the full variance decomposition using quadratic reaction norms. We start from the reaction norms (left graph, grey lines, the residual variance is not illustrated) and compute its average shape across all genotypes (left graph, red line). The phenotypic variance arising from this average shape is V_{Plas} . Centring the reaction norms along this average shape directly yields the distribution of the breeding values along environments (middle graph, purple lines), because in this quadratic case, the non-additive genetic variance is $V_{NonAdd} = 0$. The total variance of the breeding values along the environment is V_{Add} . The classical, average additive genetic variance V_A is the variance of the average of the breeding values across the environments for each genotype (middle graph, green dots). The $V_{A \times E}$ is the variance of the reminder of the breeding values after mean-centring (right graph, blue lines).

^aremoved: Schematic illustration of our variance partitioning in the case of a quadratic reaction norm, using the curve parameter approach. The variance of the expected phenotype according to each genotype’s reaction norm (light blue lines) is partitioned into the component due to the average plasticity shape (V_{Plas} , in red) and the component due to genetic variation around this average shape (V_{Gen} , in blue and corresponding to the blue area). For example, if the genetic variation (blue area) is small comparatively to the “trajectory” of the average shape (red line), then V_{Gen} will be small compared to V_{Plas} , meaning that most of the phenotypic variation comes from the direct effect of plasticity, rather than from genetic variation in plasticity.

183 [..⁹⁷] The genotypic variance V_{Gen} can be further decomposed in two steps. First, we can isolate the
 184 *additive* genetic variance (V_{Add}), from the *non-additive* genetic variance (V_{NonAdd}) arising from dominance
 185 and epistasis (Lynch & Walsh 1998; Falconer & Mackay 1996). Usually, models like Equation 2 or
 186 Equation 4 are defined using additive genetic variance-covariance matrices for their basic parameters,
 187 meaning that V_{Add} can be directly estimated from the models. As such, we will discard explicit inclusion of

⁹³removed: Each variance partitioning is relevant in what it can unveil and limited by what it hides. We explore here what the partitioning in

⁹⁴removed: can bring, both conceptually and methodologically. A more detailed and nuanced comparison, with a worked example, is provided in

⁹⁵removed: . The genetic variance can further be decomposed into an additive (heritable) component V_A and a non-additive component V_{NA} , with the latter comprising the dominance and epistasis variance, which are not our focus here.

⁹⁶removed: Contributions from the average plasticity

⁹⁷removed: We can now proceed to refine the definition of V_{Plas} and analyze its dependency on reaction norm shape. In the character-state approach, the

188 dominance or epistasis variance components in a theoretical or statistical model throughout, for the sake
189 of simplicity. However, non-additive genetic variance [⁹⁸][⁹⁹][¹⁰⁰]

[¹⁰¹]

190 [¹⁰²] can still arise from non-linearity in the (assumed) developmental system (Rice 2004; Morrissey 2015;
191 de Villemereuil et al. 2016; de Villemereuil 2018), meaning that non-additive variance can be generated
192 by the reaction norm itself. Looking at Equation 3 and Equation 4, the ultimate source of any additive
193 genetic variation in the trait z comes from the additive genetic variation in the parameters θ . As a result,
194 non-additivity in the trait arises when the function $f(\varepsilon, \theta)$ in Equation 3 is [¹⁰³] non-linear with regard to
195 θ , a situation we will refer to as “non-linearity in the parameters”. Importantly, this means that polynomial
196 (e.g. quadratic) functions, which are linear in their parameters, are such that $V_{\text{NonAdd}} = 0$ and $V_{\text{Gen}} = V_{\text{Add}}$.

197

198 When studying the evolution of plasticity, it proves useful to further decompose V_{Add} into two compo-
199 nents. The first is the marginal additive genetic variance of the trait, arising from differences in average
200 breeding values between genotypes, and typically equal to the classical V_A . In other words, V_A is the vari-
201 ance of the breeding values after averaging them across environments (Figure 1), as would be obtained if
202 the genotype-by-environment interaction was ignored altogether. For example, it would be the output of a
203 simple animal model analysis of repeated measurements of a plastic trait in a wild population. The second
204 component of V_{Add} is the additive genetic variance of plasticity, which we will note $V_{A \times E}$ (for additive
205 genetic component due to genotype-by-environment interactions). $V_{A \times E}$ is the remaining additive genetic
206 variance in the [¹⁰⁴] reaction norm after removing the mean breeding value for each genotype (Figure 1).
207 This definition is akin to the one used by Albecker et al. (2022), but here more directly expressed in terms
208 of variance of breeding values, i.e. additive genetic variance. It measures the potential for evolution of
209 plasticity in the trait. Notably, if $V_{A \times E} = 0$ but $V_{\text{Add}} > 0$, then the additive genetic variation in the
210 reaction norms is only due to average differences between genotypes, i.e. the reaction norms of different
211 genotypes are parallel. The variances V_A and $V_{A \times E}$ are exactly equivalent to the classical decomposition
212 using V_G and $V_{G \times E}$, only applied to the heritable part of the genetic variance. We show below that it is
213 possible to express V_{Add} , V_A and $V_{A \times E}$ in a way that encompasses all approaches of reaction norm, from
214 a character-state to a curve that is non-linear in its parameters, by computing reaction norm gradients

⁹⁸removed: partitioning in

⁹⁹removed: readily follows from

¹⁰⁰removed: since $E_{g|\varepsilon_k}(\hat{z}) = \mu_k$, and we have

¹⁰²removed: *i.e.* the plastic variance

¹⁰³removed: the

¹⁰⁴removed: expected character state μ_k across environmental levels k .

215 of the trait z with respect to its reaction norm parameters θ , in line with previous theoretical results for
 216 the quantitative genetics of non-linear developmental systems and non-Gaussian traits (Morrissey 2015;
 217 de Villemereuil et al. 2016),.

218 [..¹⁰⁵]

[..¹⁰⁶]

219 The complete partition of the phenotypic variance is thus:

$$V_P = V_{Plas} + V_A + V_{A \times E} + V_{NonAdd} + V_{Res}. \quad (7)$$

220 [..¹⁰⁷] From this, [..¹⁰⁸]

[..¹⁰⁹]

221 it is possible to derive unitless quantities of interest, for instance by standardising by the phenotypic variance.

222 In particular:

$$P_{RN}^2 = \frac{V_{Plas}}{V_P}, \quad (8)$$

223 is the proportion of the phenotypic variance arising from average plastic responses to environments (depend-
 224 ing on the average reaction norm shape). Variance-standardised additive genetic variances are heritabilities.

225 In our case, we can use V_{Add} , V_A or $V_{A \times E}$ as the numerator, yielding the following relationship:

$$h_{RN}^2 = \frac{V_{Add}}{V_P} = \frac{V_A}{V_P} + \frac{V_{A \times E}}{V_P} = h^2 + h_I^2. \quad (9)$$

226 [..¹¹⁰] In other words, the heritability of the trait when fully accounting for its reaction norm (h_{RN}^2) is equal
 227 to the marginal heritability of the trait (h^2 , based on the averaged breeding values across environments)
 228 plus the heritability of plasticity, arising from interaction with the environment (h_I^2). If it is not possible
 229 to measure additive genetic variances due to limitations in the experimental design (e.g. when “genotypes”
 230 correspond to populations, accessions or clones), it is possible to perform the same decomposition using
 231 “broad-sense heritabilities”,

$$H_{RN}^2 = \frac{V_{Gen}}{V_P} = \frac{V_G}{V_P} + \frac{V_{G \times E}}{V_P} = H^2 + H_I^2. \quad (10)$$

232 In all cases, the quantity:

$$T_{RN}^2 = \frac{V_{Plas} + V_{Gen}}{V_P} = P_{RN}^2 + H_{RN}^2 \quad (11)$$

¹⁰⁵removed: In the curve parameter approach, the first step is to compute the mean phenotypic conditional on the environment,

¹⁰⁷removed: where $p(\theta_g)$ is the probability density function of the parameters θ_g due to the variability across genotypes.

¹⁰⁸removed: V_{Plas} can be computed as

¹¹⁰removed: where $p(\varepsilon)$ is the probability density function of the environmental variable ε ,

233 would measure the proportion of the phenotypic variance explained by the (possibly plastic and genetically
 234 variable) reaction norm, and thus our ability to predict the individual phenotype from the genotype and
 235 the environment. In a linear context with respect to the parameters, when the environment is considered
 236 a fixed quantity, the quantities P_{RN}^2 and $[..^{111}]T_{RN}^2$ are analogous to the (resp. marginal and conditional)
 237 coefficient of determination of the reaction norm (Nakagawa & Schielzeth 2013; Johnson 2014), but
 238 their definition here is given beyond that simple context. Importantly, so far we are not making any
 239 statement about the actual reaction norm shape: P_{RN}^2 captures the contribution of the average reaction
 240 norm regardless of its shape, and the $[..^{112}]$

241 $[..^{113}]$ broad- or $[..^{114}]$ $[..^{115}]$ $[..^{116}]$

$[..^{117}]$

242 $[..^{118}]$ narrow-sense heritabilities the contribution of various aspects the genetic variation to the phenotypic
 243 variance. The contribution of detailed aspects of reaction norms shape to phenotypic variation are obtained
 244 by further partitioning V_{Plas} and the additive genetic variances, as we do below.

245 Contributions of reaction norm shape and parameters to the plastic variance

246 As stated in Equation 5, the general definition of the variance arising from the average reaction norm is

$[..^{119}]$

247 $[..^{120}] V_{Plas} = V(E_{g|\varepsilon}(\hat{z}))$. Important simplifications arise in more particular cases. For example, when the
 248 assumed curve is linear in its parameters, $E_{g|\varepsilon}(\hat{z}) = f(\varepsilon, \bar{\theta})$, where $\bar{\theta}$ is the average value of the parameters
 249 across genotypes. In particular, in the case of a quadratic reaction norm (Scheiner 1993a; Gavrillets &
 250 Scheiner 1993a; Morrissey & Liefjing 2016):

$$f(\varepsilon, \theta_g) = (\bar{a} + a_g) + (\bar{b} + b_g)\varepsilon + (\bar{c} + c_g)\varepsilon^2, \quad (12)$$

¹¹¹removed: \bar{z} is the average phenotype among genotypes and environments (*i.e.*, the grand mean phenotype). If the reaction norm function f is linear in its parameters θ (not to be confused with linearity with respect to

¹¹²removed: environment ε , *i.e.* a linear reaction norm) then $E_{g|\varepsilon}(\hat{z}) = f(\varepsilon, \bar{\theta})$ (noted simply as $f(\varepsilon)$ below), which simplifies the computation.

¹¹³removed: Although the shape of the true reaction normfunction f cannot be known with certainty and may be complex, it is often of interest to fit relatively simple functions with interpretable parameters. For instance, first-

¹¹⁴removed: second-order approximations to the reaction norm provide information on its slope or curvature. More generally, polynomial functions allow fitting reaction norms with potentially complex shapes while retaining linearity in their parameters, making them popular in studies of reaction norms, both theoretically

¹¹⁵removed: and empirically

¹¹⁶removed: . To exemplify how different components of reaction norm shape contribute to phenotypic variance, let us first focus on the quadratic case,

¹¹⁸removed: which includes linear reaction norms as a subcase when $c = 0$. In this model, the

¹²⁰removed: where bars denote averages over genetic variation.

251 where \bar{a} , \bar{b} , \bar{c} are the average intercept, first- and second-order parameters of the model, and a_g , b_g and
 252 c_g are genotype-specific deviation from these average values for the same parameters, we can express V_{Plas}
 253 simply as:

$$V_{\text{Plas}} = \bar{b}^2 V(\varepsilon) + \bar{c}^2 V(\varepsilon^2) + 2\bar{b}\bar{c}\text{cov}(\varepsilon, \varepsilon^2). \quad (13)$$

254 If the environmental variable ε has been [¹²¹] mean-centred and is symmetrical, then $\text{cov}(\varepsilon, \varepsilon^2) = 0$
 255 and the third term vanishes. [¹²²] Finally, in the case of a character-state model, the average phenotype
 256 in each environment ε_k is readily provided by the μ_k in Equation 2, so that $V_{\text{Plas}} = V(\mu)$. Once V_{Plas} is
 257 computed, its standardised version P_{RN}^2 follows by dividing by the total phenotypic variance.

258 Pushing the analysis further, we aim to compute the contributions of different aspect of reaction norm
 259 shape to the overall environmental plastic variance of the trait, notably the contribution of its slope and
 260 curvature [¹²³], which we will denote as π_{Sl} and π_{Cv} , respectively. For this, at least one of two of the
 261 following assumptions must valid: (i) ε follows a normal distribution, or (ii) the true reaction norm is
 262 quadratic. In all cases, it also require that the environmental variable has been mean-centered. A last
 263 requirement is for f to be at least twice differentiable with respect to ε (which excludes e.g. the character-
 264 state approach). In this case, these terms simply depend on the average first- and second-order derivative
 265 of $E_{g|\varepsilon}(\hat{z})$ and the variance of ε and ε^2 (see Appendix D1):

$$\pi_{\text{Sl}}^{[124]} = \frac{E\left(\frac{dE_{g|\varepsilon}}{d\varepsilon}(\hat{z})\right)^2 V(\varepsilon)}{V_{\text{Plas}}}, \quad \pi_{\text{Cv}}^{[125]} = \frac{\frac{1}{4}E\left(\frac{d^2E_{g|\varepsilon}}{d\varepsilon^2}(\hat{z})\right)^2 V(\varepsilon^2)}{V_{\text{Plas}}}. \quad (14)$$

266 An important point arising from Equation 14 is that the relative [¹²⁶] importance of variation in the
 267 slope and curvature components of reaction norm depend on variation in the environment, respectively
 268 [¹²⁷] $V(\varepsilon)$ and $V(\varepsilon^2)$. Crucially, we chose to express this partitioning using the mean environment as the
 269 reference environment (as commonly practiced, e.g. Morrissey & Liefing 2016), but any other choice
 270 of a reference environment would result in a different π -partition, notably due to a non-null value for
 271 $\text{Cov}(\varepsilon, \varepsilon^2)$. Fortunately, neither V_{Plas} nor P_{RN}^2 are impacted by this choice in the reference environment.
 272 Furthermore, if the reaction norm is linear on the parameters, the derivatives of $E_{g|\varepsilon}(\hat{z})$ can be directly taken
 273 as the derivatives of f . In particular, for a quadratic reaction norm as in Equation 12, for a mean-centred
 274 environment, those quantities simply are:

$$\pi_{\text{Sl}} = \frac{\bar{b}^2 V(\varepsilon)}{V_{\text{Plas}}}, \quad \pi_{\text{Cv}} = \frac{\bar{c}^2 V(\varepsilon^2)}{V_{\text{Plas}}}, \quad (15)$$

¹²¹removed: mean-centered and is symmetrical (e.g. Gaussian)

¹²²removed: We may then compute the relative contributions of reaction norm

¹²³removed: to the total variance attributable to the average reaction norm as

¹²⁶removed: importances of the linear and quadratic components of the curves depends

¹²⁷removed: $V_\varepsilon(\varepsilon)$ and $V_\varepsilon(\varepsilon^2)$.

275 consistent with the fact the first and second order coefficients of a quadratic polynomial correspond to
 276 its average slope and curvature, respectively. Only in this configuration do we have $\pi_{SI} + \pi_{CV} = 1$.
 277 Unfortunately, this simple, geometric interpretation of the polynomial coefficients is lost above the second-
 278 order case (see Appendix D).

279 Figure 2 [..¹²⁸] shows the values of [..¹²⁹] π_{SI} and π_{CV} for various quadratic reaction norms, assuming
 280 ε follows either a normal or uniform distribution, with same mean 0 and variance 1. The values for
 281 [..¹³⁰] π_{SI} and π_{CV} translate well the perceived “trendiness” (for large [..¹³¹] π_{SI}) or “curviness” (for
 282 large [..¹³²] π_{CV}) of reaction norms, but they may also strongly depend on the statistical distribution of
 283 the environmental variable ε , as shown especially in the third example of Figure 2. In this example, the
 284 difference arises because the assumed environmental distributions have different kurtosis (the scaled
 285 fourth central moment, related to [..¹³³] $V(\varepsilon^2)$ in Equation 15). Because [..¹³⁴] $V(\varepsilon^2)$ is larger for the
 286 Gaussian, this distribution leads to larger [..¹³⁵] π_{CV} than the uniform.

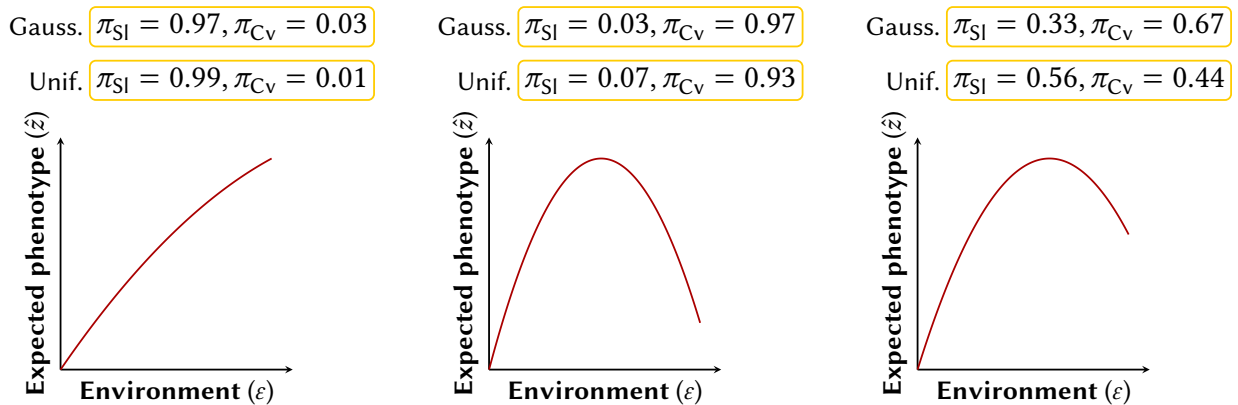


Figure 2: Computation of [..^a] $\pi_{SI} = \pi_b$ and [..^b] $\pi_{CV} = \pi_c$, the relative contributions of linear and quadratic terms to phenotypic variation caused by the mean reaction norm, for different shapes of reaction norms, and two distributions of the environmental variable ε : a standard Gaussian (of mean 0 and variance 1), and a uniform distribution between $-\sqrt{3}$ and $\sqrt{3}$ (of mean 0 and variance 1).

^aremoved: π_b

^bremoved: π_c

287 [..¹³⁶] When it is not possible to assume that ε is normally distributed (because it is discrete, or
 288 experimentally constrained) and a quadratic assumption is not a good fit to the reaction norm, it is always
 289 possible to use a higher-order polynomial model to approximate the true reaction norm, in line with

¹²⁸removed: show

¹²⁹removed: π_b and π_c

¹³⁰removed: π_b and π_c

¹³¹removed: π_b

¹³²removed: π_c

¹³³removed: $V_\varepsilon(\varepsilon^2)$ in

¹³⁴removed: $V_\varepsilon(\varepsilon^2)$

¹³⁵removed: π_c

¹³⁶removed: To generalise this reasoning to any polynomial order n , it is convenient to use linear algebra

290 theoretical work by [¹³⁷]

[¹³⁸]

291 [¹³⁹]

[¹⁴⁰]

292 [¹⁴¹]de Jong (1990), Gavrillets & Scheiner (1993a), and de Jong (1995). In this case, we can conduct
293 an alternative decomposition based on the parameters of the polynomial (rather than the mean slope
294 and curvature of the function). To distinguish this parameter-based decomposition from the specific
295 decomposition in terms of slope and curvature, we use a different notation. The relative contribution
296 of a given exponent m in the polynomial to the variance caused by the mean plasticity becomes (see
297 Appendix D2)

$$[\sup{142}] \varphi_m = [\sup{143}] \frac{\bar{\theta}_m^2 V(\varepsilon^m)}{V_{\text{Plas}}}, \quad (16)$$

298 and the contribution of the covariance between exponents l and m is

$$[\sup{144}] \varphi_{lm} = [\sup{145}] \frac{2\bar{\theta}_l \bar{\theta}_m \text{Cov}(\varepsilon^l, \varepsilon^m)}{V_{\text{Plas}}}. \quad (17)$$

299 Note that even with a symmetrical and [¹⁴⁶]mean-centred environment, the covariance between
300 [¹⁴⁷]higher-order exponents will not be zero in general, contrary to ε and ε^2 in the quadratic case.
301 Using orthogonal polynomials would solve this issue of covariances, but at the cost of a more complex
302 interpretation of the coefficients. More generally, this φ -decomposition only relies on the assumption that
303 the reaction norm is linear on its parameters, which includes polynomials as a particularly useful special
304 case. We summarise the requirements and applications for the π - and φ -decomposition depending on the
305 context in Figure 3.

306 [¹⁴⁸]

307 [¹⁴⁹]

¹³⁷removed: Gavrillets & Scheiner (1993a). A polynomial reaction norm can be written as

¹³⁹removed: where the column-vector $\mathbf{x} = (1, \varepsilon, \varepsilon^2, \dots, \varepsilon^n)^T$ (where T denotes transposition) includes all exponentiation levels (up to n) of the environmental variable ε . The variance component due to plasticity in the average reaction norm is then

¹⁴¹removed: where \mathbf{X} is the variance-covariance matrix of \mathbf{x} , recalling that $\bar{\theta}$ is the average of reaction norm parameters across the genotypes

¹⁴⁶removed: mean-centered

¹⁴⁷removed: higher-up order

¹⁴⁸removed: Contributions from genetic variation

¹⁴⁹removed: We now turn to how genetic variation in reaction norms translates into genetic

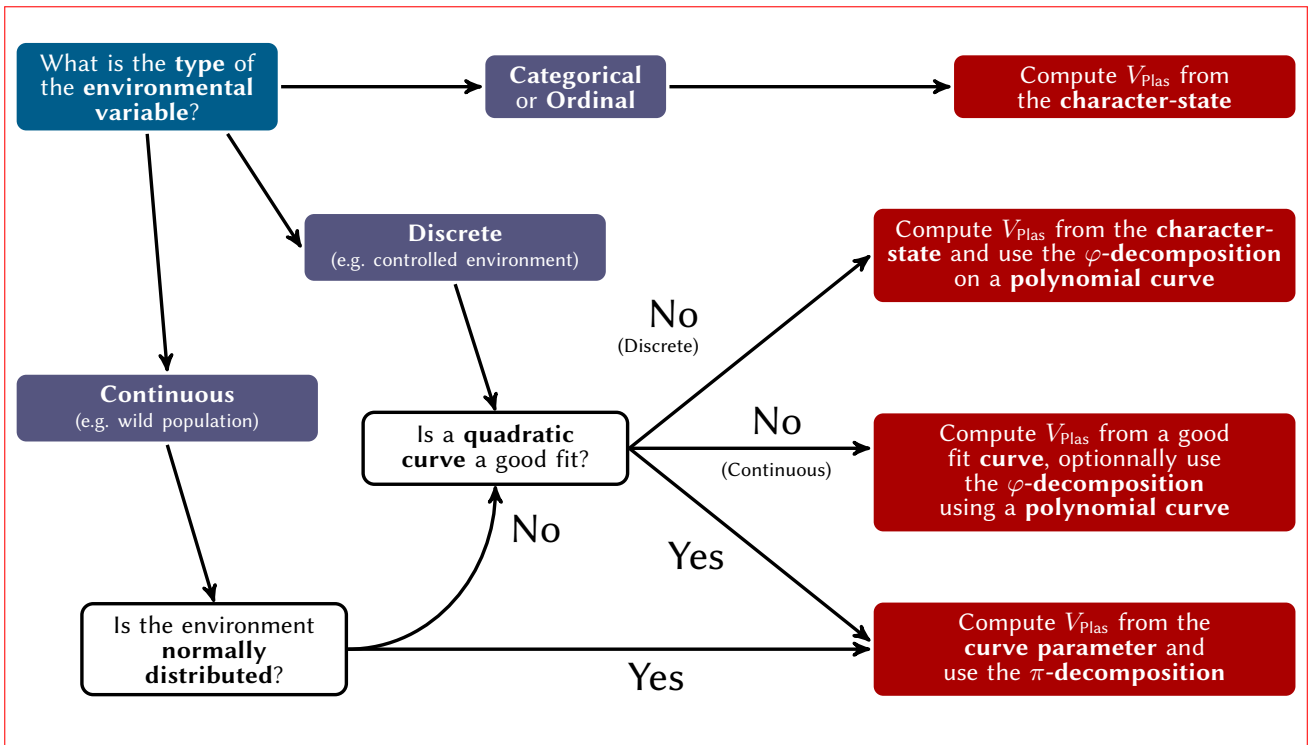


Figure 3: Decision tree summarising our suggested workflow for the computation and decomposition of V_{Plas} , depending on the nature of the environmental variable, its normality and the validity of a quadratic approximation of the reaction norm shape.

308 Contributions of reaction norm parameters to the genetic variance

309 We can expression the variance of the genotypic values of the reaction norms in Equation 5 in a slightly
 310 different, but more operational, manner:

$$V_{Gen} = V(\hat{z} - E_{g|\varepsilon}(\hat{z})) = E(V_{g|\varepsilon}(\hat{z})), \quad (18)$$

311 i.e. the total genotypic variance of the [¹⁵⁰] reaction norms is equal to the environment-specific genotypic
 312 variance averaged across environments. [¹⁵¹]

[¹⁵²]

313 [¹⁵³] From an evolutionary perspective, the component of main interest is rather the total additive genetic
 314 variance of [¹⁵⁴] [¹⁵⁵] [¹⁵⁶] the reaction norm V_{Add} , which will be the main focus of this section. As

¹⁵⁰ removed: trait
¹⁵¹ removed: In the character-state approach, the genetic variance within each environment is given by the diagonal elements of \mathbf{G}_z , so we simply have
¹⁵³ removed: that is, V_{Gen} is the average
¹⁵⁴ removed: character states across environments. Note however that this cannot be directly used to predict the mean response to selection in a variable environment, as the latter are also influenced by genetic correlations in character state across environments
¹⁵⁵ removed: . In addition, whether
¹⁵⁶ removed: actually outputs V_{Gen} , or rather its heritable component V_A , entirely depends on whether the matrix

315 a reminder, we here assume, that the experimental design allows for the inference of the additive genetic
 316 variance of the parameters of the reaction norm (\mathbf{G}_z [..157]

317 [..158] [..159]
 [..160]

318 [..161] [..162] [..163]
 [..164]

319 [..165] [..166] or \mathbf{G}_θ above), and that non-additive variance in the trait V_{NonAdd} only arises when the reaction
 320 norm is non-linear in the parameters (i.e. dominance and/or epistasis were not fitted in the statistical model).
 321 This assumption is for the sake of simplicity, as our framework can include such effects into V_{Gen} [..167] if
 322 needed.

323 A general way to relate the additive genetic variance [..168] [..169] of the trait to the additive genetic
 324 variances of the reaction norm parameters is through a vector that we describe as the reaction norm
 325 gradient, which we will note ψ_ε (following notations in de Villemereuil et al. 2016),

$$\psi_\varepsilon = \mathbb{E}_g \left(\frac{\partial z}{\partial \theta} \right)_\varepsilon, \quad (19)$$

326 where the subscript ε makes it clear that ψ_ε will generally be a function of the environment. In the case
 327 of a quadratic curve, ψ_ε is the $(1, \varepsilon, \varepsilon^2)^T$ vector (see Appendix C3 for a polynomial of arbitrary order). In
 328 the case of a character-state model, ψ_{ε_k} is a vector with 1 for the k :th environmental level (or character
 329 state), and zero elsewhere. Whether or not the reaction norm is linear in its parameters, the [..170] [..171
 330] additive genetic variance [..172] of the trait in a given environment ε is
 331 (Morrissey 2015; de Villemereuil et al. 2016, and see Appendix B),

$$V[..173]_{A|\varepsilon} = \psi[..174]_\varepsilon^T \mathbf{G}_\theta \psi[..175]_\varepsilon, \quad (20)$$

¹⁵⁷removed: is defined as containing the *total* genetic (co)variances or only the *additive* genetic (co)variances.

¹⁵⁸removed: In the curve parameter approach, expanding the second term in

¹⁵⁹removed: we get

¹⁶¹removed: From the reaction norm function in

¹⁶²removed: and under multivariate Gaussian distribution assumed in

¹⁶³removed: , the genetic variance conditional on environment becomes

¹⁶⁵removed: Numerical integration of

¹⁶⁶removed: can be used in any case to obtain

¹⁶⁷removed: . However, further analytical progress can be made when focusing more specifically on

¹⁶⁸removed: V_A , which more directly influences responses to selection

¹⁶⁹removed: . Using the property of additivity of breeding values, and relying on a multivariate extension of

¹⁷⁰removed: framework in de Villemereuil et al. (2016), it is shown in

¹⁷¹removed: that the

¹⁷²removed: in

347 centred environment as shown in Figure 1, $\psi_\varepsilon = (1, \varepsilon, \varepsilon^2)$ and thus we have (see Appendix C3)

$$\begin{aligned}
 V_{\text{Add}} &= V_a + (V_b + 2C_{ac})E(\varepsilon^2) + V_cE(\varepsilon^4), \\
 V_A &= V_a + 2C_{ac}E(\varepsilon^2) + V_cE(\varepsilon^2)^2, \\
 V_{A \times E} &= V_bV(\varepsilon) + V_cV(\varepsilon^2),
 \end{aligned}
 \tag{25}$$

348 where V_a , V_b and V_c are the additive genetic variances in the parameters a_g , b_g and c_g , and C_{ac} is the
 349 additive genetic covariance between the intercept a_g and the second-order effect c_g . Those expressions are
 350 reminiscent of classical results from the theory of evolution of plasticity (e.g. de Jong 1990; Gavrillets &
 351 Scheiner 1993a), especially regarding the crucial role of C_{ac} in the evolution of quadratic reaction norms,
 352 but here distinguishing three important components of the additive genetic variance of reaction norms. In
 353 particular, we see how the additive genetic variance in plasticity, $V_{A \times E}$, can be simply expressed as the sum
 354 of the products of the variances in the reaction norm gradients (here the environment and its squared value)
 355 and the corresponding additive genetic variance in the parameters (here b_g and c_g in Equation 12). This
 356 means that, in the quadratic case, genetic variances in slope and curvature directly translate into variance
 357 in plasticity, as they should. By contrast, V_A does not solely depend on the variance in the intercept V_a ,
 358 but also on the quadratic coefficient, more specifically its covariance with the intercept.

359 ^[.186] ^[.187] The expressions for these variance components in the character-state approach are best
 360 described directly from the \mathbf{G}_z matrix. The total additive genetic variance along the reaction norm ^[.188]
 361 ^[.189] ^[.190] ^[.191]

$$\sup[.192]$$

362 ^[.193] V_{Add} , is the average of the additive genetic variance in each environment, i.e. the average of the
 363 ^[.194] ^[.195] diagonal elements of the ^[.196] \mathbf{G}_z . The marginal additive genetic variance of the trait, V_A ,
 364 is the average of all the elements of the \mathbf{G}_z matrix. Finally, the variance $V_{A \times E}$ is the sum of the products of
 365 the (co)variances in the frequency of each environment and the additive genetic (co)variances in \mathbf{G}_z . We
 366 illustrate in Appendix C4 the relationship between the structure in the \mathbf{G}_z matrix and the additive genetic
 367 variances, but a simplified statement is that $V_{A \times E} > 0$ as soon as the correlation between environments
 368 are different from 1 or variances in the diagonal are not all equal.

¹⁸⁶removed: We can illustrate the general decomposition of V_{Gen} in the case of polynomial reaction norms

¹⁸⁷removed: , as done above for V_{Plas} . When

¹⁸⁸removed: is a polynomial function of the environment

¹⁸⁹removed: then the gradient of \hat{z} with respect to reaction norm parameters is simply the vector of exponents of the environment defined below

¹⁹⁰removed: , $\psi = \mathbf{x}$. Then using

¹⁹¹removed: , we have

¹⁹³removed: where $\bar{\mathbf{x}}$ is the vector of

¹⁹⁴removed: average of the exponentiated environments, \mathbf{X} their covariance matrix defined in

¹⁹⁵removed: and Tr stands for the trace of a matrix . Note that

¹⁹⁶removed: trace of a matrix product is the sum of element-wise products of their terms. With

369 To further decompose genetic variation in the reaction norms, we first note that here, the reaction norm
 370 parameters are the focus of the decomposition, rather than shape characteristics like the slope or curvature
 371 (with the exception of a quadratic reaction norm^[..197]^[..198]

[..199]

372 ^[..200], the only case were they are formally linked). Because Equation 21 is a sum of products, and since
 373 G_θ is a constant, we can isolate each term of the resulting sum as:

$$\gamma_i = \frac{E_\varepsilon(\psi_{\varepsilon,i}^2) V_g(\theta_i)}{V_{\text{Add}}}, \quad \gamma_{ij} = \frac{2E_\varepsilon(\psi_{\varepsilon,i}\psi_{\varepsilon,j}) \text{Cov}_g(\theta_i, \theta_j)}{V_{\text{Add}}}, \quad \sum_i \gamma_i + \sum_{i<j} \gamma_{ij} = 1. \quad (26)$$

374 Here, γ_i provides the contribution of the i th parameter in the model to the total additive genetic variance
 375 V_{Add} , while γ_{ij} provides the contribution of the covariation between parameters i and ^[..201] j to V_{Add} . As
 376 such, this “ γ -decomposition” (where gamma refers to g for Genetics) measures the relative importance of
 377 genetic variances and covariances of the ^[..202]^[..203]parameters to the evolvability of the plastic trait.
 378 Large values of γ_i indicate that genetic variation in the i th parameter translate into a large proportion of
 379 the genetic variation in the trait. Also, large positive or negative values for γ_{ij} indicate that covariation
 380 between parameters i and j can have a large impact in increasing or reducing genetic variation in the trait.

381
 382 It is also possible to focus on the additive genetic variation in plasticity, $V_{\text{A}\times\text{E}}$, rather than the reaction
 383 norm itself, which yields:

$$\iota_i = \frac{V(\psi_{\varepsilon,i}) V_g(\theta_i)}{V_{\text{A}\times\text{E}}}, \quad \iota_{ij} = \frac{2\text{Cov}_\varepsilon(\psi_{\varepsilon,i}, \psi_{\varepsilon,j}) \text{Cov}_g(\theta_i, \theta_j)}{V_{\text{A}\times\text{E}}}, \quad \sum_i \iota_i + \sum_{i<j} \iota_{ij} = 1. \quad (27)$$

384 This “ ι -decomposition” (where iota refers to i for Interaction) highlights the fact that $V_{\text{A}\times\text{E}}$ is the sum
 385 of the products of (co)variances in elements of the reaction norm gradient ψ_ε and the additive genetic
 386 (co)variances in the parameters.

387 For a quadratic reaction norm as in Equation 12 with a mean-centred environment, this yields:

$$\gamma_a = \frac{V_a}{V_{\text{Add}}}, \quad \gamma_b = \frac{V_b E(\varepsilon^2)}{V_{\text{Add}}}, \quad \gamma_c = \frac{V_c E(\varepsilon^2)^2}{V_{\text{Add}}}, \quad \gamma_{ac} = \frac{2C_{ac} E(\varepsilon^2)}{V_{\text{Add}}}, \quad \iota_b = \frac{V_b V(\varepsilon)}{V_{\text{A}\times\text{E}}}, \quad \iota_c = \frac{V_c V(\varepsilon^2)}{V_{\text{A}\times\text{E}}}. \quad (28)$$

¹⁹⁷removed: as in

¹⁹⁸removed: , this becomes

²⁰⁰removed: where terms in V

²⁰¹removed: C denote additive

²⁰²removed: reaction norm parameters defined in

²⁰³removed: . If the environmental variable is symmetrical and

388 Note that since the environment has been mean-centred, [..²⁰⁴]

[..²⁰⁵]

389 [..²⁰⁶] we have $V(\varepsilon) = E(\varepsilon^2)$ since $E(\varepsilon) = 0$, and thus $\gamma_b = \iota_b$, i.e. in the quadratic case, all of the
390 genetic [..²⁰⁷] variation in the slope contributes to the genetic variance in plasticity. Note also that genetic
391 variance in reaction norm intercept a does not contribute to the heritability of plasticity ($\iota_a = 0$).

392 For the character-state, such decomposition can be performed but yields as many parameters as there
393 are environments for γ , and pairwise combinations of environments for ι . They directly depend on the
394 additive genetic variance in each environment, weighed by its frequency in the experimental setting for γ ;
395 and on the product between the (co)variance in frequency of the environment and the additive genetic
396 (co)variance in or between environments for ι . While these quantities can be informative about particular
397 (couple of) environment (e.g. large γ_k would sign that the k th environment is associated with a large
398 genetic variance, compared to the others), they are certainly not summary quantities of the \mathbf{G}_z matrix and
399 are difficult to easily relate to evolvability and constraints on reaction norms shape. The variances V_{Add} ,
400 V_A and [..²⁰⁸] [..²⁰⁹] [..²¹⁰]

[..²¹¹]

401 $V_{A \times E}$ are more interesting summary statistics in this particular context. Another interesting summary
402 quantity can be provided by the toolbox of multivariate quantitative genetics. Following (Kirkpatrick
403 2009), we can define the effective number of character states as

$$n_e = \sum_i \frac{\lambda_i}{\lambda_1}, \quad (29)$$

404 [..²¹²] [..²¹³] [..²¹⁴] where λ_i is the i^{th} eigenvalue of \mathbf{G}_z ranked by size (i.e., λ_1 is the largest eigenvalue).
405 Large n_e close to the actual number of assayed environments means that genetic variance is well balanced
406 and little correlated across environments. Conversely, n_e near 1 means that most genetic variation lies along
407 a single combination of character states, such that reaction norm evolution is highly constrained, i.e. the
408 genetic correlations are very high between the environments. However, it would be wrong to equate $n_e = 1$

²⁰⁴removed: then $E(\varepsilon) = E(\varepsilon^3) = 0$, such that

²⁰⁶removed: Note the importance

²⁰⁷removed: covariance between the intercept

²⁰⁸removed: the curvature component C_{ac} , which can have a critical evolutionary role

²⁰⁹removed: . From

²¹⁰removed: , we can compute the contribution of each component of genetic variance in reaction norm to the total genetic variance (averaged across environments):

²¹²removed: As noted above for components of V_{Plas} in

²¹³removed: , the components of V_{Gen} in

²¹⁴removed: depend on the distribution of environments, through its moments $E(\varepsilon^n)$

409 with an absence of genetic variance in plasticity: if the genetic variances within environments (i.e. the
410 diagonal elements of \mathbf{G}_z) are variable while $n_e = 1$, this results in more evolvability in some environments,
411 thus $V_{A \times E} > 0$. Reciprocally, a maximal value for n_e (i.e. equal to the number of environments) does not
412 mean that the genetic variance in plasticity is maximised at the expense of additive genetic variance in the
413 trait: for example, when there is no genetic covariances between environments and equal genetic variances
414 within environments, n_e is maximised, but V_A is not zero. As a result, a combined interpretation of n_e and
415 the ratio $V_{A \times E}/V_{Add}$ (i.e. how much of the total genetic variance in the reaction norm consists of genetic
416 variance in plasticity) generates an interesting summary of the main properties of the \mathbf{G}_z matrix in the
417 context of a character-state.

418 Parameter estimation and variance partitioning in practice

419 Estimating the parameters

420 All the parameters mentioned [..²¹⁵] in the previous section can be estimated through commonly used
421 statistical frameworks. [..²¹⁶] [..²¹⁷] [..²¹⁸] [..²¹⁹] [..²²⁰] For the character-state approach (Equation 2),
422 a random-intercept model can be used, or alternatively a “multi-trait” model (Rovelli et al. 2020;
423 Mitchell & Houslay 2021). We will focus here on the former, which is more easily implemented while
424 seemingly scarcely used in the literature on plasticity. In a random-intercept model, the environment
425 is considered as a categorical variable, to which a random effect is added using the genotype as the
426 grouping factor. In the [..²²¹] curve-parameter approach, the appropriate models will be random-slope
427 models for a polynomial approach (as mentioned in Morrissey & Liefting 2016), or non-linear mixed
428 models [..²²²], fitting the reaction norm function $f(\varepsilon, \boldsymbol{\theta})$ [..²²³] to the data. Random effects are fitted to
429 the parameters of this function (with the genotype as grouping factor) [..²²⁴], e.g. the intercept, slope,
430 and any higher-order effects for a polynomial function.

431 Since the parameters are estimated with noise, it is important to account for the impact of es-
432 timation uncertainty when computing variance components. In particular, while variances directly
433 obtained using random effects (e.g. [..²²⁵] genetic variances) are expected to be unbiased, the vari-

²¹⁵removed: above

²¹⁶removed: A tutorial is available at

²¹⁷removed: github.com/devillemereuil/TutoPartReacNorm

²¹⁸removed: showing how to implement such models using e.g. the frequentist lme4

²¹⁹removed: and Bayesian brms R packages

²²⁰removed: .

²²¹removed: curve parameter

²²²removed: . Such a model is based on

²²³removed: , possibly written as a linear model (e.g. for a polynomial function), to which random effects

²²⁴removed: are added for all of its parameters

²²⁵removed: variances related to V_{Gen}

434 ances arising from fixed effects (e.g. variances related to V_{Plas}) should be corrected for biases due to
435 uncertainty [..²²⁶]

[..²²⁷]

436 [..²²⁸](as the adjusted R^2 does for example). Details are provided in Appendix E[..²²⁹]

[..²³⁰]

437 [..²³¹][..²³²].

438 [..²³³]

439 To compute the total phenotypic variance required to get the estimates \hat{P}_{RN}^2 , \hat{H}_{RN}^2 and \hat{h}_{RN}^2 , we advise
440 using the sum of all estimated components rather the raw sample variance. The former is common practice
441 in most quantitative genetics inference to account for potential imbalance in the experimental or sampling
442 design (Wilson et al. 2010; de Villemereuil et al. 2018).

443 We provide an R package, named `Reacnorm` github.com/devillemereuil/Reacnorm, providing functions
444 implementing the variance decomposition based on raw outputs of statistical models. A tutorial is shipped
445 with the package, as an R vignette, showing how to implement such models using the Bayesian `brms` R
446 packages (Bürkner 2017), along with `Reacnorm`.

447 Perfect modelling of quadratic curves

448 We simulated phenotypic data conforming to a quadratic reaction norm, to evaluate the performance of
449 the proposed approach when the [..²³⁴]reaction norm truly is quadratic. We considered both a discrete
450 and continuous environment. For the discrete environment, we considered $N_{\text{Gen}} = 20$ or 5 different
451 genotypes and an environmental gradient of [..²³⁵] $N_{\text{Env}} = 10$ or 4 values, equally spaced from -2
452 to [..²³⁶]2. We sampled $N_{\text{Rep}} = N_{\text{Gen}}$ individual measures for each genotype with a residual variance
453 $V_{\text{Res}} = 0.25$. For the continuous environment, we drew $N_{\text{Env}} = 10$ or 4 values from a normal distribution
454 for each of the $N_{\text{Gen}} = 200$ or 50 genotypes. Residual noise was applied around each measure for each
455 genotype with a residual variance $V_{\text{Res}} = 0.25$. In all cases, we defined a quadratic curve with average

²²⁶removed: . For example, the unbiased estimator of V_{Plas} in a polynomial model would be:

²²⁸removed: where \mathbf{S}_θ is the variance-covariance matrix of errors around the $\hat{\theta}$ estimators (see

²²⁹removed:). The unbiased estimator for a character-state model would be:

²³¹removed: where s_k is the standard-error of μ_k at environment k (see

²³²removed:).

²³³removed: Perfect modelling of polynomial curves

²³⁴removed: true reaction norm is correctly modeled

²³⁵removed: 10

²³⁶removed: 2, over which we

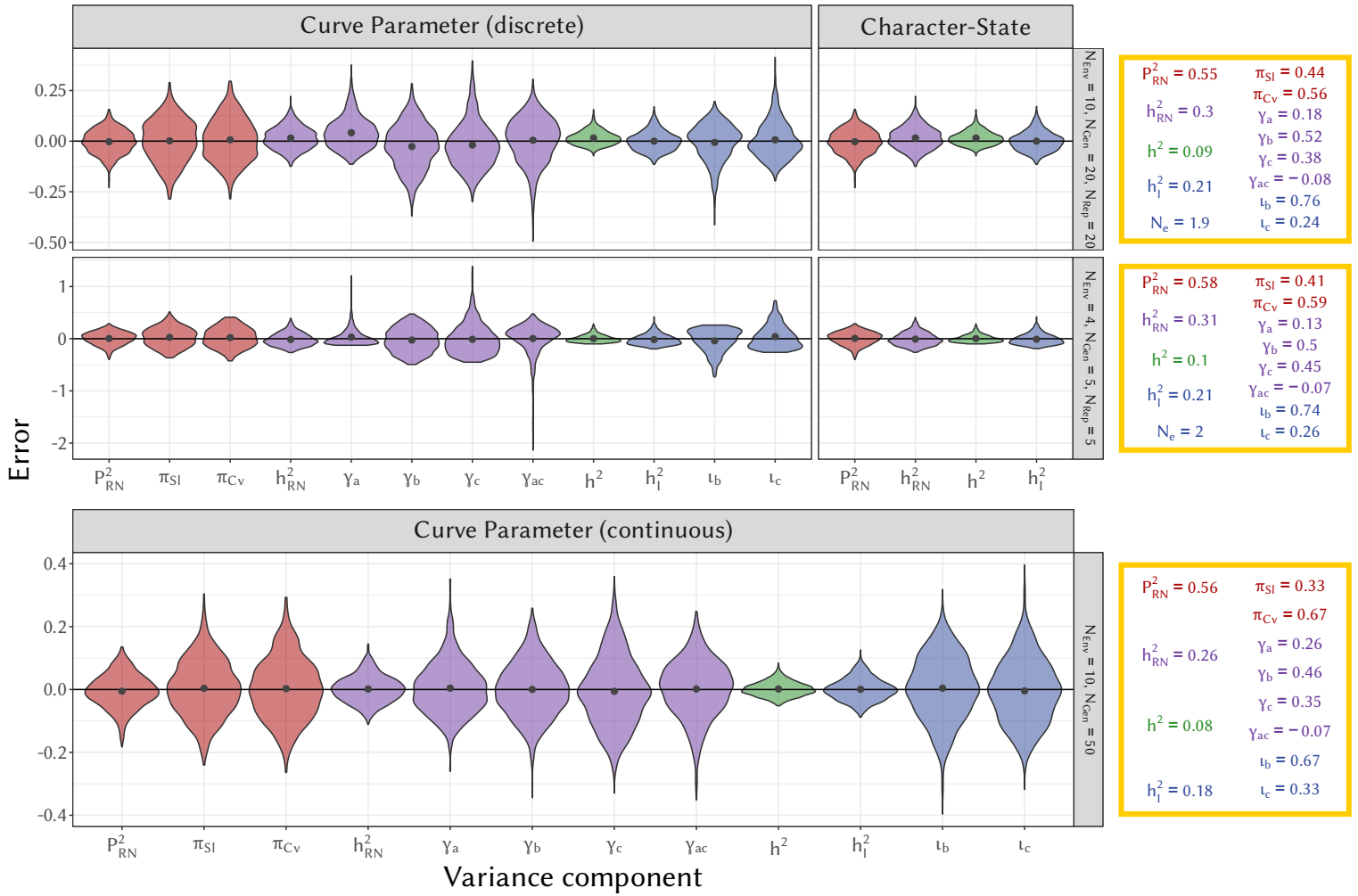


Figure 4: Distribution of the error (difference between the inferred and true value) for each the inferred variance components for three scenarios: two discrete (N_{env} : number of environments, N_{Gen} : number of different genotypes, N_{Rep} : number of replicates per genotype) and one continuous (N_{env} : number of environment tested per genotype, N_{Gen} : number of different genotypes). The grey dots correspond to the average over the 1000 simulations. The character-state approach was impossible for the continuous environment scenario. The yellow boxes on the right show the estimates for \hat{P}_{RN}^2 (proportion of variance generated by the plasticity in the mean reaction norm), \hat{h}_{RN}^2 (total heritability of the reaction norm), \hat{h}^2 (heritability based on average breeding values) and \hat{h}_1^2 (heritability of plasticity) for both the curve-parameter and character-state approaches. For the curve-parameter, the π -decomposition of \hat{P}_{RN}^2 into π_{SI} (contribution of the slope) and π_{Cv} (contribution of the curvature); the γ -decomposition of \hat{h}_{RN}^2 into γ_a (genetic contribution of the intercept), γ_b (genetic contribution of the slope), γ_c (genetic contribution of the curvature) and γ_{ac} (genetic contribution of the covariance between the intercept and the curvature) and the ι -decomposition of \hat{h}_1^2 into ι_b (slope) and ι_c (curvature) are also shown. The effective number of dimensions n_e from the character-state is not shown, due to an important bias impacting the comparison with the other parameters.

456 parameters $\bar{\theta} = (1.5, 0.5, -0.5)$ for intercept, slope and curvature. We then drew [\dots ²³⁷] N_{Gen} different
 457 genotype-specific vectors of [\dots ²³⁸] **curve-parameter** θ from a multivariate normal distribution with

²³⁷removed: 20

²³⁸removed: curve parameter

458 mean $\bar{\theta}$ and (genotypic) variance-covariance matrix

$$[..^{239}] \mathbf{G}_{\theta} = \begin{pmatrix} 0.090 & -0.024 & -0.012 \\ -0.024 & 0.160 & 0.008 \\ -0.012 & 0.008 & 0.040 \end{pmatrix}.$$

459 Figure 1 displays examples of curves resulting from these parameters. [..²⁴⁰] The simulation process
 460 was repeated [..²⁴¹] 1000 times for each scenario, and for each simulated dataset, we ran estimations
 461 using the lme4 R package (Bates et al. 2015) under [..²⁴²] the curve-parameter (for discrete and continu-
 462 ous environment) and character-state (only for discrete environment) approaches, in order to check how
 463 these approaches compare in practice.

464 [..²⁴³]

465 [..²⁴⁴] From the curve-parameter models, we computed \hat{V}_{Plas} [..²⁴⁵] [..²⁴⁶] (accounting for the uncer-
 466 tainty in fixed effects), then \hat{P}_{RN}^2 . We also computed the π -decomposition ($\hat{\pi}_{\text{SI}}$ and $\hat{\pi}_{\text{CV}}$, Equation 14) [..²⁴⁷
 467] [..²⁴⁸], since the true reaction norm is quadratic here, as well as \hat{h}_{RN}^2 , \hat{h}^2 and \hat{h}_I^2 as in Equation 9. We then
 468 applied the γ -decomposition to \hat{h}_{RN}^2 (Equation 26): $\hat{\gamma}_a$ [..²⁴⁹] impact of the genetic variation of the
 469 intercept), [..²⁵⁰] $\hat{\gamma}_b$ (for the slope), [..²⁵¹] $\hat{\gamma}_c$ (for of the curvature) and [..²⁵²] $\hat{\gamma}_{ac}$ (for the covariance
 470 between the intercept and curvature). Similarly, we applied the ι -decomposition to \hat{h}_I^2 (Equation 27):
 471 ι_b (for the slope) and ι_c (for the curvature). From the character-state model, we computed [..²⁵³] [..²⁵⁴

²⁴⁰removed: Finally, we sampled 20 individual measures for each genotype with a residual variance $V_{\text{Res}} = 0.25$. This scenario corresponds to expected values $V_{\text{Plas}} = 0.92$ and $V_{\text{Gen}} = 0.5$, for a total phenotypic variance of 1.67. Our simulated conditions resulted in $20 \times 10 \times 20 = 4000$ data points per simulation, which is on the higher-end of the realm of practical datasets, since the aim was not to perform a power analysis, but to evaluate the soundness of the approach in practice. However the results were qualitatively unchanged when using 4 instead of 10 environments.

²⁴¹removed: 100 times in R

²⁴²removed: both the curve parameter and

²⁴³removed: Distribution of the relative error (difference between the inferred and true value, divided by the true value) for each the inferred variance components. Estimates are for \hat{V}_{Plas} , \hat{V}_{Gen} and \hat{V}_{Tot} for both the curve parameter and character-state approaches. For the parameter curve, the π -decomposition of \hat{V}_{Plas} into π_b (contribution of the slope) and π_c (contribution of the curvature) and the γ -decomposition of \hat{V}_{Gen} into γ_a (genetic contribution of the intercept), γ_b (genetic contribution of the slope), γ_c (genetic contribution of the curvature) and γ_{ac} (genetic contribution of the covariance between the intercept and the curvature) is also shown. The red dots correspond to the average over the 1000 simulations. The yellow box provides the expected values for all of the estimates.

²⁴⁴removed: From the curve parameter

²⁴⁵removed: as in

²⁴⁶removed: , as well as its

²⁴⁷removed: into π_b (part explained by the average linear trend) and π_c (part explained by the average curvature). We also computed \hat{V}_{Gen} as in

²⁴⁸removed: and its

²⁴⁹removed:) into γ_a (

²⁵⁰removed: γ_b

²⁵¹removed: γ_c

²⁵²removed: γ_{ac}

²⁵³removed: \hat{V}_{Plas} as in

²⁵⁴removed: and \hat{V}_{Gen} as in

472] [.255] only \hat{P}_{RN}^2 , \hat{h}_{RN}^2 , \hat{h}^2 and \hat{h}_1^2 .

473 The yellow boxes in Figure 4 display the theoretical expected values for the different parameters for
474 three scenarios of environmental variation (two discrete, one continuous; other scenarios are shown in
475 Appendix F). Using the first discrete scenario as a reference for now, most of the total phenotypic
476 variance comes from the average plasticity ($P_{RN}^2 = 0.55$). This, in turns, includes a large contribution from
477 the curvature ($\pi_{CV} = 0.56$) of the average reaction norm, more than from its slope ($\pi_{SI} = 0.44$). The
478 total heritability of the reaction norm is substantial ($h_{RN}^2 = 0.3$), but interestingly most of it is due to the
479 heritability of plasticity ($h_{RN}^2 = 0.21$), while the marginal heritability of the trait is only $h^2 = 0.08$. Contrary
480 to the [.256] [.257] average shape, most of the additive genetic variation comes from the slope, both when
481 considering the total reaction norm ($\gamma_b = 0.52$), or plasticity alone ($\iota_b = 0.76$). All scenarios share the
482 same underlying parameters θ and \mathbf{G}_θ , resulting in very comparable values for our variance decomposition
483 (i.e. P_{RN}^2 and the heritabilities) across the different environmental sampling scheme. By contrast, the
484 environmental sampling scheme (especially discrete v. continuous distribution) can substantially impact
485 the expected values of the π -, γ - and ι -decompositions. This is especially true when switching from the
486 discrete to the continuous scenarios (e.g. $\pi_{SI} = 0.44$ for the first discrete scenario while $\pi_{SI} = 0.33$ for
487 the continuous scenario). Interestingly, the theoretical effective number of environment n_e is very stable
488 when comparing the first (4 environments) and second (10 environments) discrete scenarios ($n_e = 2$ v.
489 $n_e = 1.9$), which is due to the constraining shape of the quadratic reaction norm.

490 [.258] Switching to the error in the estimation of the parameters (left panels of Figure 4 [.259]),
491 we see first that both the character-state and curve-parameter approaches allow for unbiased inference
492 (Wilcoxon's rank test, $p > 0.05$ [.260]), apart from a slight bias in the heritabilities (\hat{h}_{RN}^2 , [.261] \hat{h}^2 and
493 [.262] \hat{h}_1^2) and some of their γ and ι components in the discrete scenarios ($< 5\%$ relative bias, Wilcoxon's
494 rank test, $p < 0.05$), notably due to a slight overestimation of the genetic variance of the intercept
495 (visible in the top row of Figure 4). A notable exception, not shown in the graphics of Figure 4, was
496 the effective number of dimensions, n_e , for the character-state. The relative bias was between -12% and
497 -35% (Wilcoxon's rank test, $p < 0.05$), and was mainly explained by an overestimation of the dominant
498 eigenvalue λ_1 in Equation 29. For the discrete case, the precision of the estimates was not much influenced

²⁵⁵removed: . Finally for both models, we computed the total inferred variance as the sum $\hat{V}_{Plas} + \hat{V}_{Gen} + V_{Res}$, and compared it to

²⁵⁶removed: sample phenotypic variance, to verify the ability of both approaches to implement the variance partitioning in

²⁵⁷removed: .

²⁵⁸removed: The results of the inferences are available in

²⁵⁹removed: . First, they show that both methods

²⁶⁰removed: for all components) of all estimates, showing that our variance partitioning is easily implemented with existing tools. There was

²⁶¹removed: however, considerable uncertainty in the estimation of γ_{ac} , as covariances are typically more difficult to estimate. Second,

²⁶²removed: as a consequence,

499 by the number of environments and depended more on the number of genotypes (see Figure S1). For the
500 continuous case, both the number of environments and genotypes influenced the precision of estimates (see
501 Figure S2). As a sanity check, we also verified that \hat{V}_{Tot} ^[..263](not shown in Figure 4) reflected the raw
502 phenotypic variance with extreme precision (correlation > 99%) ^[..264]in the discrete case and very good
503 precision (correlation > 87%) in the continuous case. The difference between these two types of scenarios
504 is explained by how the stochasticity in environmental values differs among them. Importantly, the ^{[..265}
505]results in Figure 4) also illustrate the exact equivalence, in the discrete case, between the curve-parameter
506 and character-state ^[..266]approaches, as the distributions of ^[..267] \hat{P}_{RN}^2 and \hat{h}_{RN}^2 were nearly identical
507 (Figure 4, correlation > 99%) between the two approaches. This means that our variance partitioning
508 is not impacted by which approach is chosen to study plasticity, as long as the ^[..268]curve-parameter
509 approach captures the true reaction norm shape. When this does not hold, the differences between
510 estimates from these alternative approaches can be exploited efficiently, as we describe below.

511 ^[..269]Imperfect modelling of a non-polynomial reaction norm

512 The true shapes of reaction norms are generally unknown and may be complex, such that any ^{[..270}
513]curve-parameter model is likely to be mis-specified to some extent. ^[..271]In the case of a discrete
514 environment, the character-state approach is ^[..272]arguably more general, as it does not assume
515 anything about the “true” shape of the reaction norm (as pointed out previously by de Jong 1995).
516 Nonetheless, having access to ^[..273]curve-parameters is often very interesting and more actionable
517 ^[..274](even in cases where the linear and quadratic components cannot be interpreted as the average
518 slope and curvature), especially to predict evolution of phenotypic plasticity (see also de Jong 1995).
519 To get the best of both worlds, we ^[..275]rely on the ^[..276]ability of the character-state approach to
520 recover ^[..277] P_{RN}^2 , using it as an “anchor”^[..278], to assess the performance of a given curve. Note that,
521 under these circumstances, it is not possible to obtain the most natural π -decomposition in Equation 14,

²⁶³removed: retrieved the total

²⁶⁴removed: . Third, and most interestingly, the results illustrate

²⁶⁵removed: equivalence between the curve parameter

²⁶⁶removed: approaches

²⁶⁷removed: \hat{V}_{Plas} and \hat{V}_{Gen} were correlated at

²⁶⁸removed: curve parameter

²⁶⁹removed: Assessing goodness-of-fit under imperfect

²⁷⁰removed: curve parameter

²⁷¹removed: The

²⁷²removed: arguable

²⁷³removed: curve parameters

²⁷⁴removed: and interpretable

²⁷⁵removed: offer to

²⁷⁶removed: robust

²⁷⁷removed: V_{Plas}

²⁷⁸removed: to test the goodness-of-fit of an assumed curve

522 so we instead rely on the φ -decomposition in Equation 16 (here taken at the second order). Because of
 523 this, we need to assess how “bad” our simplification using an imperfect curve is. To do so, we compute the
 524 ratio of the variance modelled by the polynomial curve to the total variance due to phenotypic plasticity:

$$M_{\text{Plas}}^2 = \frac{\hat{V}_{\text{mod}}}{\hat{V}_{\text{Plas}}}. \quad (30)$$

525 It is important to note here that M_{Plas}^2 is just a convenient way to quantify the amount of \hat{V}_{Plas} explained
 526 by the chosen parametric curve, and should not be used to perform model selection. Model selection is
 527 a complex matter and we refer the readers to published reviews on this subject (e.g. Johnson & Omland
 528 2004; Tredennick et al. 2021).

529 In order to demonstrate the soundness and usefulness of this approach, we simulated datasets
 530 following relatively common curves that are not well-captured by a second order polynomial: a logistic
 531 sigmoid (hereafter sigmoid scenario), or a Gompertz-Gaussian thermal performance curve (hereafter TPC
 532 scenario, see Figure 5). We assumed that the environment is sampled at either 10 or 4 values. For
 533 each of these conditions, we simulated 1000 datasets, with 10 measures *per* environment (for the
 534 sake of simplicity, and given the focus on \hat{P}_{RN}^2 here, we did not include different genotypes in
 535 these simulations). We estimated the parameters of a polynomial model, and computed the relative
 536 contributions of the first- and second-order parameters using Equation 16. In addition, we
 537 computed the unbiased estimates of the variance explained by our polynomial or character-
 538 state models to obtain M_{Plas}^2 .

539 \hat{P}_{RN}^2

\hat{V}_{Plas}

540 Our results show that, as expected, the polynomial function is an imperfect proxy of our complex
 541 shapes (Figure 5, $M_{\text{Plas}}^2 = 0.89$ for the sigmoid and $M_{\text{Plas}}^2 = 0.65$ for the TPC), but using
 542 the character-state approach allows retrieving the total plastic variance without bias. The approach
 543 described here is thus useful to compare a given reaction norm model (e.g. a polynomial function)
 544 to an unknown true shape of the reaction norm, in a case where environment is discretised. In

²⁷⁹removed: \hat{V}_{Plas}

²⁸⁰removed: slope and curvature using

²⁸¹removed: model as in

²⁸²removed: (here specifically termed \hat{V}_{mod}), and compared it to \hat{V}_{Plas} estimated from a

²⁸³removed: model (here a simple ANOVA, since genotypes are not modelled)

²⁸⁴removed: As a measure of goodness-of-fit, we computed the ratio of the variance explained by the polynomial curve to the total variance due to phenotypic plasticity:

²⁸⁶removed: $R_{\text{mod}}^2 = 0.89$

²⁸⁷removed: $R_{\text{mod}}^2 = 0.65$ for the performance curve

²⁸⁸removed: compute a measure of goodness-of-fit of a

²⁸⁹removed: . Here, while a linear function might be acceptable for the sigmoid curve, with $R_{\text{mod}}^2 = 0.89$, even a quadratic function can be considered as a bad fit to the Gompertz-Gaussian performance curve ($R_{\text{mod}}^2 = 0.65$)

545 more [..²⁹⁰] **detail, the linear component** was the most important component to explain the phenotypic
 546 variation for the sigmoid [..²⁹¹] **scenario** ($\varphi_1 = 0.89$, same as the total model). This was because [..²⁹²
 547] **the quadratic component** was always estimated close to zero ($< 10^{-3}$), [..²⁹³] **thus no variance was**
 548 explained by the [..²⁹⁴] **quadratic component** ($\varphi_2 = 0$). Of course, the sigmoid is not a straight line
 549 either, and some remaining variance unexplained by the polynomial curve ($1 - 0.89 = 0.11$) could
 550 have been explained by higher-order effects (e.g. cubic effect **and higher**). By contrast, for the [..²⁹⁵
 551] **TPC scenario**, while the [..²⁹⁶] **linear component** was an important factor ([..²⁹⁷] $\varphi_1 = 0.47$), the
 552 [..²⁹⁸] **quadratic component** also explained quite a lot of the variance as well ([..²⁹⁹] $\varphi_2 = 0.2$). Again,
 553 higher-order effect, including at least a cubic effect, would have explained more of the variance arising
 554 from the average shape of plasticity.

555 This example illustrates the usefulness of a combined [..³⁰⁰] **curve-parameter** and character-state
 556 approach to study the shape of reaction norms **of a discretely sampled environment**. While the character-
 557 state approach provides a [..³⁰¹] **widely applicable estimation of \hat{P}_{RN}^2** (if the environment is discretised),
 558 **the curve-parameter** approach provides interpretable information about [..³⁰²] **(at least) first- and [..³⁰³**
 559 **second-order parameters** of the reaction norm **(although they might depart more or less strongly from**
 560 **its average slope and curvature)**, which helps describing where most phenotypic variance lies. [..³⁰⁴
 561] **Our ratio M_{Plas}^2 can then be used to evaluate** how well a chosen polynomial function models an actual
 562 reaction norm. [..³⁰⁵]

563 Estimation of non-linear models

564 Although we have focused so far on models that are linear in [..³⁰⁶] **its parameters, the main strength**
 565 **of our approach is its generality: it can** be applied to [..³⁰⁷] **any arbitrary functions (provided it is**

²⁹⁰removed: details, the average slope

²⁹¹removed: curve ($\pi_b = 0.89$)

²⁹²removed: , as the average curvature of a sigmoid is zero, the

²⁹³removed: resulting in no variance

²⁹⁴removed: curvature in this case ($\pi_c = 0$)

²⁹⁵removed: Gompertz-Gaussian performance curve

²⁹⁶removed: average slope

²⁹⁷removed: $\pi_b = 0.47$

²⁹⁸removed: average curvature

²⁹⁹removed: $\pi_c = 0.2$

³⁰⁰removed: curve parameter

³⁰¹removed: robust estimation of V_{Plas} , the curve parameter

³⁰²removed: the average slope and curvature (

³⁰³removed: higher-orders if needed)

³⁰⁴removed: Using our measure of goodness-of-fit R_{mod}^2 , this analysis can be performed to assess

³⁰⁵removed: Note that R_{mod}^2 is not penalised for the number of parameters, and thus should not be used for model selection.

³⁰⁶removed: the parametersto estimate (*e.g.*, the coefficients associated to each exponent of the environment for a polynomial reaction norm), the approach we propose can also

³⁰⁷removed: arbitrary functions

566 differentiable). This requires numerically computing [..³⁰⁸] integrals for V_{Plas} [..³⁰⁹](for \hat{P}_{RN}^2), π_{SI} , π_{CV}
567 and ψ_ε (for the heritabilities), but this can be solved with efficient algorithms. We illustrate this [..³¹⁰] by
568 introducing genetic variation in the parameters [..³¹¹] of the sigmoid and TPC reaction norms illustrated
569 in Figure 5 (top panels). [..³¹²][..³¹³] We used a non-zero, but small, residual variance ($V_{\text{R}} = 0.0001$) to
570 avoid numerical issues typical when running thousands of non-linear models. We focused on a continuous
571 environment, and estimated the actual functions used to generate the datasets, using the non-linear
572 modelling function of nlme package (Pinheiro et al. 2009). We used the cubature package (Narasimhan
573 et al. 2023), as in the QGglmm package (de Villemereuil et al. 2016), to compute [..³¹⁴] parameters
574 linked to the variance decomposition, and, further, the π -, γ - and ι -decomposition. We simulated 1000
575 datasets for each scenario, consisting of [..³¹⁵] 200 genotypes measured each in 10 [..³¹⁶] different
576 environments, randomly sampled from a normal distribution.

577 We retrieved our simulated parameters without bias using the nlme function [..³¹⁷][..³¹⁸][..³¹⁹],
578 except for a slight bias (Wilcoxon’s rank test, $p < 0.05$) in the variance of r (latent slope) in the sigmoid
579 model and in C (height of the peak) in the TPC model. This translated into significant (Wilcoxon’s rank
580 test, [..³²⁰] $p < 0.05$) [..³²¹]

581 , but very limited bias (relative bias $< 5\%$) in our derived parameters (Figure 6, bottom panels).
582 Moreover, the sum of variance components ([..³²²] \hat{V}_{Tot}) successfully reflects the total phenotypic
583 variance, with a correlation between the two quantities [..³²³] $> 91\%$.

584 First focusing the average shape of the reaction norm (Figure 6, top panel), one unfortunate aspect
585 of running a non-linear model is that [..³²⁴][..³²⁵] our bias correction described in Appendix E can
586 no longer be applied. However, this bias is generally small provided the standard error is small for

³⁰⁸removed: the integrals in the most general definitions of
³⁰⁹removed: and V_{Gen} above
³¹⁰removed: here using the sigmoid and performance curve shapes above,
³¹¹removed: , beyond the mean curves
³¹²removed: Instead of fitting polynomials as in
³¹³removed: , we
³¹⁴removed: ψ_ε and $V_{\text{A}|\varepsilon}$
³¹⁵removed: 100 individuals (i.e. the “genotype”) measured in each of
³¹⁶removed: environments (say at 10 different temperatures)
³¹⁷removed: . As a result, we successfully recovered all the variance components defined in
³¹⁸removed: (
³¹⁹removed: , bottom panels) . This includes the estimation of the total additive genetic variance of the trait V_{A} .
Indeed, almost all components of variance were unbiased
³²⁰removed: all $p > 0.05$ but one). The only exceptions (
³²¹removed: were V_{Gen} and V_{A} in the Performance Curve case, although the relative bias is extremely small (resp.
1.20% and 1.13%), especially with regard to the uncertainty surrounding the estimates. This results from a slight bias
in the estimation of the Θ matrix by the nlme function. Because of this, there is a slighter bias in V_{Tot} (0.39%).
³²²removed: V_{Tot} in
³²³removed: $> 99.9\%$. One
³²⁴removed: the correction method offered in
³²⁵removed: no longer holds, precisely because of non-linearity in the model

587 most parameters, and the resulting bias in $[\dots^{326}] \hat{P}_{RN}^2$ is extremely small, $[\dots^{327}] [\dots^{328}]$ and even non-
588 significant $[\dots^{329}]$ for the sigmoid model. An important distinction here is the difference between the
589 curve defined by the average parameters $f(\varepsilon, \bar{\theta})$ (Figure 6, top panel, black curve) and the one defined
590 by the local average phenotype $E_{g|\varepsilon}(\hat{z})$ (Figure 6, top panel, red curve), recalling that $[\dots^{330}] \hat{P}_{RN}^2$ is
591 linked to the latter. While the two are very close for the sigmoid case, they differ quite $[\dots^{331}]$ visibly
592 for the TPC one, due to a more pronounced non-linearity in the parameters in the latter. The average
593 slope contributed the most to the overall plastic variance of the mean reaction norm for the sigmoid shape
594 ($\pi_{SI} = 0.88$), with no impact of average curvature ($\pi_{CV} = 0$), close to the φ -decomposition in Figure 5.
595 For the TPC scenario, the contribution of the average slope ($\pi_{SI} = 0.31$) and curvature ($\pi_{CV} = 0.35$)
596 are similar. In this case, the values are very different from the φ -decomposition in Figure 5 (although
597 note that the distribution of the environment is different between these two scenarios). It might appear
598 as counter-intuitive that the slope contributes so much to variance, since the curve increases from 0 and
599 then decreases toward 0, but this is linked to the fact that the environment is normally distributed, so most
600 values are near $\varepsilon = 0$, an area where the slope of the curve is close to be maximised.

601 Although the variation between $[\dots^{332}]$ genotypes in the top panel of Figure 6 seems quite large, the
602 $[\dots^{333}]$ contribution from the average plasticity $[\dots^{334}] \hat{P}_{RN}^2$ is 1.7 to 3.4 times higher than the $[\dots^{335}]$ one
603 of the genetic variance \hat{H}_{RN}^2 (Figure 6, yellow box in $[\dots^{336}]$ first- and second-row panels). This occurs
604 because the genetic variance is actually very low in most environments (Figure 6, $[\dots^{337}]$ brown and
605 purple lines of the second-row panels), and scarcely as high as V_{Plas} . $[\dots^{338}]$

606 $[\dots^{339}] [\dots^{340}]$ As mentioned above, non-linearity in the parameters is less strong for the sigmoid case
607 than for the TPC case, resulting in almost exactly equal values for \hat{H}_{RN}^2 and \hat{h}_{RN}^2 for the former, while
608 they are slightly different for the latter. In both cases, the low difference between \hat{H}_{RN}^2 and \hat{h}_{RN}^2 can
609 be explained by the disproportionate importance in the γ -decomposition of parameters that are actually
610 linearly related to the trait ($\gamma_L = 0.98$ for the sigmoid and $\gamma_C = 0.81$ for the TPC scenarios). In terms

³²⁶removed: V_{Plas}

³²⁷removed: especially with regard to the imprecision, as can be seen in

³²⁸removed: and the

³²⁹removed: result of Wilcoxon's rank test. In general, this bias will be small in regards to other sources of imprecision, unless the standard error of the estimates is extremely large (e.g. for very small sample size)

³³⁰removed: V_{Plas}

³³¹removed: strongly for the performance curve one.

³³²removed: individuals (i.e. genotypes in this simulation) in

³³³removed: variance due to

³³⁴removed: V_{Plas} is two to four

³³⁵removed: genetic variance V_{Gen}

³³⁶removed: top

³³⁷removed: blue violins of the middle

³³⁸removed: This illustrates how our variance partitioning can quantify and objectify variations that may be counter-intuitive for the human eye, notably because of non-linearities.

³³⁹removed: An important aspect of such modelling of the reaction norm is that there is no longer an equivalence between the genetic variance V_{Gen} and the additive genetic variance V_A , due to the non-linearity of the system

³⁴⁰removed: . In this regard the sigmoid model does unexpectedly yield extremely close values for V_{Gen} and V_A

611 of heritability of plasticity, it is substantial in both cases ($h_1^2 = 0.081$ for the sigmoid and $h_1^2 = 0.133$ for
612 the TPC scenario), as can be expected from the non-parallel reaction norms (Figure 6[.341]). However,
613 it remains smaller than the marginal heritability of the trait in both cases ($h^2 = 0.143$ for the sigmoid and
614 $h^2 = 0.216$ for the TPC scenarios). Interestingly, for the TPC scenario, and contrary to what happens with
615 the γ -decomposition, a majority of the additive genetic variance in plasticity comes from the variation in
616 the [.342] location of the optimum ($\iota_{\varepsilon_0} = 0.525$). This is because variation in the location of the optimum
617 shifts the reaction norm along the environment axis (i.e. on the “x-axis”), meaning that even a small shift
618 can generate considerable variation that is non-parallel along the phenotype axis (i.e. along the “y-axis”).

619 An interesting aspect of our framework is that we can explore the variation of $V_{\text{Gen},\varepsilon}$, $V_{\text{A},\varepsilon}$ and the γ -
620 decomposition of $V_{\text{A},\varepsilon}$ along the environmental gradient, which can be very informative from an evolutionary
621 perspective. In the case of the sigmoid curve (Figure 6, second and third rows, left panels), the analysis
622 is relatively simple : as the value of the environment increases, the parameter L is [.343] multiplied by
623 an increased value (going from 0 to 1 due to the sigmoid function) and thus its genetic variance plays a
624 stronger role. This translates into $V_{\text{Gen},\varepsilon}$ and $V_{\text{A},\varepsilon}$ increasing with the environment, and γ_L accounting for
625 almost all of the genetic variance after the sigmoid inflexion point in 0. The TPC scenario is even more
626 interesting. First, we can see that both $V_{\text{Gen},\varepsilon}$ and $V_{\text{A},\varepsilon}$ (Figure 6, second row, right panels) are close to zero
627 in the [.344] extreme environments and maximised in a region between the optimum and critical maximal
628 temperature, where the reaction norm suddenly drops after the optimum. This maximum also corresponds
629 to the region where $V_{\text{Gen},\varepsilon}$ and $V_{\text{A},\varepsilon}$ are the most different (and where the red and black departs the most
630 in Figure 6, [.345] top row, right panel). [.346] Regarding the γ -decomposition (Figure 6, third row, right
631 panels), the influence of the location of the optimum (γ_{ε_0}) is maximised at extreme environments, while
632 the influence of the maximum value at the peak (γ_C) is exactly maximised at the average location of the
633 peak. The influence of the covariation between both ($\gamma_{C\varepsilon_0}$) is negative before the peak and positive after.

634 [.347] As these simulations illustrate, our framework allows very finely describing the characteristics of
635 reaction norms, such as how its average shape (slope/curvature) and genetic variation in the parameters

³⁴¹removed: , yellow box in top panels, blue and green violins in middle panels). This is the result of the disproportionate importance of the genetic

³⁴²removed: L parameter is this model ($\gamma_L = 0.99$), even though the genetic variance in

³⁴³removed: only twice that in r in the Θ matrix. Since L is only a mere scaling factor for the model, its relation with the phenotype is linear and thus $V_{\text{Gen}} \simeq V_{\text{A}}$. On the contrary, V_{Gen} and V_{A} differ for

³⁴⁴removed: performance curve model, especially in parts of the model where the local shape differs strongly between individuals (e.g. the two last environmental values,

³⁴⁵removed: right middle

³⁴⁶removed: In this case, V_{A} depends less exclusively on variation in the scaling factor C ($\gamma_C = 0.68$), with $\gamma_{\varepsilon_0} = 0.33$. Hence in this model, the non-linearity due to the exponential function of ε_0 causes more substantial difference between V_{Gen} and V_{A}

³⁴⁷removed: Despite being slightly more complex to implement, this non-linear approach can be highly relevant in practice, as it offers an in-depth analysis of the shape and genetic features of phenotypic plasticity. Moreover, although the environment simulated here was discretised for the sake of simplicity (and to favour good convergence in nlme), this approach would be most relevant when the (measured) environment is continuous rather than discretised, as in analysis of natural, uncontrolled environments

636 influence the phenotypic variance in the trait, while discriminating between total genetic variation of the
637 trait and genetic variation exclusively linked with plasticity itself.

638 Discussion

639 The variance [³⁴⁸]decomposition in Equation 7 is very general, and applicable to any approach used
640 to estimate a reaction norm. In particular, it applies equally well to both the character-state and curve-
641 parameter approaches. Each component and its variance-standardisation provide a different information
642 on the reaction norms: P_{RN}^2 quantifies the proportion of phenotypic variance due to the average plastic
643 response across genotypes, while H_{RN}^2 or h_{RN}^2 quantify the contributions from (broad or additive) genetic
644 variance in the reaction norms. Further, these genetic components can be separated into the marginal
645 heritability of the trait (h^2) based on the average breeding values across environments, and the heritability
646 of plasticity (h_1^2) which is solely based on the gene-by-environment interactions at the level of breeding
647 values. Finally, the sum $T_{RN}^2 = P_{RN}^2 + H_{RN}^2$ quantifies how well we can predict the individual phenotypes
648 based on their genotypes and environments (i.e. genetically variable reaction norms). Those components
649 are efficient summary statistics yielding important information regarding the evolutionary potential of both
650 the trait and its plasticity. Importantly, they are very generally applicable, with a strict equivalence between
651 e.g. a character-state or a curve-parameter approach. However, they do not provide information regarding
652 the actual shape of the reaction norms. To that end, we further decomposed some of these components
653 in terms of characteristics of the shape or parameters of reaction norms.

654 The most difficult problem is to decompose the average plastic variance P_{RN}^2 into terms arising ei-
655 ther from the linear trend (π_{SI}) or from the curvature (π_{CV}) of the reaction norm, which we called π -
656 decomposition. Unfortunately, our estimates for π_{SI} and [³⁴⁹][³⁵⁰] π_{CV} are only valid if the environment
657 is normally distributed, or the true reaction norm is quadratic. In other cases, mean slope and curvature
658 lose their simple interpretation, preventing a meaningful π -decomposition. Nonetheless, for polynomial
659 reaction norms of higher order, we described an alternative decomposition, based on the polynomial coeffi-
660 cients rather than actual slope and curvature, which we called φ -decomposition. While not as interpretable
661 as the π -decomposition, this decomposition can serve as a way to compare polynomial shapes across con-
662 texts. Based on the equivalence between the curve-parameter and [³⁵¹]character-state, we introduced
663 M_{Plas}^2 as a way to quantify the ability of a polynomial model to recover V_{Plas} compared to an “agnostic”

³⁴⁸removed: partitioning that we implement here has several conceptual and practical advantages. First, being based on the law of total variance, it

³⁴⁹removed: does not rely on any particular assumptions, such as Independence between the genotype and the environment. Note that contrary to the common genotype/environment/genotype-by-environment partition, the law of total variance is not symmetrical. Indeed,

³⁵⁰removed: takes averages and variances first over genotypes,

³⁵¹removed: then over environments

664 model such as the character-state. Our proposed framework is summarised in Figure 3. [..³⁵²]
 665 [..³⁵³]Decomposing h_{RN}^2 and h_I^2 is comparatively easier, because the model assumed in Equation 3
 666 and Equation 4 ensures that we can always translate additive genetic variance in the parameters θ into
 667 additive genetic variance in the trait z , even if the function f is not linear in its parameters. Decom-
 668 position of the total heritability of the reaction norm h_{RN}^2 into the impact of the parameters θ leads to
 669 the γ -decomposition. It quantifies the relative importance of genetic variance in different reaction norm
 670 parameters to the evolvability of the trait. [..³⁵⁴]For instance if a given selection episode concerns indi-
 671 viduals that all experienced the same plasticity-inducing environment (i.e. when spatial environmental
 672 variation is negligible [..³⁵⁵]relative to temporal variation), using the multivariate breeder's equation
 673 (Lande 1979)[..³⁵⁶], the relative contribution of genetic variation in parameter θ_i to the response to
 674 selection for the [..³⁵⁷]trait z is

$$[..³⁵⁸] \frac{\Delta_{\theta_i} \bar{z}}{\Delta \bar{z}} = [..³⁵⁹] \gamma_i [..³⁶⁰] + \frac{1}{2} \sum [..³⁶¹]_{i \neq j} \gamma_{ij} [..³⁶²], \quad (31)$$

675 where [..³⁶³]the γ_i and γ_{ij} are defined in Equation 26. In other words, the contributions of responses to
 676 selection by different reaction norm parameters [..³⁶⁴]to overall response to selection by the plastic trait
 677 z is directly proportional to their contribution to its genetic variance. Importantly, these contributions
 678 will depend on the reaction norm gradient ψ_ε defined in Equation 19, and thus on the environment, as
 679 illustrated in Equation 26. In fact, the environment-specific additive genetic variance $V_{A,\varepsilon}$ is a critical
 680 piece of information regarding evolutionary potential, and we can apply the γ -decomposition within
 681 each environment as well. For example, in the [..³⁶⁵]TPC scenario investigated above [..³⁶⁶](Figure 6,
 682 right panels), the contribution of the peak height parameter C is maximised at the average location of the
 683 optimum, where it accounts for 100% of the additive genetic variance [..³⁶⁷] [..³⁶⁸]. On the contrary,
 684 the influence of additive genetic variation in the location of the optimum ε_0 is more important in extreme
 685 environments. The complex interaction between the role of C and ε_0 generates a peak for $V_{A,\varepsilon}$ in the area
 686 between the peak and critical maximal value for the environment (where the performance curve reaches

³⁵²removed: This allows recovering intuitive metrics of the influence of the average reaction norm (V_{Plas}), and the average genetic variance (V_{Gen}).

³⁵³removed: Second, in combination with polynomial modelling (or other forms of parametric approaches), this partitioning allows quantifying the impacts of different aspects of reaction norm shape on the mean plastic variance, versus the genetic variance

³⁵⁴removed: This should prove especially relevant with respect to responses to selection.

³⁵⁵removed: relative

³⁵⁶removed: the

³⁵⁷removed: expressed plastic

³⁶³removed: β is the selection gradient on the expressed trait, and the

³⁶⁴removed: (e.g. slope, curvature, etc)

³⁶⁵removed: Performance Curve

³⁶⁶removed: , there is a peak of

³⁶⁷removed: close to the performance optimum, followed by a sharp decrease at higher temperatures (

³⁶⁸removed: , middle right panel

687 zero). In the context of predicting eco-evolutionary response to warming, this would mean that a slight
688 temperature rise above the optimum would provide a very short window of higher evolvability, but
689 followed by a sharp decrease thereof if warming persists. Beyond these simple scenarios, how selection
690 acts on reaction norms and plasticity depends on how the environment varies in space and/or time
691 [..³⁶⁹] [..³⁷⁰] (Scheiner 1993b; de Jong 1999; Tufto 2015; King & Hadfield 2019), and how the reaction
692 norm gradient ψ_ε and direction selection on the expressed trait z covary across environments. However, an
693 in-depth exploration of how to estimate these selection responses is beyond the scope of the present
694 work.

695 [..³⁷¹] While the γ -decomposition is key to understanding and predicting evolution of the trait, it is
696 based on the total heritability of the reaction norm h_{RN}^2 , which combines additive genetic variation in the
697 trait and its plasticity. To study plasticity in isolation from the marginal additive genetic variance in the trait,
698 we decomposed h_{I}^2 in a similar fashion as h_{RN}^2 , which we called the ν -decomposition. The components of
699 the ν -decomposition measure the contribution of each parameter to the evolutionary potential of plasticity,
700 i.e. to the evolvability of reaction norm shape. In our thermal performance case (TPC) example, the ν
701 associated to C and ε_0 were close to 0.5, meaning that evolution can roughly equally impact the peak
702 height C or the location of the optimum ε_0 , should selection on the shape of reaction norms occur.

703 The detailed decomposition that we propose opens the door to better commensurability and compara-
704 tibility across studies, which can be a challenge in meta-analyses of plasticity. Murren et al. (2014)
705 performed such a meta-analysis, comparing genetic variation in different parameters of reaction norm
706 shape across published datasets. However they [..³⁷²] (i) computed these parameters using only ex-
707 treme environmental values, instead of the whole range of environments; [..³⁷³] (ii) did not account for
708 uneven spacing between environments where relevant; [..³⁷⁴] (iii) did not account for uncertainty in
709 estimations of reaction norms (as previously highlighted by Morrissey & Liefing 2016); and [..³⁷⁵] (iv)
710 assumed the modeled reaction norm shape is true. More detail about the analyses in that study is
711 provided in Appendix G. Our approach overcomes all these issues (some of which had been dealt with
712 already by Morrissey & Liefing 2016). Unfortunately the dataset compiled by Murren et al. (2014)
713 does not provide information on uncertainty of phenotypic estimates (related to V_{Res}), precluding
714 proper meta-analysis of reaction norm shape variation.

³⁶⁹removed: add ref: Tufto 2015 Evolution, king & Hadfield 2019 Evol Lett

³⁷⁰removed: , but

³⁷¹removed: Third, our general framework treats the curve-parameter and character-state approaches under the same umbrella, allowing evaluation of any chosen parametrical model through the goodness-of-fit parameter R_{mod}^2 . This also opens the

³⁷²removed: (i)

³⁷³removed: (ii)

³⁷⁴removed: (iii)

³⁷⁵removed: (iv)

715 [..³⁷⁶]**Importantly**, our variance partitioning can be implemented through commonly used statistical
716 models, notably (**non-**)linear mixed models. [..³⁷⁷]**We** showed that even complex non-linear modelling
717 can perform well, only at the cost of using dedicated libraries to compute integrals numerically. This
718 means that biologists can readily seize all the modelling tools introduced here. In particular, although
719 a character-state approach can be performed using a simple random-intercept model, studies of genetic
720 variance in plasticity seem to rather use a multi-trait model, which offers more control, but is more
721 difficult to implement (but see Stirling & Roff 2000). In order to make the variance partitioning
722 introduced here more accessible, we [..³⁷⁸][..³⁷⁹][..³⁸⁰]**have** implemented the computation of [..³⁸¹
723] \hat{P}_{RN}^2 and the heritabilities, as well as their different decompositions as an R package named **Reacnorm**
724 github.com/devillemereuil/Reacnorm. The package also included a tutorial as a vignette, showing how
725 **to implement the models in the Bayesian package brms and use functions from Reacnorm to study the**
726 **properties of reaction norms**. We hope that this will further stimulate interest in investigating variation
727 and evolutionary potential of reaction norms.

728 **Code availability** The code for the data simulation and analyses performed in this article is available
729 at the following repository: [github.com/devillemereuil/](https://github.com/devillemereuil/CodePartReacnorm)[..³⁸²]**CodePartReacnorm**

730 **Acknowledgements** We are grateful to Jarrod Hadfield, Thibaut Morel-Journel, Stéphane Robin and John
731 **Stinchcombe for useful discussions and/or comments that much improved the quality of the paper.**

732 **References**

- 733 Albecker, M. A., Trussell, G. C., & Lotterhos, K. E. (2022) A novel analytical framework to quantify
734 co-gradient and countergradient variation. *Ecology Letters*, 25:(2022), 1521–1533. doi: [10.1111/ele.](https://doi.org/10.1111/ele.14020)
735 [14020](https://doi.org/10.1111/ele.14020).
- 736 Angilletta, M. J. (2009) *Thermal adaptation: a theoretical and empirical synthesis*. OUP Oxford,
737 Jan. 29, 2009. 304 pp.
- 738 Bates, D., Mächler, M., Bolker, B., & Walker, S. (2015) Fitting linear mixed-effects models using lme4.
739 *Journal of Statistical Software*, 67:(2015), 48.

³⁷⁶removed: Fourth and finally

³⁷⁷removed: Furthermore, we

³⁷⁸removed: provide a tutorial on how to use linear and non-linear modelling to analyse data at the following address:

³⁷⁹removed: github.com/devillemereuil/TutoPartReacNorm

³⁸⁰removed: . We have also

³⁸¹removed: V_{plas} , V_{Gen} and V_{A} for non-linear models as a new feature of the QGglmm R package

³⁸²removed: CodePartReacNorm

- 740 Bonamour, S., Chevin, L.-M., Charmantier, A., & Teplitsky, C. (2019) Phenotypic plasticity in re-
741 sponse to climate change: the importance of cue variation. *Philosophical Transactions of the Royal*
742 *Society B: Biological Sciences*, 374:(Mar. 18, 2019), 20180178. doi: [10.1098/rstb.2018.0178](https://doi.org/10.1098/rstb.2018.0178).
- 743 Bradshaw, A. D. (1965) Evolutionary significance of phenotypic plasticity in plants. *Advances in*
744 *Genetics*. Ed. by E. W. Caspari & J. M. Thoday. Vol. 13. Cambridge (MA, USA): Academic Press,
745 Jan. 1, 1965, pp. 115–155. doi: [10.1016/S0065-2660\(08\)60048-6](https://doi.org/10.1016/S0065-2660(08)60048-6).
- 746 Brown, G. G. & Rutenmiller, H. C. (1977) Means and variances of stochastic vector products with
747 applications to random linear models. *Management Science*, 24:(Oct. 1977), 210–216. doi: [10.](https://doi.org/10.1287/mnsc.24.2.210)
748 [1287/mnsc.24.2.210](https://doi.org/10.1287/mnsc.24.2.210).
- 749 Bürkner, P.-C. (2017) Advanced bayesian multilevel modeling with the R package brms. *ArXiv170511123*
750 *Stat*:(May 31, 2017).
- 751 Charmantier, A., McCleery, R. H., Cole, L. R., Perrins, C., Kruuk, L. E. B., & Sheldon, B. C. (2008)
752 Adaptive phenotypic plasticity in response to climate change in a wild bird population. *Science*,
753 320:(May 9, 2008), 800–803. doi: [10.1126/science.1157174](https://doi.org/10.1126/science.1157174).
- 754 Chevin, L.-M., Collins, S., & Lefèvre, F. (2013) Phenotypic plasticity and evolutionary demographic
755 responses to climate change: taking theory out to the field. *Functional Ecology*, 27:(2013), 967–979.
756 doi: [10.1111/j.1365-2435.2012.02043.x](https://doi.org/10.1111/j.1365-2435.2012.02043.x).
- 757 Chevin, L.-M., Lande, R., & Mace, G. M. (2010) Adaptation, plasticity, and extinction in a changing
758 environment: towards a predictive theory. *PLOS Biology*, 8:(Apr. 27, 2010), e1000357. doi: [10.1371/](https://doi.org/10.1371/journal.pbio.1000357)
759 [journal.pbio.1000357](https://doi.org/10.1371/journal.pbio.1000357).
- 760 de Jong, G. (1990) Quantitative genetics of reaction norms. *Journal of evolutionary biology*, 3:(1990),
761 447–468.
- 762 de Jong, G. (1995) Phenotypic plasticity as a product of selection in a variable environment. *The*
763 *American Naturalist*, 145:(Apr. 1, 1995), 493–512. doi: [10.1086/285752](https://doi.org/10.1086/285752).
- 764 de Jong, G. (1999) Unpredictable selection in a structured population leads to local genetic differen-
765 tiation in evolved reaction norms. *Journal of Evolutionary Biology*, 12:(1999), 839–851.
- 766 Des Marais, D. L., Hernandez, K. M., & Juenger, T. E. (2013) Genotype-by-environment interaction
767 and plasticity: exploring genomic responses of plants to the abiotic environment. *Annual Review of*
768 *Ecology, Evolution, and Systematics*, 44:(2013), 5–29. doi: [10.1146/annurev-ecolsys-110512-135806](https://doi.org/10.1146/annurev-ecolsys-110512-135806).
- 769 Deutsch, C. A., Tewksbury, J. J., Huey, R. B., Sheldon, K. S., Ghalambor, C. K., Haak, D. C., & Martin,
770 P. R. (2008) Impacts of climate warming on terrestrial ectotherms across latitude. *Proceedings of*
771 *the National Academy of Sciences*, 105:(May 6, 2008), 6668–6672. doi: [10.1073/pnas.0709472105](https://doi.org/10.1073/pnas.0709472105).

- 772 de Villemereuil, P. (2018) Quantitative genetic methods depending on the nature of the phenotypic
773 trait. *Annals of the New York Academy of Sciences*. The Year in Evolutionary Biology 1422:(June 1,
774 2018), 29–47. doi: [10.1111/nyas.13571](https://doi.org/10.1111/nyas.13571).
- 775 de Villemereuil, P., Morrissey, M. B., Nakagawa, S., & Schielzeth, H. (2018) Fixed-effect variance and
776 the estimation of repeatabilities and heritabilities: issues and solutions. *Journal of Evolutionary*
777 *Biology*, 31:(2018), 621–632. doi: [10.1111/jeb.13232](https://doi.org/10.1111/jeb.13232).
- 778 de Villemereuil, P., Schielzeth, H., Nakagawa, S., & Morrissey, M. B. (2016) General methods for
779 evolutionary quantitative genetic inference from generalised mixed models. *Genetics*, 204:(Nov. 1,
780 2016), 1281–1294. doi: [10.1534/genetics.115.186536](https://doi.org/10.1534/genetics.115.186536).
- 781 de Villemereuil, P. et al. (2020) Fluctuating optimum and temporally variable selection on breeding
782 date in birds and mammals. *Proceedings of the National Academy of Sciences*, 117:(2020), 31969–
783 31978. doi: [10.1073/pnas.2009003117](https://doi.org/10.1073/pnas.2009003117).
- 784 Falconer, D. S. (1952) The problem of environment and selection. *The American Naturalist*, 86:(Sept. 1,
785 1952), 293–298. doi: [10.1086/281736](https://doi.org/10.1086/281736).
- 786 Falconer, D. S. & Mackay, T. F. (1996) *Introduction to quantitative genetics*. 4th ed. Harlow, Essex
787 (UK): Benjamin Cummings, Feb. 16, 1996.
- 788 Gavrillets, S. & Scheiner, S. M. (1993a) The genetics of phenotypic plasticity. V. Evolution of reaction
789 norm shape. *Journal of Evolutionary Biology*, 6:(1993), 31–48. doi: [10.1046/j.1420-9101.1993.](https://doi.org/10.1046/j.1420-9101.1993.6010031.x)
790 [6010031.x](https://doi.org/10.1046/j.1420-9101.1993.6010031.x).
- 791 Gavrillets, S. & Scheiner, S. M. (1993b) The genetics of phenotypic plasticity. VI. Theoretical predic-
792 tions for directional selection. *Journal of Evolutionary Biology*, 6:(1993), 49–68.
- 793 Gienapp, P., Teplitsky, C., Alho, J. S., Mills, J. A., & Merilä, J. (2008) Climate change and evolution:
794 disentangling environmental and genetic responses. *Molecular Ecology*, 17:(Jan. 1, 2008), 167–178.
795 doi: [10.1111/j.1365-294X.2007.03413.x](https://doi.org/10.1111/j.1365-294X.2007.03413.x).
- 796 Gomulkiewicz, R. & Kirkpatrick, M. (1992) Quantitative genetics and the evolution of reaction norms.
797 *Evolution*, 46:(Apr. 1, 1992), 390–411. doi: [10.1111/j.1558-5646.1992.tb02047.x](https://doi.org/10.1111/j.1558-5646.1992.tb02047.x).
- 798 Hammill, E., Rogers, A., & Beckerman, A. P. (2008) Costs, benefits and the evolution of inducible
799 defences: a case study with *Daphnia pulex*. *Journal of Evolutionary Biology*, 21:(May 1, 2008),
800 705–715. doi: [10.1111/j.1420-9101.2008.01520.x](https://doi.org/10.1111/j.1420-9101.2008.01520.x).
- 801 Johnson, J. B. & Omland, K. S. (2004) Model selection in ecology and evolution. *Trends in Ecology*
802 *& Evolution*, 19:(Feb. 2004), 101–108. doi: [doi:DOI:10.1016/j.tree.2003.10.013](https://doi.org/10.1016/j.tree.2003.10.013).
- 803 Johnson, P. C. (2014) Extension of Nakagawa & Schielzeth’s R2GLMM to random slopes models.
804 *Methods in Ecology and Evolution*, 5:(Sept. 1, 2014), 944–946. doi: [10.1111/2041-210X.12225](https://doi.org/10.1111/2041-210X.12225).

- 805 King, J. G. & Hadfield, J. D. (2019) The evolution of phenotypic plasticity when environments fluctuate
806 in time and space. *Evolution Letters*, 3:(Feb. 1, 2019), 15–27. doi: [10.1002/evl3.100](https://doi.org/10.1002/evl3.100).
- 807 Kirkpatrick, M. (2009) Patterns of quantitative genetic variation in multiple dimensions. *Genetica*,
808 136:(June 1, 2009), 271–284. doi: [10.1007/s10709-008-9302-6](https://doi.org/10.1007/s10709-008-9302-6).
- 809 Kirkpatrick, M. & Heckman, N. (1989) A quantitative genetic model for growth, shape, reaction norms,
810 and other infinite-dimensional characters. *Journal of Mathematical Biology*, 27:(Aug. 1, 1989), 429–
811 450. doi: [10.1007/BF00290638](https://doi.org/10.1007/BF00290638).
- 812 Lande, R. (1979) Quantitative genetic analysis of multivariate evolution, applied to brain:body size
813 allometry. *Evolution*, 33:(1979), 402–416.
- 814 Lande, R. (2009) Adaptation to an extraordinary environment by evolution of phenotypic plasticity
815 and genetic assimilation. *Journal of Evolutionary Biology*, 22:(July 1, 2009), 1435–1446. doi: [10.1111/j.1420-9101.2009.01754.x](https://doi.org/10.1111/j.1420-9101.2009.01754.x).
- 816
- 817 Lande, R. & Arnold, S. J. (1983) The measurement of selection on correlated characters. *Evolution*,
818 37:(1983), 1210–1226. doi: [10.2307/2408842](https://doi.org/10.2307/2408842).
- 819 Landsman, Z. & Nešlehová, J. (2008) Stein’s Lemma for elliptical random vectors. *Journal of Multi-*
820 *variate Analysis*, 99:(May 1, 2008), 912–927. doi: [10.1016/j.jmva.2007.05.006](https://doi.org/10.1016/j.jmva.2007.05.006).
- 821 Landsman, Z., Vanduffel, S., & Yao, J. (2013) A note on Stein’s lemma for multivariate elliptical
822 distributions. *Journal of Statistical Planning and Inference*, 143:(Nov. 1, 2013), 2016–2022. doi:
823 [10.1016/j.jspi.2013.06.003](https://doi.org/10.1016/j.jspi.2013.06.003).
- 824 Lynch, M. & Walsh, B. (1998) *Genetics and analysis of quantitative traits*. Sunderland, Massachussets
825 (US): Sinauer Associates, 1998.
- 826 Lynch, M. & Gabriel, W. (1987) Environmental tolerance. *The American Naturalist*, 129:(Feb. 1, 1987),
827 283–303. doi: [10.1086/284635](https://doi.org/10.1086/284635).
- 828 Merilä, J. & Hendry, A. P. (2014) Climate change, adaptation, and phenotypic plasticity: the problem
829 and the evidence. *Evolutionary Applications*, 7:(2014), 1–14. doi: [10.1111/eva.12137](https://doi.org/10.1111/eva.12137).
- 830 Mitchell, D. J. & Houslay, T. M. (2021) Context-dependent trait covariances: how plasticity shapes
831 behavioral syndromes. *Behavioral Ecology*, 32:(Jan. 1, 2021), 25–29. doi: [10.1093/beheco/araa115](https://doi.org/10.1093/beheco/araa115).
- 832 Moczek & Emlen (1999) Proximate determination of male horn dimorphism in the beetle *Onthophagus*
833 *taurus* (Coleoptera: Scarabaeidae). *Journal of Evolutionary Biology*, 12:(1999), 27–37. doi: [10.1046/
834 j.1420-9101.1999.00004.x](https://doi.org/10.1046/j.1420-9101.1999.00004.x).
- 835 Morrissey, M. B. (2015) Evolutionary quantitative genetics of nonlinear developmental systems. *Evo-*
836 *lution*, 69:(Aug. 1, 2015), 2050–2066. doi: [10.1111/evo.12728](https://doi.org/10.1111/evo.12728).

- 837 Morrissey, M. B. & Liefting, M. (2016) Variation in reaction norms: Statistical considerations and
838 biological interpretation. *Evolution*, 70:(Sept. 1, 2016), 1944–1959. doi: [10.1111/evo.13003](https://doi.org/10.1111/evo.13003).
- 839 Murren, C. J., Maclean, H. J., Diamond, S. E., Steiner, U. K., Heskell, M. A., Handelsman, C. A.,
840 Ghalambor, C. K., Auld, J. R., Callahan, H. S., & Pfennig, D. W. (2014) Evolutionary change in
841 continuous reaction norms. *The American Naturalist*, 183:(2014), 453–467.
- 842 Nakagawa, S. & Schielzeth, H. (2013) A general and simple method for obtaining R² from generalized
843 linear mixed-effects models. *Methods in Ecology and Evolution*, 4:(2013), 133–142. doi: [10.1111/j.
844 2041-210x.2012.00261.x](https://doi.org/10.1111/j.2041-210x.2012.00261.x).
- 845 Narasimhan, B., Johnson, S. G., Hahn, T., Bouvier, A., & Kiêu, K. (2023) *Cubature: Adaptive multi-*
846 *variate integration over hypercubes*. manual. 2023.
- 847 Nussey, D. H., Postma, E., Gienapp, P., & Visser, M. E. (2005) Selection on heritable phenotypic
848 plasticity in a wild bird population. *Science*, 310:(Oct. 14, 2005), 304–306. doi: [10.1126/science.
849 1117004](https://doi.org/10.1126/science.1117004).
- 850 Pinheiro, J., Bates, D., DebRoy, S., Sarkar, D., & {the R Core team} (2009) *Nlme: Linear and*
851 *Nonlinear Mixed Effects Models*. 2009.
- 852 Pletcher, S. D. & Geyer, C. J. (1999) The genetic analysis of age-dependent traits: modeling the
853 character process. *Genetics*, 153:(Oct. 1, 1999), 825–835. doi: [10.1093/genetics/153.2.825](https://doi.org/10.1093/genetics/153.2.825).
- 854 Reed, T. E., Waples, R. S., Schindler, D. E., Hard, J. J., & Kinnison, M. T. (2010) Phenotypic plasticity
855 and population viability: the importance of environmental predictability. *Proceedings of the Royal*
856 *Society B: Biological Sciences*, 277:(Nov. 22, 2010), 3391–3400. doi: [10.1098/rspb.2010.0771](https://doi.org/10.1098/rspb.2010.0771).
- 857 Rice, S. H. (2004) *Evolutionary Theory: Mathematical and Conceptual Foundations*. Sinauer, Sept. 1,
858 2004. 348 pp.
- 859 Robertson, A. (1966) A mathematical model of the culling process in dairy cattle. *Animal Science*,
860 8:(1966), 95–108. doi: [10.1017/S0003356100037752](https://doi.org/10.1017/S0003356100037752).
- 861 Rovelli, G. et al. (2020) The genetics of phenotypic plasticity in livestock in the era of climate change:
862 a review. *Italian Journal of Animal Science*, 19:(Dec. 14, 2020), 997–1014. doi: [10.1080/1828051X.
863 2020.1809540](https://doi.org/10.1080/1828051X.2020.1809540).
- 864 Schaum, C. E. & Collins, S. (2014) Plasticity predicts evolution in a marine alga. *Proceedings of the*
865 *Royal Society B: Biological Sciences*, 281:(Oct. 22, 2014), 20141486. doi: [10.1098/rspb.2014.1486](https://doi.org/10.1098/rspb.2014.1486).
- 866 Scheiner, S. M. (1993a) Genetics and evolution of phenotypic plasticity. *Annual Review of Ecology and*
867 *Systematics*, 24:(Nov. 1993), 35–68. doi: [10.1146/annurev.es.24.110193.000343](https://doi.org/10.1146/annurev.es.24.110193.000343).
- 868 Scheiner, S. M. (1993b) Plasticity as a selectable trait: reply to Via. *The American Naturalist*, 142:(Aug. 1,
869 1993), 371–373. doi: [10.1086/285544](https://doi.org/10.1086/285544).

- 870 Scheiner, S. M. & Lyman, R. F. (1989) The genetics of phenotypic plasticity I. Heritability. *Journal*
871 *of Evolutionary Biology*, 2:(Mar. 1989), 95–107. doi: [10.1046/j.1420-9101.1989.2020095.x](https://doi.org/10.1046/j.1420-9101.1989.2020095.x).
- 872 Schlichting, C. D. & Pigliucci, M. (1998) Phenotypic evolution: a reaction norm perspective. *Pheno-*
873 *typic evolution: a reaction norm perspective.*:(1998).
- 874 Stinchcombe, J. R., Function-valued Traits Working Group, & Kirkpatrick, M. (2012) Genetics and
875 evolution of function-valued traits: understanding environmentally responsive phenotypes. *Trends*
876 *in Ecology & Evolution*, 27:(Nov. 1, 2012), 637–647. doi: [10.1016/j.tree.2012.07.002](https://doi.org/10.1016/j.tree.2012.07.002).
- 877 Stirling, G. & Roff, D. A. (2000) Behaviour plasticity without learning: phenotypic and genetic vari-
878 ation of naïve *Daphnia* in an ecological trade-off. *Animal Behaviour*, 59:(May 1, 2000), 929–941.
879 doi: [10.1006/anbe.1999.1386](https://doi.org/10.1006/anbe.1999.1386).
- 880 Suzuki, Y. & Nijhout, H. F. (2006) Evolution of a polyphenism by genetic accommodation. *Science*,
881 311:(Feb. 3, 2006), 650–652. doi: [10.1126/science.1118888](https://doi.org/10.1126/science.1118888).
- 882 Teplitsky, C., Mills, J. A., Alho, J. S., Yarrall, J. W., & Merilä, J. (2008) Bergmann’s rule and climate
883 change revisited: Disentangling environmental and genetic responses in a wild bird population.
884 *Proceedings of the National Academy of Sciences*, 105:(Sept. 9, 2008), 13492–13496. doi: [10.1073/
885 pnas.0800999105](https://doi.org/10.1073/pnas.0800999105).
- 886 Tredennick, A. T., Hooker, G., Ellner, S. P., & Adler, P. B. (2021) A practical guide to selecting
887 models for exploration, inference, and prediction in ecology. *Ecology*, 102:(2021), e03336. doi: [10.
888 1002/ecy.3336](https://doi.org/10.1002/ecy.3336).
- 889 Tufto, J. (2000) The evolution of plasticity and nonplastic spatial and temporal adaptations in the
890 presence of imperfect environmental cues. *The American Naturalist*, 156:(Aug. 1, 2000), 121–130.
891 doi: [10.1086/303381](https://doi.org/10.1086/303381).
- 892 Tufto, J. (2015) Genetic evolution, plasticity, and bet-hedging as adaptive responses to temporally
893 autocorrelated fluctuating selection: A quantitative genetic model. *Evolution*, 69:(2015), 2034–
894 2049. doi: [10.1111/evo.12716](https://doi.org/10.1111/evo.12716).
- 895 Vedder, O., Bouwhuis, S., & Sheldon, B. C. (2013) Quantitative assessment of the importance of
896 phenotypic plasticity in adaptation to climate change in wild bird populations. *PLOS Biology*,
897 11:(2013), e1001605. doi: [10.1371/journal.pbio.1001605](https://doi.org/10.1371/journal.pbio.1001605).
- 898 Via, S. & Lande, R. (1985) Genotype-environment interaction and the evolution of phenotypic plas-
899 ticity. *Evolution*, 39:(May 1, 1985), 505–522. doi: [10.1111/j.1558-5646.1985.tb00391.x](https://doi.org/10.1111/j.1558-5646.1985.tb00391.x).
- 900 Wilson, A. J., Réale, D., Clements, M. N., Morrissey, M. M., Postma, E., Walling, C. A., Kruuk,
901 L. E. B., & Nussey, D. H. (2010) An ecologist’s guide to the animal model. *Journal of Animal*
902 *Ecology*, 79:(Jan. 2010), 13–26. doi: [10.1111/j.1365-2656.2009.01639.x](https://doi.org/10.1111/j.1365-2656.2009.01639.x).

903 Woltereck, R. (1909) Weitere experimentelle Untersuchungen über Artveränderung, speziell über das
904 Wesen quantitativer Artunterschiede bei Daphniden. *Verh. D. Tsch. Zool. Ges.*, 1909:(1909), 110–
905 172.

Appendix

A [..³⁸³] A unified formalism for the curve-parameters and character-state approaches

[..³⁸⁴]

[..³⁸⁵][..³⁸⁶] Despite having different mechanics, the curve-parameter and character-state approaches can be shown to be mathematically equivalent de Jong (1995). We can use this to express both approaches under the same, unified formalism. More precisely, we can express the character-state approach as being a special case of the curve-parameters approach. Under a curve-parameters approach, the [..³⁸⁷] reaction norm is seen as a function f of the environment ε and a vector of parameters θ_g :

$$\hat{z} = f(\varepsilon, \theta_g). \quad (\text{S1})$$

The θ_g 's covary across genotypes with a variance-covariance matrix \mathbf{G}_θ :

$$\theta_g \sim \mathcal{N}(\bar{\theta}, \mathbf{G}_\theta). \quad (\text{S2})$$

By contrast, in a [..³⁸⁸][..³⁸⁹][..³⁹⁰]

[..³⁹¹]

³⁸³removed: Comparison between alternative variance partitionings

³⁸⁴removed: A schematic example

³⁸⁵removed: To illustrate the difference between the variance partitioning in

³⁸⁶removed: and

³⁸⁷removed: ‘classical’ variance partitioning between V_G , V_E and $V_{G \times E}$, we will first consider a very schematic example.

Let us consider two scenarios with 3 genotypes in 2 environments. For now, we will consider the environmental variable is mean-centered, so that the zero for the environment is exactly at mid-value between the two environments. In the first scenario, all of the reaction norms are parallel between each genotype, such that this is

³⁸⁸removed: typical case where there is no genotype-by-environment interaction (

³⁸⁹removed: , left panel). In the second scenario, we invert the values of the most extremes genotypes in the second environment, so that the reaction norms are now crossing with considerable genotype-by-environment interaction (

³⁹⁰removed: , right panel). An interesting feature of such scenarios is that, since we only reassigned values to different genotypes, we conserved the genetic variance within each environments. Note that the reaction norms are directly considered here, so that V_{Res} is ignored in this section. Also, in the second scenario, since all reaction norms cross exactly at the mid-point between environments, there is no variation in the intercept.

³⁹¹removed: Two different scenarios with the same total variance. On the left: all reaction norms are parallel, so that $V_{G \times E} = 0$, by definition. On the right, the two extreme values on the second environment were switched, resulting in the crossing of reaction norms and thus substantial $V_{G \times E}$, at the full expanse of V_G . Our variance partition in V_{Plas} and V_{Gen} is equal in both scenarios, however, the γ -decomposition (where a stands for the intercept and b for the slope) of the genetic variance V_{Gen} is completely different, reflecting the (co)variation of the intercept and slope of reaction norms on the second scenario (right).

918 [..³⁹²] [..³⁹³] character-state approach, the [..³⁹⁴] [..³⁹⁵] [..³⁹⁶]
 919 [..³⁹⁷] reaction norm values of different genotypes across environments are directly provided by sampling
 920 from a multivariate normal distribution:

$$\hat{\mathbf{z}} \sim \mathcal{N}(\boldsymbol{\mu}, \mathbf{G}_z). \quad (\text{S3})$$

921 One way to express the character-state using the same formalism as the curve-parameter is to recognise
 922 that Equation S3 can be written as

$$\begin{aligned} \hat{z} &= \boldsymbol{\mu}_g^T \mathbf{u}_k, \\ \boldsymbol{\mu}_g &\sim \mathcal{N}(\boldsymbol{\mu}, \mathbf{G}_z), \end{aligned} \quad (\text{S4})$$

923 where \mathbf{u}_k is the unit vector with 1 [..³⁹⁸] at the k th value (corresponding to environment ε_k) and 0
 924 elsewhere. Thus, the character-state model can be expressed using the formalism of Equation S1 and
 925 Equation S2, where $\boldsymbol{\mu}_g$ in Equation S4 plays the role of $\boldsymbol{\theta}_g$, and thus \mathbf{G}_z plays the role of \mathbf{G}_θ . In this
 926 case, the function f is a function taking the level k of the environment and [..³⁹⁹] the parameters $\boldsymbol{\mu}_g$ of
 927 the genotype g as input, and [..⁴⁰⁰] yielding the evaluated reaction norm \hat{z} as the output. Evidently, this
 928 function f is not continuous and not differentiable along the (categorical) environment.

929 [..⁴⁰¹] However, it is a continuous, differentiable and even linear function along the (continuous)
 930 parameters $\boldsymbol{\mu}_g$. As such, all properties mentioned in the main text and the Appendices pertaining to
 931 reaction norms that are “linear in its parameters” also apply to the character-state approach. [..⁴⁰²]

³⁹²removed: In the first scenario, since all reaction norms are parallel we have $V_{G \times E} = 0$, and there is a perfect correspondence between terms in both partitionings, with that $V_{\text{Plas}} = V_E$ and $V_{\text{Gen}} = V_G$ (

³⁹³removed: , left and center). All of the genetic variance in the trait comes from variation in the intercept of reaction norms, which is reflected by

³⁹⁴removed: γ -decomposition from

³⁹⁵removed: (

³⁹⁶removed: , left).

³⁹⁷removed: In contrast in the second scenario, all genotypes have the same mean phenotype averaged across environments, leading to $V_G = 0$ in the classical partitioning. However, V_{Gen} is not zero, and is in fact exactly equal to that in the first scenario, in this example. In other words, both scenarios lead to the same amount of genetic variation available for responding to selection across the two environments where phenotypes have been measured. The only thing that differs between these scenarios is the constraints they impose on evolution of reaction norms. Scenario

³⁹⁸removed: facilitates responses to phenotypic selection that goes in the same direction in both environments, while scenario 2 facilitates responses to selection in opposite directions across environments. Although the value for V_{Gen} is unchanged, these constraints are adequately reflected by the γ -decomposition of V_{Gen} , for which we now have $\gamma_a = 0$

³⁹⁹removed: $\gamma_b = 1$. Note that in this scenario, we instead have $V_{\text{Plas}} = V_E$

⁴⁰⁰removed: $V_{\text{Gen}} = V_{G \times E}$

⁴⁰¹removed: As a final note on this example, let us imagine that, instead of choosing the mid-point between environments as reference (set to zero), we choose the first environment

⁴⁰²removed: In this case, the intercept is defined in this first environment, and there is now considerable variation in the intercept. Such arbitrary choice has no impact on the values of neither V_{Plas} and V_{Gen} , nor on V_G , V_E and $V_{G \times E}$. However, this new definition of the intercept and its variation leads to a different γ -decomposition: $\gamma_a = 1$, $\gamma_b = 4$ and $\gamma_{ab} = -4$. In other words, redefining the zero in the scale of the environment changed the definition of the parameter “intercept”, and made apparent the negative genetic correlation between the intercept and slope (a perfect one in this scenario), whereby steeper negative slopes are associated with higher intercept (phenotype in environment 1). Nevertheless, the evolutionary dynamics are not sensitive to the arbitrary choice of a zero in the environmental scale, as the distribution of genetic variation along environments is the same in both versions of the second scenario.

932 [..⁴⁰³]

933 [..⁴⁰⁴]

934 [..⁴⁰⁵][..⁴⁰⁶][..⁴⁰⁷]

935 [..⁴⁰⁸][..⁴⁰⁹]

936 B Computation of the additive genetic variance holding 937 environment constant

938 B1 Preliminary results

939 **Multiple regression** [..⁴¹⁰]slopes expressed using a **variance-covariance matrix** Let us assume a
940 multiple regression between a random variable y and a [..⁴¹¹]set of random variables $\mathbf{x} = (x_1, \dots, x_n)^T$
941 such that:

$$y = \mu + \mathbf{x}^T \beta + e, \quad (\text{S5})$$

942 where μ is the intercept and e is the residual of the model. Note that in practical regression, the
943 realised sampling of \mathbf{x} will be contained in the design matrix of the model. If it exists and is unique,
944 the solution for [..⁴¹²]the vector of multiple regression slopes β can be formulated in terms variance-
945 covariance matrices (see e.g. p.179, Lynch & Walsh 1998):

$$\beta = \mathbf{V}(\mathbf{x})^{-1} \text{cov}(\mathbf{x}, y), \quad (\text{S6})$$

⁴⁰³removed: General comparison

⁴⁰⁴removed: This example illustrates how our variance partitioning differs from the classical one with genotype, environment, and genotype-by-environment interaction effects.

⁴⁰⁵removed: In particular, there is no distinction between V_G and $V_{G \times E}$ in our partitioning, as $V_{\text{Gen}} = V_G + V_{G \times E}$. This is due to our use of the total variance, which integrates over genotypes in each environment, before integrating over environments. However, this does not mean that our framework is degenerate and loses information on how genetic variance is distributed across environments, and how this constrains evolution of reaction norm shape. Instead, these aspects are captured by two things. The first is the γ -decomposition in

⁴⁰⁶removed: , which provides an explicit measure of genetic variation in different components of reaction norm shape. The second is the environment-specific amount of genetic variance, as detailed in our worked example of non-linear reaction norm models (

⁴⁰⁷removed:).

⁴⁰⁸removed: Regarding the environmental variance V_E and V_{Plas} , there were considered equal on our example, but this is because we considered directly the reaction norms, and thus ignored V_{Res} . In many contexts, we can consider V_{Plas} and V_{Res} as respectively measuring the *general* (environment shared by a group of individuals) and *specific* (environment-specific to an individual) environmental variance as defined by Falconer

⁴⁰⁹removed: . A complication is that, in reality, V_{Plas} is not defined relative to groups of individuals (or genotype), but rather to a singled-out environmental variable. In that regard, V_{Res} contains the part of what could be considered the general environment, which results from the influence of other environmental variable. In any case, if no distinction is made between general and specific environment components in V_E and the phenotypic trait is under consideration rather than reaction norms themselves, then we can write $V_E = V_{\text{Plas}} + V_{\text{Res}}$.

⁴¹⁰removed: from

⁴¹¹removed: series a random variables $\mathbf{x} = (x_1, \dots, x_n)$

⁴¹²removed: β

946 where $\mathbf{V}(\mathbf{x})$ is the variance-covariance matrix of \mathbf{x} , $\mathbf{V}(\mathbf{x})^{-1}$ is its inverse matrix and $\text{cov}(\mathbf{x}, y)$ is the
 947 column-vector of covariances between the x_i and y .

948 **Multivariate version of Stein's lemma** Let us assume that $\mathbf{x} = (x_1, \dots, x_{p_x})$ and
 949 $\mathbf{y} = (y_1, \dots, y_{p_y})$ follow multivariate normal distributions, and that g is a differentiable, $R^{p_x} \rightarrow R$
 950 function such that $E(\nabla g)$, where ∇g is the gradient of g (the vector of partial derivatives), is
 951 a vector with finite values, then it can be shown (Landsman & Nešlehová 2008; Landsman et al.
 952 2013) that:

$$\text{cov}(g(\mathbf{x}), \mathbf{y}) = \text{cov}(\mathbf{x}, \mathbf{y})E(\nabla g). \quad (\text{S7})$$

953 Note that covariance matrices of vectors (also known as cross-covariance matrices) are not commutative,
 954 but are such that $\text{cov}(\mathbf{x}, \mathbf{y}) = \text{cov}(\mathbf{y}, \mathbf{x})^T$. In the case where $p_y = 1$, then $\mathbf{y} = y$ follows a normal
 955 distribution and:

$$\text{cov}(g(\mathbf{x}), y) = \text{cov}(y, \mathbf{x})E(\nabla g). \quad (\text{S8})$$

956 Note that $\text{cov}(y, \mathbf{x})$ is a row-vector and $\text{cov}(\mathbf{x}, y)$ is a column-vector by convention.

957 B2 Breeding values in a given environment

958 Genetics of reaction norms As mentioned in the main text, a general formalism (including
 959 the character-state as a special case) for the reaction norm \hat{z} is given by Equation 3 in the main text, i.e.

$$\hat{z} = f(\varepsilon, \boldsymbol{\theta}_g). \quad (\text{S9})$$

960 The phenotype predicted by the reaction norm \hat{z} thus depends on the environmental value ε , and the
 961 reaction norm parameters $\boldsymbol{\theta}_g$ specific to the genotype g . When holding the environment ε constant, the
 962 genetic variance is simply the variance of reaction norms across genotypes:

$$V_{G|\varepsilon} = V_{g|\varepsilon}(f(\varepsilon, \boldsymbol{\theta}_g)) \quad (\text{S10})$$

963 If the reaction norms are estimated in such a way that non-additive genetic variance can be separated
 964 out from additive genetic variance (e.g. if "genotype" refers to individuals) or are known to be

⁴¹³removed: $\mathbf{y} = (x_1, \dots, x_{p_y})$ follows a multivariate normal distribution, that

⁴¹⁴removed: follows a multivariate normal distribution

⁴¹⁵removed: $R^{p_x} \rightarrow R$

⁴¹⁶removed: differentials

⁴¹⁷removed: of

⁴¹⁹removed: The

⁴²⁰removed: V_A is the variance

negligible on the one hand; and if the reaction norm is linear in its parameters (i.e. f is a linear function of θ_g , as for a polynomial function) on the other hand, then the additive genetic variance conditional on the environment is readily given by Equation S10, i.e. $V_{A|\varepsilon} = V_{G|\varepsilon}$. In the case where f is not linear in its parameters, it is necessary to rely on the theory in non-linear quantitative genetics (Morrissey 2015; de Villemereuil et al. 2016), as we do below.

Linear relationship between breeding values The relationship between the breeding value of the trait \mathcal{A}_z and the breeding values of the ^[.421]reaction norm parameters θ_g is the key towards developing a framework that works for any reaction norm, linear in its parameters or not. Let us note ^[.422] \mathcal{A}_θ the vector of breeding values of all the parameters in θ . We will follow the same demonstration as in de Villemereuil et al. (2016), which starts from the point that, by definition, breeding values are ^[.423]all linked through linear relationships (see also Robertson 1966), since they are all linearly linked to the genotype (Lynch & Walsh 1998). More precisely, the breeding value ^[.424] \mathcal{A}_z of the phenotypic trait z of an individual ^[.425]linearly depends on a linear combination of ^[.426]its breeding values for the reaction norm parameters \mathcal{A}_θ , so that:

$$\sup[.427]\mathcal{A}_z\sup[.428] = \mu\sup[.429]\mathcal{A} + \mathcal{A}_\theta^T \psi\sup[.430] \quad (\text{S11})$$

where ^[.431] μ_a is a constant chosen such that $E(\mathcal{A}_z) = 0$, ψ ^[.432]is a vector of slopes that we will shortly describe as the reaction norm gradient.

Derivation of ψ To derive an expression of ψ , we can apply the results in Equation S6 to Equation S11, yielding

$$\psi = \mathbf{G}_\theta^{-1} \text{cov}(\mathcal{A}_\theta, \hat{z}). \quad (\text{S12})$$

This assumes that $\text{cov}(\mathcal{A}_\theta, \mathcal{A}_z) = \text{cov}(\mathcal{A}_\theta, \hat{z})$, i.e. that there is no covariance between the environmental values of the phenotype as predicted by the reaction norm and the breeding values of the parameters. This results also assumes that \mathbf{G}_θ is invertible. However, such assumption is already necessary to most statistical algorithms available to infer \mathbf{G}_θ in practice, so that this assumption is not limiting here. Noting

⁴²¹removed: breeding values a_z of the phenotypic trait z

⁴²²removed: $a_{\theta,i}$ as the breeding value of the parameter θ_i . Here, we will assume that we are working within a given (and fixed) environment ε .

⁴²³removed: linked through a linear relationship

⁴²⁴removed: the trait a_z

⁴²⁵removed: linearly

⁴²⁶removed: the breeding values of the parameters $a_{\theta,i}$ of the same individual

⁴³¹removed: e is the residual variance of the regression (assumed independent of the breeding values)

⁴³²removed: is a vector containing the slopes and \mathbf{a}_θ is a vector containing the breeding values for all parameters

987 that $\hat{z} = f(\varepsilon, \theta)$, we can apply the multivariate version of Stein's lemma (Equation S7):

$$\psi = \mathbf{G}_\theta^{-1} \text{cov}(\mathcal{A}_\theta, \theta_g) \mathbf{E}(\nabla_\theta f) = \mathbf{G}_\theta^{-1} \mathbf{G}_\theta \mathbf{E}(\nabla_\theta f) = \mathbf{E}(\nabla_\theta f), \quad (\text{S13})$$

988 where we have used the fact that the covariance of breeding values of reaction norm parameters with their
 989 breeding values is their additive genetic covariance matrix \mathbf{G}_θ . Again, note that this assumes that f is
 990 partially differentiable with respect to all elements of θ_g . Given that this demonstration was applied when
 991 holding the environment constant, the values in ψ generally depend on the environment ε , so below and
 992 in the main text, we use the notation ψ_ε .

993 Values of ψ_ε in specific contexts When the reaction norm is linear in its parameters, the values in
 994 ψ_ε are (trivially) the linear coefficients of such relation. For a quadratic reaction norm, where $\hat{z} =$
 995 $(\bar{A} + a_g) + (\bar{b} + b_g)\varepsilon + (\bar{c} + c_g)\varepsilon^2$, such linear coefficients are respectively 1, ε and ε^2 for a_g , b_g and c_g . It
 996 results that $\psi_\varepsilon = (1, \varepsilon, \varepsilon^2)^T$ as mentioned in the main text. More generally, if f is a polynomial of order
 997 N , then $\psi_\varepsilon = (1, \varepsilon, \dots, \varepsilon^N)^T$. In the context of a character-state, it can be seen from Equation S4 that
 998 the gradient ψ_ε in the parameters will be equal to \mathbf{u}_k , i.e. a vector of 1 for the k th value (corresponding
 999 to the environment chosen to be hold constant) and 0 elsewhere.

1000 B3 Additive genetic variance

1001 By definition, the additive genetic variance of the trait conditional on the environment $V_{A|\varepsilon}$ is the variance
 1002 of the breeding values defined in Equation S11. We can thus express it from the breeding values of the
 1003 reaction norm parameters (right hand side of Equation S11) as

$$V_{A|\varepsilon} = V_{\mathbf{g}|\varepsilon}(\mathcal{A}_\theta^T \psi_\varepsilon) = \psi_\varepsilon^T \mathbf{G}_\theta \psi_\varepsilon. \quad (\text{S14})$$

1004 This formula holds whether the reaction norm is linear on its parameters or not, and also holds for the
 1005 character-state approach (although in this case, this formula merely selects the k th element of the diagonal
 1006 of \mathbf{G}_z).

1007 [..⁴³³] [..⁴³⁴] [..⁴³⁵] [..⁴³⁶]

⁴³³removed: Defining the value of ψ

⁴³⁴removed: To compute the value of ψ , we can solve the linear equation in

⁴³⁵removed: using

⁴³⁶removed: :

1008 **C** Derivation of the general decomposition of variance

1009 **C1** Distinguishing between V_{Plas} , V_{Gen} and V_{Add}

1010 The phenotype predicted by the reaction norm \hat{z} depends on the environment, and the reaction norm
1011 parameters θ_g specific to the genotype g . The impacts of environment and genotype are intricately related
1012 via the reaction norm shape, but in a given environment, one can still isolate the average impact of the
1013 environment from variation among genotypes by computing the average value of the reaction norm across
1014 genotypes conditional on the environment, i.e. $E_{g|\varepsilon}(\hat{z})$. The variance of $E_{g|\varepsilon}(\hat{z})$, taken across environments,
1015 is the component $V_{\text{Plas}} = V(E_{g|\varepsilon}(\hat{z}))$ in the main text, i.e. the phenotypic variance arising from plasticity
1016 after averaging across genotypes. The genotypic value \mathcal{G}_z of genotype g within the environment ε is then
1017 given by

$$\mathcal{G}_z = \hat{z} - E_{g|\varepsilon}(\hat{z}). \quad (\text{S15})$$

1018 Note that, although we removed the average effect of the environment, the genotypic value \mathcal{G}_z still depends
1019 on both the genotype g and the environment ε , because genotypes can vary in their response to the
1020 environment. The total genetic variance in the reaction norm is thus $V_{\text{Gen}} = V(\mathcal{G}_z)$. It is possible to get
1021 to the breeding values of the trait in each environment \mathcal{A}_z following the process described in [Appendix B](#),
1022 i.e. $\mathcal{A}_z = \mu_a + \mathcal{A}_\theta^T \psi_\varepsilon$. The total additive genetic variance in the reaction norm is then

$$V_{\text{Add}} = V(\mathcal{A}_z) = E(V_{g|\varepsilon}(\mathcal{A}_z)) + V(E_{g|\varepsilon}(\mathcal{A}_z)) = E(\psi_\varepsilon^T \mathbf{G}_\theta \psi_\varepsilon), \quad (\text{S16})$$

1023 using the law of total variance and noting that $E_{g|\varepsilon}(\mathcal{A}_z) = 0$ by construction. In [Figure 1](#) in the main text,
1024 the average $E_{g|\varepsilon}(\hat{z})$ corresponds to the red line in the left panel of [Figure 1](#) in the main text, while
1025 \mathcal{A}_z corresponds to the purple lines in the middle panel.

1026 **C2** Distinguishing between V_{Add} , V_{A} and $V_{\text{A} \times \text{E}}$

1027 We can separate the total additive genetic variance of the reaction norm, V_{Add} , into two components: the
1028 marginal additive genetic variance of the trait V_{A} and the additive genetic variance of plasticity $V_{\text{A} \times \text{E}}$. The
1029 first component is given by considering, for a given genotype, its average breeding value across environment:

$$[\dots^{437}] \bar{\mathcal{A}} = [\dots^{438}] E_{e|g}([\dots^{439}] \mathcal{A}_z). \quad (\text{S17})$$

1031 [⁴⁴⁰][⁴⁴¹] This average corresponds to the breeding value that would be predicted for the same genotype
 1032 present in all environments (or moving across them, being measured several times), ignoring the impact
 1033 of the environment. In other words, this average is the predicted breeding value after the impact of the
 1034 environment has been marginalised. Graphically, it depicts the average shift in the y -axis of the reaction
 1035 norm, as can be seen in the middle panel of Figure 1 in the main text. The marginal additive genetic
 1036 variance of the trait is

$$V_A = V(\bar{\mathcal{A}}) = \mathbf{E}(\boldsymbol{\psi}_\varepsilon)^\top \mathbf{G}_\theta \mathbf{E}(\boldsymbol{\psi}_\varepsilon) \quad (\text{S18})$$

1037 The remaining additive genetic variation after accounting for the marginal breeding value is linked to the
 1038 impact of genetic variation in plasticity, arising from genotype-by-environment interactions. We can define
 1039 the part of the breeding values strictly linked to that genotype-by-environment interaction by mean-centring
 1040 the breeding values, for each genotype:

$$\mathcal{A}_I = \mathcal{A}_z - \bar{\mathcal{A}}. \quad (\text{S19})$$

1041 The right panel of Figure 1 depicts these interaction breeding values. The additive genetic variance linked
 1042 to genotype-by-environment, and thus to variation in plasticity, is:

$$V_{A \times E} = V(\mathcal{A}_I) = V(\mathcal{A}_z) + V(\bar{\mathcal{A}}) - 2\text{cov}(\mathcal{A}_z, \bar{\mathcal{A}}) = V(\mathcal{A}_z) - V(\bar{\mathcal{A}}) = V_{\text{Add}} - V_A, \quad (\text{S20})$$

1043 noting that, by construction, $\text{cov}(\mathcal{A}_z, \bar{\mathcal{A}}) = \text{cov}(\bar{\mathcal{A}}, \bar{\mathcal{A}}) = V(\bar{\mathcal{A}})$. By substituting V_{Add} and V_A with their
 1044 values in Equation S16 and Equation S18, we obtain

$$V_{A \times E} = \mathbf{E}(\boldsymbol{\psi}_\varepsilon^\top \mathbf{G}_\theta \boldsymbol{\psi}_\varepsilon) - \mathbf{E}(\boldsymbol{\psi}_\varepsilon)^\top \mathbf{G}_\theta \mathbf{E}(\boldsymbol{\psi}_\varepsilon) = \text{tr}(\boldsymbol{\Psi} \mathbf{G}_\theta) = \sum_{l,k} \Psi_{l,k} \mathbf{G}_{\theta(l,k)}, \quad (\text{S21})$$

1045 where $\boldsymbol{\Psi}$ is the variance-covariance matrix of the reaction norm gradient $\boldsymbol{\psi}_\varepsilon$ across the environment. In
 1046 other words, $V_{A \times E}$ is the sum of the products, for all pairs of parameters, of the (co)variance in the
 1047 reaction norm gradient and the additive genetic (co)variance. The γ - and ι -decomposition directly comes
 1048 from dividing each elements of the sums in Equation S16 and Equation S21 respectively by V_{Add} and
 1049 $V_{A \times E}$, so that the total sums to 1.

1050 C3 Variance decomposition for a polynomial model

⁴⁴⁰removed: Noting that $z = f(\varepsilon, \boldsymbol{\theta})$, we can apply the multivariate version of Stein's lemma (
⁴⁴¹removed:) :

1051 In this section, we will assume a polynomial reaction norm:

$$\hat{z} = \sum_{n=0}^N (\bar{\theta}_n + \theta_{n,g}) \varepsilon^n \quad (\text{S22})$$

1052 where $\theta_n = \bar{\theta}_n + \theta_{n,g}$ is the n th order coefficient of the polynomial. In this form, it is easy to remark that
 1053 polynomial reaction norms are linear in their parameters, i.e. there is a linear relationship between the θ_n 's
 1054 and \hat{z} , so that $\mathcal{G}_z = \mathcal{A}_z$. It results that:

$$\mathcal{G}_z = \mathcal{A}_z = \hat{z} - E_{g|\varepsilon}(\hat{z}) = \sum_{n=0}^N (\bar{\theta}_n + \theta_{n,g}) \varepsilon^n - \sum_{n=0}^N \bar{\theta}_n \varepsilon^n = \sum_{n=0}^N \theta_{n,g} \varepsilon^n. \quad (\text{S23})$$

1055 Taking the derivative of this expression with respect to each of $\theta_{n,g}$ in a given environment ε would yield
 1056 a reaction norm gradient equal to the value of each exponent of ε , i.e. $\psi_\varepsilon = (1, \varepsilon, \dots, \varepsilon^N)^T$. The total
 1057 (additive) genetic variance is thus:

$$[\dots] V_{\text{Gen}} = [\dots] V_{\text{Add}} = E([\dots] \psi_\varepsilon^T \mathbf{G}_\theta [\dots] \psi_\varepsilon) = [\dots] \sum_n V_n E([\dots] \varepsilon^{2n}) [\dots] + 2 \sum_{n < m} C_{nm} E([\dots] \varepsilon^{n+m}) [\dots] \quad (\text{S24})$$

1058 $[\dots]$ where V_n is the additive genetic variance for $\theta_{n,g}$ and C_{nm} is the additive genetic
 1059 covariance between $\theta_{m,g}$ and $\theta_{n,g}$. For the quadratic case, if ε has been mean-centred and is symmetrical,
 1060 we have $E(\varepsilon) = E(\varepsilon^3) = 0$ and the expression reduces to

$$V_{\text{Gen}} = V_{\text{Add}} = V_0 + (V_1 + C_{03})E(\varepsilon^2) + V_3E(\varepsilon^4). \quad (\text{S25})$$

1061 For a given genotype, its average breeding value across environments is

$$\bar{\mathcal{A}} = E_{\varepsilon|g}(\mathcal{A}_z) = E_{\varepsilon|g} \left(\sum_{n=0}^N \theta_{n,g} \varepsilon^n \right) = \sum_{n=0}^N \theta_{n,g} E(\varepsilon^n) \quad (\text{S26})$$

1062 The marginal (additive) genetic variance of the trait $[\dots]$ is

$$V_G = V_A = E(\psi_\varepsilon)^T \mathbf{G}_\theta E(\psi_\varepsilon) = \sum_n V_n E(\varepsilon^n)^2 + 2 \sum_{n < m} C_{nm} E(\varepsilon^n) E(\varepsilon^m) \quad (\text{S27})$$

⁴⁵³removed: Additive genetic variance

⁴⁵⁴removed: From

⁴⁵⁵removed: , the additive

⁴⁵⁶removed: V_A is given by:

1063 For the quadratic case with mean-centred and symmetrical ε , this yields:

$$V_A = [..^{457}]V_0 + 2C_{02}E([..^{458}][..^{459}]\varepsilon^2)[..^{460}][..^{461}][..^{462}] + V_2E(\varepsilon^2)^2 \quad (\text{S28})$$

1064 [$..^{463}$] Finally, the additive genetic variance in plasticity itself is

$$V_{A \times E} = V_{\text{Add}} - V_A = \sum_n V_n E(\varepsilon^{2n}) + 2 \sum_{n < m} C_{nm} E(\varepsilon^{n+m}) - \sum_n V_n E(\varepsilon^n)^2 + 2 \sum_{n < m} C_{nm} E(\varepsilon^n) E(\varepsilon^m). \quad (\text{S29})$$

1065 By recognising that $V(\varepsilon^n) = E(\varepsilon^{2n}) - E(\varepsilon^n)^2$ and [$..^{464}$] $\text{cov}(\varepsilon^n, \varepsilon^m) = E(\varepsilon^{n+m}) - E(\varepsilon^n)E(\varepsilon^m)$, we can
1066 further simplify this expression as:

$$V_{A \times E} = \sum_n V_n V(\varepsilon^n) + 2 \sum_{lk} C_{nm} \text{cov}(\varepsilon^n, \varepsilon^m). \quad (\text{S30})$$

1067 For the quadratic case, for a mean-centred and symmetrical ε , all the covariances between the different
1068 exponents of ε are 0, yielding

$$V_{A \times E} = V_1 V(\varepsilon) + V_2 V(\varepsilon^2). \quad (\text{S31})$$

1069 **C4** Variance decomposition for the character-state approach

1070 As mentioned in [Appendix A](#), the character-state can be written using a function f such that in environ-
1071 ment ε_k and for genotype g , we have

$$\hat{z} = f(\boldsymbol{\mu}_g, \varepsilon_k) = \boldsymbol{\mu}_g^T \mathbf{u}_k. \quad (\text{S32})$$

1072 In a given environment ε_k , the unit vector \mathbf{u}_k is equal to 1 at the k th index and 0 elsewhere. The reaction
1073 norm gradient is equal to this unit vector, i.e. $\boldsymbol{\psi}_{\varepsilon_k} = \mathbf{u}_k$. In the first environment, for example, we have
1074 $\boldsymbol{\psi}_{\varepsilon_1} = \mathbf{u}_1 = (1, 0, \dots)^T$. As mentioned in [Appendix A](#), the character-state approach is linear in its
1075 parameters. We can thus compute the genotypic/breeding values in a given environment ε_k as

$$\mathcal{G}_z = \mathcal{A}_z = \hat{z} - E_{g|\varepsilon}(\hat{z}) = \boldsymbol{\mu}_g^T \mathbf{u}_k - \boldsymbol{\mu}^T \mathbf{u}_k = \mu_{g,k} - \mu_j, \quad (\text{S33})$$

⁴⁶³removed: We worked at a given environment,

⁴⁶⁴removed: to reflect this, these quantities are named $\boldsymbol{\psi}_\varepsilon$ and $V_{A|\varepsilon}$ in

1076 where $\mu_{g,k}$ and μ_j are the k th values of the vectors $\boldsymbol{\mu}_g$ and $\boldsymbol{\mu}$. The total (additive) genetic variance is the
 1077 variance of the breeding values across environments:

$$V_{\text{Gen}} = V_{\text{Add}} = V(\mathcal{A}_z) = V(\mu_{g,k}). \quad (\text{S34})$$

1078 Since the variance-covariance matrix of $\boldsymbol{\mu}_g$ is the \mathbf{G}_z matrix, the variance of all elements $\mu_{g,k}$ taken together
 1079 is the average of the diagonal elements of \mathbf{G}_z , which we will note V_k . Assuming that all environments are
 1080 equiprobable for the sake of simplicity (releasing this assumption merely requires to use weighted average),
 1081 we have

$$V_{\text{Add}} = \frac{1}{K} \sum_{k=1}^K V_k. \quad (\text{S35})$$

1082 In other words, V_{Add} is the average of the diagonal elements of the \mathbf{G}_z matrix.

1083 The marginal (additive) genetic variance of the trait depends on the average of the breeding values
 1084 across environment for a given genotype:

$$\bar{\mathcal{A}} = \frac{1}{K} \sum_k \mathcal{A}_{z,k}, \quad (\text{S36})$$

1085 where $\mathcal{A}_{z,k}$ is the breeding value evaluated at the ⁴⁶⁵ k th environment for a given genotype, still
 1086 assuming equiprobable environments. It results that the marginal (additive) genetic variance of the trait is

$$V_G = V_A = \frac{1}{K^2} \left(\sum_k V_k + 2 \sum_{k<l} C_{kl} \right), \quad (\text{S37})$$

1088 where C_{kl} is the genetic covariance between the environment k and l . In other words, V_A is the average of
 1089 all the elements of the \mathbf{G}_z matrix.

1090 Finally, the (additive) genetic variance of plasticity can be computed as the difference between V_{Add}
 1091 and V_A :

$$V_{G \times E} = V_{A \times E} = V_{\text{Add}} - V_A = \frac{1}{K^2} \left((K-1) \sum_k V_k - 2 \sum_{k<l} C_{kl} \right) \quad (\text{S38})$$

1092 A few particular cases are important to note here. The first case is when all environments harbour the
 1093 same additive genetic variance, say V , and are all perfectly correlated with one another. This is a situation
 1094 generally describe as a total absence of genetic variation in plasticity. In our framework, this situation would
 1095 indeed result in $V_{\text{Add}} = V_A = V$ and, indeed, no genetic variation in plasticity with $V_{A \times E} = 0$. Note that
 1096 uneven additive genetic variances across environments, even if genetic correlation are kept perfect across
 1097 environments, would result in slightly positive genetic variance in plasticity with $V_{A \times E} > 0$. This is because,

⁴⁶⁵removed: main text.

1098 in such context, the trait can still evolve faster in some environments compared to other, hence plasticity
1099 can evolve. The second extreme case, is when the marginal additive genetic variance of the trait is null,
1100 i.e. $V_A = 0$, while all the additive genetic variance in reaction norm is composed of the additive genetic
1101 variance in plasticity, i.e. $V_{\text{Add}} = V_{A \times E}$. This happens when the sum of covariances (the total of which must
1102 be negative) exactly compensates the sum of diagonal variances in the \mathbf{G}_z , meaning that strong negative
1103 genetic correlation must exist between environments. In this case, it is impossible for directional selection
1104 to act on average value of the trait across all environments, but the evolvability of plasticity is maximised.
1105 A third, interesting case is when there is absolutely no genetic correlation between environments, i.e. the
1106 off-diagonal elements of \mathbf{G}_z are all equal to 0. In such case, it is important to note that, because evolution
1107 can freely operate across environments, then both $V_A = \frac{1}{K^2} \sum_k V_k$ and $V_{A \times E} = \frac{K-1}{K^2} \sum_k V_k$ are non-zero.
1108

1109 **D Derivation of π - and φ -partition of V_{Plas}**

1110 **D1 The π -decomposition**

1111 We have seen in [Appendix C](#) how to compute the variance arising from the average shape of reaction
1112 norm V_{Plas} . In order to go further, we now separate this into a component linked to the average slope
1113 of the reaction norm and another linked to the average curvature. For this, we need one or two of the
1114 following assumptions to hold true: (i) the environment ε follows a normal distribution; or (ii) the function
1115 f is quadratic. In such context, we can isolate the contribution of the slope, V_{Sl} , from the contribution of
1116 the curvature, V_{Cv} to V_{Plas} , based on the best quadratic approximation of $E_{g|\varepsilon}(\hat{z})$ (akin to the reasoning
1117 in Lande & Arnold 1983, for estimates of selection gradients), as:

$$1118 \quad V_{\text{Sl}} = E \left(\frac{dE_{g|\varepsilon}}{d\varepsilon}(\hat{z}) \right)^2 V(\varepsilon), \quad V_{\text{Cv}} = \frac{1}{4} E \left(\frac{d^2 E_{g|\varepsilon}}{d\varepsilon^2}(\hat{z}) \right)^2 V(\varepsilon^2). \quad (\text{S39})$$

1118 As an illustration of why the assumptions above are needed, if ε follows a uniform distribution between -2
1119 and 2; and the average shape of plasticity is the following cubic function, $f(\varepsilon) = 2\varepsilon - 0.5\varepsilon^2 - \varepsilon^3$, then the
1120 average slope is -2, while the slope from the best quadratic approximation of $E_{g|\varepsilon}(\hat{z})$ is -0.4. In such cases,
1121 the decomposition in [Equation S39](#) is not valid anymore, due to (i) the impossibility to apply Stein's lemma
1122 to a non-normal distribution and (ii) strong covariation between the slope and curvature. This means that
1123 whenever the environment is non-normal and the reaction norm is non-quadratic, the π -decomposition can
1124 bear little meaning (in the cubic example above, V_{Sl} would be 5.4, while $V_{\text{Plas}} = 2.0$, so that π_{Sl} would be
1125 largely above 1). A truly quadratic reaction norm is the only case where $\pi_{\text{Sl}} + \pi_{\text{Cv}} = 1$.

1126 D2 The φ -decomposition

1127 In such cases where the environment is non-normal and the reaction norm is non-quadratic, it is always
1128 possible to approximate the true shape of the reaction norm using a polynomial function:

$$\hat{z} = \sum_{n=0}^N (\bar{\theta}_n + \theta_{n,g}) \varepsilon^n \quad (\text{S40})$$

1129 In the context of decomposing V_{Plas} , such polynomial approximation provides a possibility to isolate the
1130 (co-)contribution of the (pairs of) coefficients in $E_{g|\varepsilon}(\hat{z}) = \sum_{n=0}^N \bar{\theta}_n \varepsilon^n$:

$$V_{\text{Plas}} = V(E_{g|\varepsilon}(\hat{z})) = \sum_n \bar{\theta}_n^2 V(\varepsilon^n) + 2 \sum_{n < m} \bar{\theta}_n \bar{\theta}_m \text{cov}(\varepsilon^n, \varepsilon^m) \quad (\text{S41})$$

1131 From this, we suggest the alternative φ -decomposition of V_{Plas} , with $\varphi_n = \frac{\bar{\theta}_n^2 V(\varepsilon^n)}{V_{\text{Plas}}}$ and $\varphi_{nm} = \frac{2\bar{\theta}_n \bar{\theta}_m \text{cov}(\varepsilon^n, \varepsilon^m)}{V_{\text{Plas}}}$.
1132 It is important to note that this decomposition is based on the *coefficients* of the polynomial function and,
1133 thus, it is unfortunately impossible to simply interpret the φ_n in terms of slope (for φ_1), curvature (for φ_2),
1134 and so on. The only exception is when the reaction norm shape is quadratic, in which case $\pi_{\text{SI}} = \varphi_1$ and
1135 $\pi_{\text{CV}} = \varphi_2$.

1136 E Correcting for uncertainty in the estimation of fixed 1137 effects

1138 **Character-state approach** It is easier to start with the character-state approach [⁴⁶⁶] based on the
1139 ANOVA model [⁴⁶⁷]. We want to compute V_{Plas} as the variance of the group-level effects μ [⁴⁶⁸
1140] [⁴⁶⁹] [⁴⁷⁰]:

$$V_{\text{Plas}} = V(\mu) \quad (\text{S42})$$

1141 However, we do not have access to the real-world values for μ , [⁴⁷¹] but only to the estimated $\hat{\mu}$ from
1142 the model. Such estimates, if unbiased, have an expected value of μ_k [⁴⁷²] in environment k and
1143 a standard-error (i.e. the estimation of the sampling standard deviation) s_k . In other words, we can

⁴⁶⁶removed: and

⁴⁶⁷removed: it is based on

⁴⁶⁸removed: (see

⁴⁶⁹removed: and

⁴⁷⁰removed: in the main text)

⁴⁷¹removed: instead, we have access

⁴⁷²removed: at

1144 state that $\hat{\mu}_k$ is equal to μ_k up to an additive error:

$$\hat{\mu}_k = \mu_k + \tilde{\mu}_k \quad (\text{S43})$$

1145 where $\tilde{\mu}$ is of mean 0 and variance s_k^2 . Considering each [\[.473\]](#) virtual repeat r of the experiment, we
 1146 can apply the law of total variance[\[.474\]](#):

$$V(\hat{\mu}) = V_\varepsilon(\mathbb{E}_{r|\varepsilon}(\hat{\mu})) + \mathbb{E}_\varepsilon(V_{r|\varepsilon}(\hat{\mu})) = V_\varepsilon(\mu) + \mathbb{E}_\varepsilon(s^2). \quad (\text{S44})$$

1147 We thus have:

$$V_{\text{Plas}} = V_\varepsilon(\mu) = V_\varepsilon(\hat{\mu}) - \mathbb{E}_\varepsilon(s^2) \quad (\text{S45})$$

1148 This result is equivalent to e.g. the classical computation of the “sire variance” in sire models in
 1149 quantitative genetics (Lynch & Walsh 1998), although [\[.475\]](#) the latter is generally expressed using
 1150 sums-of-squares.

1151 [\[.476\]](#) **Curve-parameter approach** There is unfortunately no simple solution to the problem of ac-
 1152 counting for the uncertainty of fixed effects in the general context of non-linear modelling. However,
 1153 for the particular case where the model can be framed as a linear model, as is the case for the poly-
 1154 nomial function[\[.477\]](#) [\[.478\]](#), then $\hat{z} = \mathbf{X}\boldsymbol{\theta}$ [\[.479\]](#), where \mathbf{X} is the design matrix containing the values for
 1155 the environment. Noting $\boldsymbol{\Sigma}_X$ the variance-covariance matrix of \mathbf{X} , we can define V_{Plas} as[\[.480\]](#) [\[.481\]](#):

$$V_{\text{Plas}} = \text{[.482]}\boldsymbol{\theta}^T \text{[.483]}\text{[.484]}\boldsymbol{\Sigma}_X\boldsymbol{\theta}. \quad (\text{S46})$$

1156 Again, the problem is that $\boldsymbol{\theta}$ is unknown, we only have access to the estimated values of the parameters,
 1157 $\hat{\boldsymbol{\theta}}$, that are inferred with an error provided by the variance-covariance matrix of standard errors, \mathbf{S}_θ .

1158 We can write again:

$$\hat{\boldsymbol{\theta}} = \bar{\boldsymbol{\theta}} + \tilde{\boldsymbol{\theta}}, \quad (\text{S47})$$

⁴⁷³removed: sampling

⁴⁷⁴removed: , although in a different context than in the main text

⁴⁷⁵removed: this later

⁴⁷⁶removed: Parameter curve

⁴⁷⁷removed: (see

⁴⁷⁸removed: ,

⁴⁷⁹removed:). In this case

⁴⁸⁰removed: (

⁴⁸¹removed:):

1159 ^[..485] Noting that the error is independent from the true value, we have:

$$\text{[..486]} \hat{\boldsymbol{\theta}}^T \boldsymbol{\Sigma}_X \hat{\boldsymbol{\theta}} \text{[..487]} = \text{[..488]} \text{[..489]} \boldsymbol{\theta}^T \text{[..490]} \boldsymbol{\Sigma}_X \boldsymbol{\theta} + \text{[..491]} \tilde{\boldsymbol{\theta}}^T \boldsymbol{\Sigma}_X \tilde{\boldsymbol{\theta}} \text{[..492]} \quad (\text{S48})$$

1160 To express ^[..493] $\tilde{\boldsymbol{\theta}}^T \boldsymbol{\Sigma}_X \tilde{\boldsymbol{\theta}}$, it is important to note that $S_{\theta,ij} = \text{E}(\tilde{\theta}_i \tilde{\theta}_j)$, since $\text{E}(\tilde{\boldsymbol{\theta}}) = \mathbf{0}$. Then, we
 1161 can note that, the error being unknown, we actually want to compute ^[..494] $\text{E}_r(\tilde{\boldsymbol{\theta}}^T \boldsymbol{\Sigma}_X \tilde{\boldsymbol{\theta}})$ taken across
 1162 virtual repeats r ^[..495] of the experiment:

$$\text{E}_r(\text{[..496]} \tilde{\boldsymbol{\theta}} \text{[..497]}^T \text{[..498]} \boldsymbol{\Sigma}_X \tilde{\boldsymbol{\theta}}) = \text{E}_r\left(\sum_{ij} \tilde{\theta}_i \tilde{\theta}_j \text{[..499]} \boldsymbol{\Sigma}_{X,ij}\right) = \sum_{ij} \text{E}_r(\tilde{\theta}_i \tilde{\theta}_j) \text{[..500]} \boldsymbol{\Sigma}_{X,ij} = \sum_{ij} S_{\theta,ij} \text{[..501]} \boldsymbol{\Sigma}_{X,ij} = \text{Tr}(\mathbf{S}_\theta \text{[..502]}) \quad (\text{S49})$$

1163 This is similar to the result of Brown & Rutemiller (1977). Finally, we have ^[..503] ^[..504]:

$$V_{\text{Plas}} = \hat{\boldsymbol{\theta}}^T \text{[..505]} \boldsymbol{\Sigma}_X \hat{\boldsymbol{\theta}} - \text{Tr}(\mathbf{S}_\theta \text{[..506]} \boldsymbol{\Sigma}_X). \quad (\text{S50})$$

1164 **F Full results for the section “Perfect modelling of quadratic curves”**

1165 This section provides the full results corresponding to the section “Perfect modelling of quadratic curves” in
 1166 the main text. The results of all investigated values for the number of environments (10 or 4) and number
 1167 of genotypes (20 or 5 for the discrete case, 200 or 50 for the continuous case) are provided for the discrete
 1168 and continuous cases.

⁴⁸⁵ removed: where $\tilde{\boldsymbol{\theta}}$ has a null mean and a variance-covariance matrix \mathbf{S}_θ .

⁴⁹³ removed: the variance $\text{V}(\mathbf{X}\tilde{\boldsymbol{\theta}})$

⁴⁹⁴ removed: $\text{E}_r(\text{V}(\mathbf{x}^T \tilde{\boldsymbol{\theta}}))$ taken across all possible sampling

⁴⁹⁵ removed: :

⁵⁰³ removed: proven

⁵⁰⁴ removed: :

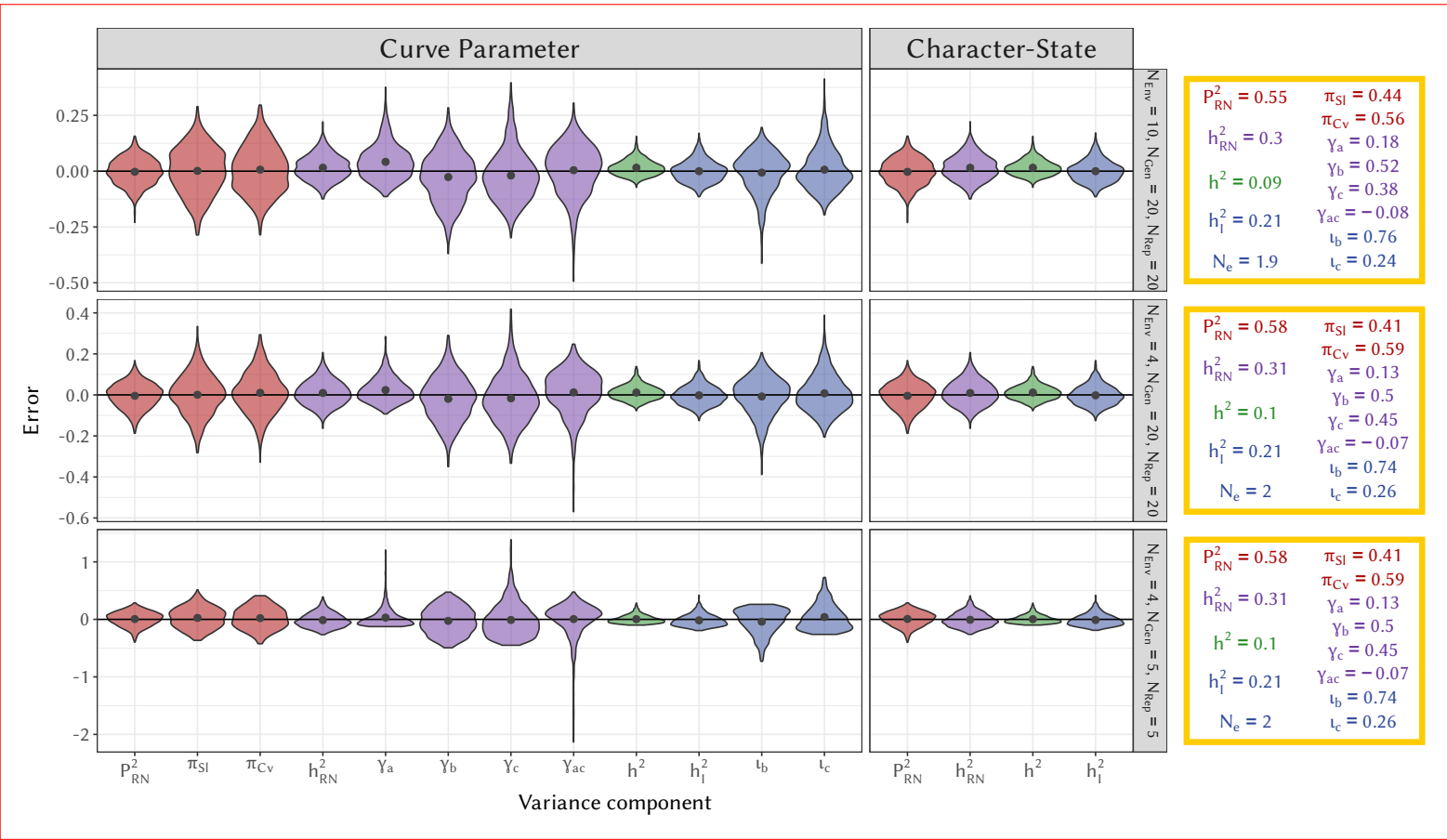


Figure S1: Distribution of the error (difference between the inferred and true value) for each the inferred variance components for three discrete scenarios: N_{env} : number of environments, N_{Gen} : number of different genotypes, N_{Rep} : number of replicates per genotype. Estimates are for \hat{P}_{RN}^2 (proportion of variance generated by plasticity after averaging across genotypes), \hat{h}_{RN}^2 (total heritability of the reaction norm), \hat{h}^2 (heritability based on average breeding values) and \hat{h}_1^2 (heritability of plasticity) for both the curve-parameter and character-state approaches. For the curve-parameter, the π -decomposition of \hat{P}_{RN}^2 into π_{SI} (contribution of the slope) and π_{Cv} (contribution of the curvature); the γ -decomposition of \hat{h}_{RN}^2 into γ_a (genetic contribution of the intercept), γ_b (genetic contribution of the slope), γ_c (genetic contribution of the curvature) and γ_{ac} (genetic contribution of the covariance between the intercept and the curvature) and the ι -decomposition of \hat{h}_1^2 into ι_b (slope) and ι_c (curvature) are also shown. The grey dots correspond to the average over the 1000 simulations. The effective number of dimensions n_e from the character-state is not shown, due to an important bias impacting the comparison with the other parameters.

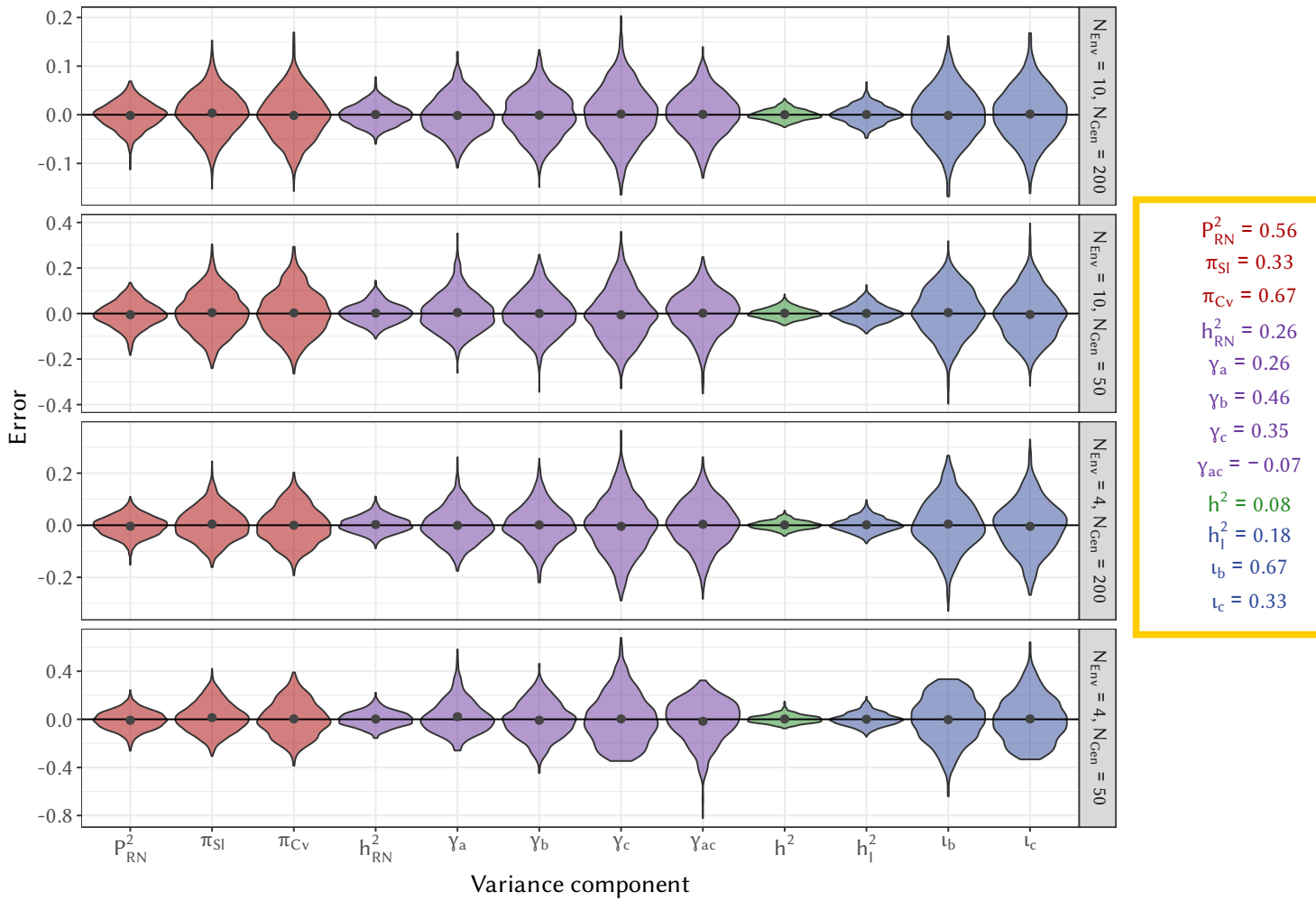


Figure S2: Distribution of the error (difference between the inferred and true value) for each the inferred variance components for four continous scenarios: N_{env} : number of environment tested per genotype, N_{Gen} : number of different genotypes. The character-state approach was impossible for the continuous environment scenario. Estimates are for \hat{P}^2_{RN} (proportion of variance generated by plasticity after averaging across genotypes), \hat{h}^2_{RN} (total heritability of the reaction norm), \hat{h}^2 (heritability based on average breeding values) and \hat{h}^2_I (heritability of plasticity) for both the curve-parameter and character-state approaches. For the curve-parameter, the π -decomposition of \hat{P}^2_{RN} into π_{SI} (contribution of the slope) and π_{Cv} (contribution of the curvature); the γ -decomposition of \hat{h}^2_{RN} into γ_a (genetic contribution of the intercept), γ_b (genetic contribution of the slope), γ_c (genetic contribution of the curvature) and γ_{ac} (genetic contribution of the covariance between the intercept and the curvature) and the l -decomposition of \hat{h}^2_I into l_b (slope) and l_c (curvature) are also shown. The grey dots correspond to the average over the 1000 simulations. The effective number of dimensions n_e from the character-state is not shown, due to an important bias impacting the comparison with the other parameters.

1169 G Comparison with the approach from Murren *et al.* (2014)

1170 Murren *et al.* (2014) studied variation of the reaction norm shapes across different datasets, using their
 1171 own metrics. We argue in the main text that our variance decomposition is more appropriate than the ones
 1172 suggested by Murren *et al.* (2014), and we develop here why.

1173 The first step in the approach of Murren *et al.* (2014) is to choose a reference reaction norm in
 1174 each of the studies and compute contrasts (*i.e.* difference with) to that particular reaction norm. The

1175 contrasts are then analysed, rather than the **reaction** norms themselves. For the sake of simplicity, and
 1176 because this does not (or marginally) impact our comments on this approach, we will overlook that
 1177 step and consider reaction norms directly.

1178 For each genotype k and from its given reaction norm (or contrast) $\mathbf{z}_k = \{z_{k,1}, \dots, z_{k,n}\}$, Murren et al.
 1179 (2014) compute four statistics (we removed the absolute values for the sake of simplicity here):

1180 1. The offset, O_M , measures the “location” of the reaction norm, i.e. its mean. Comparison of
 1181 the offsets allows detecting whether reaction norms are “shifted” toward higher or lower values.
 1182 It is computed, for each genotype k , as the absolute value of the average of the norm across
 1183 environments:

$$O_{M,k} = \frac{\sum_i^n |z_{k,i}|}{n}. \quad (\text{S51})$$

1184 2. The slope, S_M , measures the linear trend of the **reaction** norms. Formally, it is the absolute sum
 1185 of the differences between two consecutive environments, divided by the number of intervals
 1186 ($n - 1$):

$$S_{M,k} = \frac{\sum_i^{n-1} |z_{k,i+1} - z_{k,i}|}{n - 1}. \quad (\text{S52})$$

1187 3. The curvature, C_M , is computed as the absolute value of the average change in [⁵⁰⁷] **phenotype**
 1188 between two consecutive [⁵⁰⁸] **pairs** of environments:

$$C_{M,k} = \frac{\sum_i^{n-2} |(z_{k,i+2} - z_{k,i+1}) - (z_{k,i+1} - z_{k,i})|}{n - 2}. \quad (\text{S53})$$

1189 4. The wiggle, W_M , is, according to the authors the “the variability in shape not described by any
 1190 of the previous three measures”:

$$W_{M,k} = \frac{\sum_i^{n-2} |(z_{k,i+2} - z_{k,i+1}) - (z_{k,i+1} - z_{k,i})|}{n - 2} - C_{M,k}. \quad (\text{S54})$$

1191 Given the lower interest in this **latter** statistics, we will not comment on it any further. Most of
 1192 the comments on the other statistics also apply to this one.

1193 One strong assumption underlying the calculations above is that environmental values [⁵⁰⁹] $\varepsilon =$
 1194 $\{\varepsilon_1, \dots, \varepsilon_n\}$ on which the reaction norms were evaluated are evenly spaced, e.g. that the differences
 1195 [⁵¹⁰] $\varepsilon_{i+1} - \varepsilon_i$ are equal for all possible values of i . [⁵¹¹] **The assumption is actually** that the space

⁵⁰⁷removed: norms

⁵⁰⁸removed: couples

⁵⁰⁹removed: $\mathbf{x} = \{x_1, \dots, x_n\}$

⁵¹⁰removed: $x_{i+1} - x_i$

⁵¹¹removed: More, this calculation assumes

1196 between two measures is equal to 1 (which, admittedly, is only a matter of rescaling when evenly-
 1197 spaced values are already assumed). If this is **the** case, then there is indeed no loss in generality in
 1198 using the number of components (n , $n-1$ and $n-2$) rather than actual values of x in the denominator.
 1199 Although it is common for studies on reaction norms to use evenly-spaced environmental values, it is
 1200 an unnecessary assumption that shall not be satisfied by all studies.

1201 [⁵¹²] **Second**, developing the sums in S_M and C_M above show that the intermediate values cancel
 1202 each other out, leaving only the values at each extreme of the environmental range in the estimate:

$$\begin{aligned}
 S_{M,k} &= \frac{z_{k,n} - z_{k,1}}{n-1}, \\
 C_{M,k} &= \frac{(z_{k,n} - z_{k,n-1}) - (z_{k,2} - z_{k,1})}{n-2}.
 \end{aligned}
 \tag{S55}$$

1203 The issue here is double[⁵¹³]: **(i)** the estimation is highly sensitive to the random noise coming from
 1204 a small number of values (two or three/four)[⁵¹⁴]; **and (ii)** the intermediate values in the reaction
 1205 norm are simply thrown out and not used for a more robust estimation. In other words, it would have
 1206 been exactly the same to not measure the reaction norm at these intermediate values, since they are
 1207 not accounted for in the calculation.

1208 A final issue [⁵¹⁵] **is that the approach uses the** measured values of the reaction norms without
 1209 accounting for the uncertainty in their estimation (i.e. standard-deviation and sample size for each
 1210 genotype and environmental value) **which** poses the well-known issue of non-propagation of the error
 1211 when doing “statistics on statistics”.

1212 Although we also provide estimators of the impact of [⁵¹⁶] **several aspects** of reaction norms
 1213 on the phenotypic variation, our approach differs from the one from Murren *et al.* (2014) by many
 1214 aspects. First, [⁵¹⁷] **our variance decomposition makes** the explicit distinction between the average
 1215 shape of the reaction norm and the genetic variance surrounding it. As such, to O_M , S_M and C_M
 1216 corresponds not only the [⁵¹⁸] π -, but also the [⁵¹⁹] γ - and ι -decomposition. **We clearly delimit the**
 1217 **domain of validity of each of these decomposition.** We also account for possible [⁵²⁰] **correlation between**
 1218 **those** components. Second, we use the whole of the statistical inference to define our [⁵²¹] **variance**

⁵¹²removed: Another issue does not specifically stems from assumptions underlying the estimators, but rather from the fact that these estimators are applied to the estimated values themselves, rather than on a fitted function for the reaction norms. Indeed,

⁵¹³removed: . First,

⁵¹⁴removed: . Second,

⁵¹⁵removed: , closely related to the second one, is that using the

⁵¹⁶removed: the intercept, slope and curvature

⁵¹⁷removed: using the law of total variance , we make

⁵¹⁸removed: genetic component r_{ga}^2 , r_{gb}^2 and r_{gc}^2 ,

⁵¹⁹removed: average plasticity components (r_{pb}^2 and r_{pc}^2). We

⁵²⁰removed: genetic correlation between

⁵²¹removed: estimates of contribution of intercept, slope and curvature to the phenotypic variance

1219 **decomposition estimates.** Third, we explicitly account for the uncertain estimation of reaction norms.

Table 1: List of the main notations, as well as their source of variation. We here distinguish the “focal” environment, which only concerns the environmental variable used to parametrise the reaction norm, from other putative sources of environmental variation that may influence the phenotypic trait (sometimes described as micro-environmental variation). “Everything” in the table thus includes all (focal and other) sources of environmental and genetic variation, developmental noise and measurement error.

| Notation | Explanation | Varies over |
|------------------------------------|---|------------------------------|
| z | Phenotypic value for the trait | Everything |
| \hat{z} | Phenotype as predicted from the environment and the genotype | Focal environment, genotypes |
| ε | Environmental variable | — |
| μ | Vector of the average value of the phenotypic in each environment | Focal environment |
| \mathbf{G}_z | Additive genetic variance-covariance matrix of trait values across environments (character states) | — |
| θ_g | Vector of parameter values of the reaction norm for genotype g | Genotypes |
| $\bar{\theta}$ | Vector of mean values of the reaction parameters over the genotypes | — |
| \mathbf{G}_θ | Additive genetic variance-covariance matrix of the reaction norm parameters | — |
| ψ_ε | Reaction norm gradient, the vector of partial derivatives of the phenotype z against reaction norm parameters θ_g , averaged over the genotypes at environment ε | Focal environment |
| Ψ | Variance-covariance matrix of ψ_ε across environments | — |
| V_P | Total phenotypic variance in the trait z | — |
| V_{Res} | Residual variance, not explained by the reaction norm | — |
| $V_{\text{Plas}}, P_{\text{RN}}^2$ | Phenotypic variance arising from changes in the mean reaction norm across environments; divided by V_P for P_{RN}^2 | — |
| $V_{\text{Gen}}, H_{\text{RN}}^2$ | Total genetic variance in the trait across environments; divided by V_P for H_{RN}^2 | — |
| $V_{\text{Add}}, h_{\text{RN}}^2$ | Total additive genetic variance in the trait across environments; divided by V_P for h_{RN}^2 | — |
| V_A, h^2 | Marginal additive genetic variance of the trait, i.e. based on the mean breeding values across environments, divided by V_P for h^2 | — |
| $V_{A \times E}, h_1^2$ | Additive genetic variance in plasticity, i.e. variance of the mean-centred breeding values, divided by V_P for h_1^2 | — |
| $\pi_{\text{SI}}, \pi_{\text{CV}}$ | Proportion of V_{Plas} explained by the average slope (π_{SI}) or curvature (π_{CV}) of the average reaction norm | — |
| φ_i, φ_{ij} | Proportion of V_{Plas} explained by parameter i , or by covariation between parameter i and j for a polynomial reaction norm | — |
| γ_i, γ_{ij} | Proportion of V_{Add} explained by the additive genetic (co)variation in parameter i (and j) | — |
| ι_i, ι_{ij} | Proportion of $V_{A \times E}$ explained by the additive genetic (co)variation in parameter i (and j) | — |

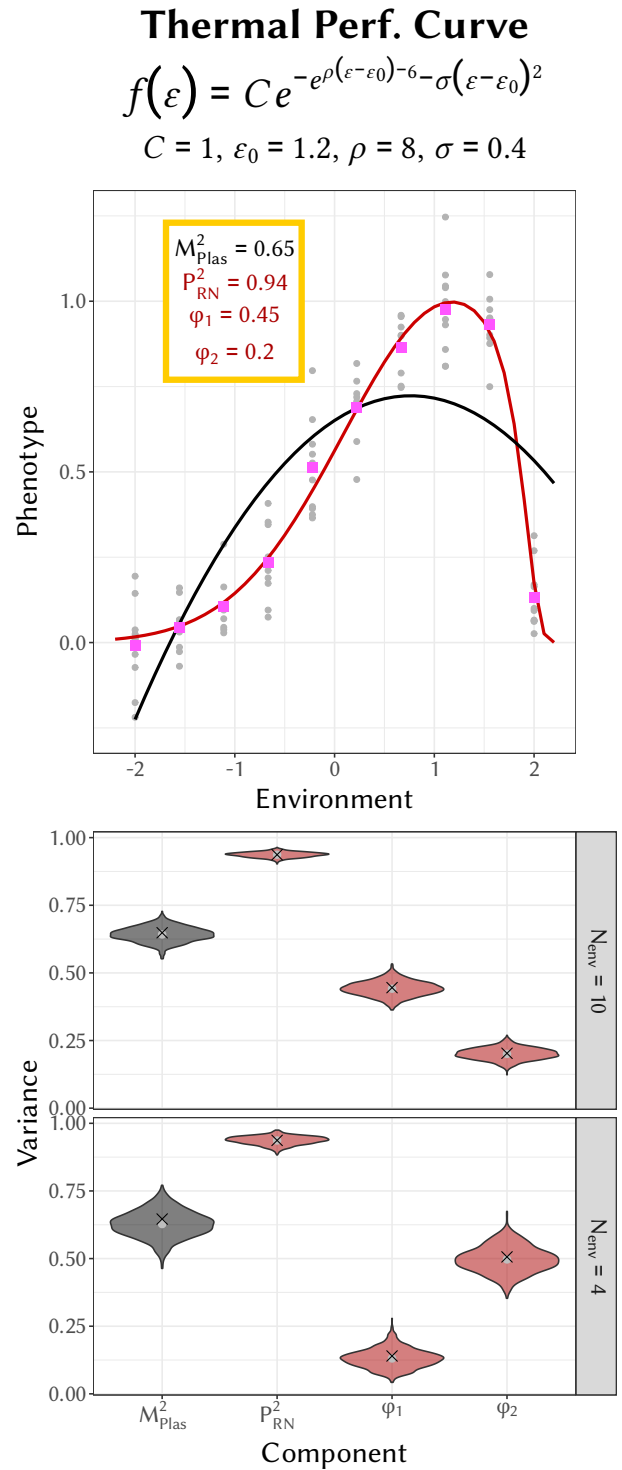
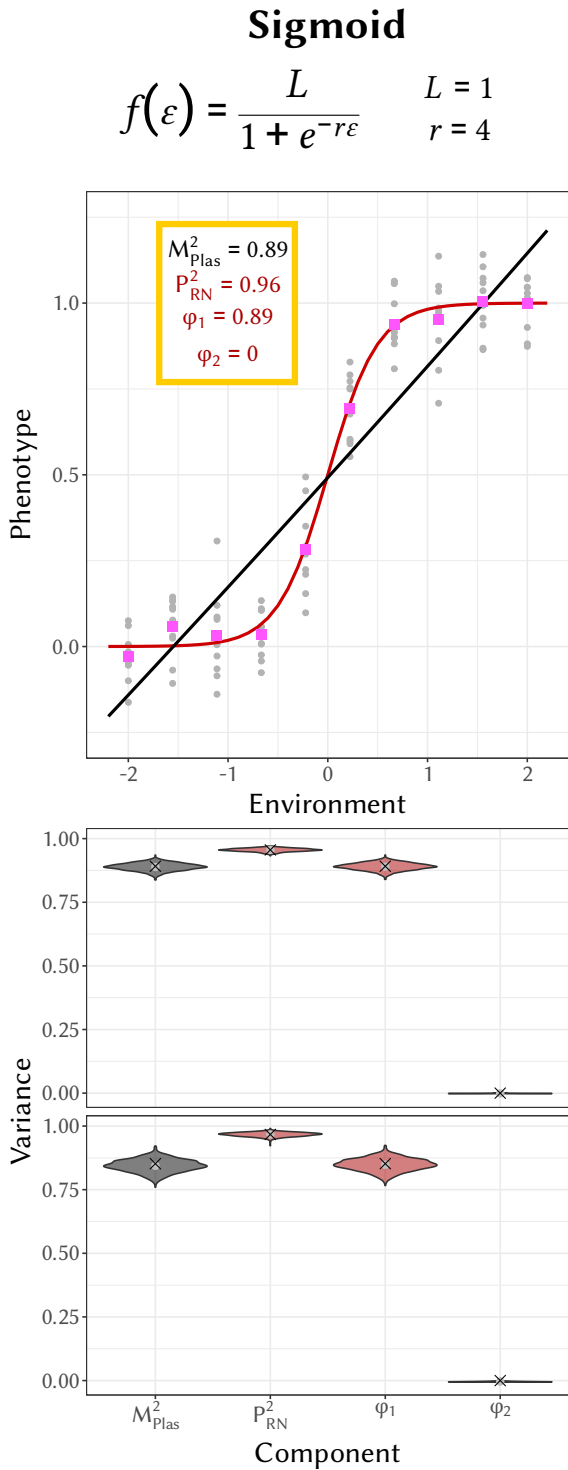


Figure 5: Estimation of the variance of the reaction norm when the true shape (sigmoid on the left, Gompertz-Gaussian performance curve on the right, red lines on top graphs) is unknown and approximated from a polynomial function. The estimated [..^a]black line, top graphs) only account for a part of the reaction norm shape, while the ANOVA estimation ([..^b]pink dots, top graphs) fit the true shape more accurately. As a result, the model is expected to explain only a part [..^c] M_{Plas}^2 of phenotypic variance due to plasticity[..^d]. [..^e]On the [..^f]bottom rows, [..^g]the [..^h]error distribution are shown for M_{Plas}^2 , P_{RN}^2 , φ_1 and φ_2 ([..ⁱ]grey dots [..^j]are the average estimated values[..^k], black crosses [..^l]are the expected true values)[..^m][..ⁿ]

^aremoved: blue

^bremoved: green

^cremoved: \hat{V}_{mod}

^dremoved: (see R_{Mod}^2)

^eremoved: The part of

^fremoved: total phenotypic variance explained by overall plasticity

^gremoved: $R_{Plas}^2 = \hat{V}_{Plas}/V(z)$, is also provided for information. Replicating

^hremoved: simulation 1000 times shows that our estimation process is without bias

ⁱremoved: red

^jremoved: :

^kremoved: :

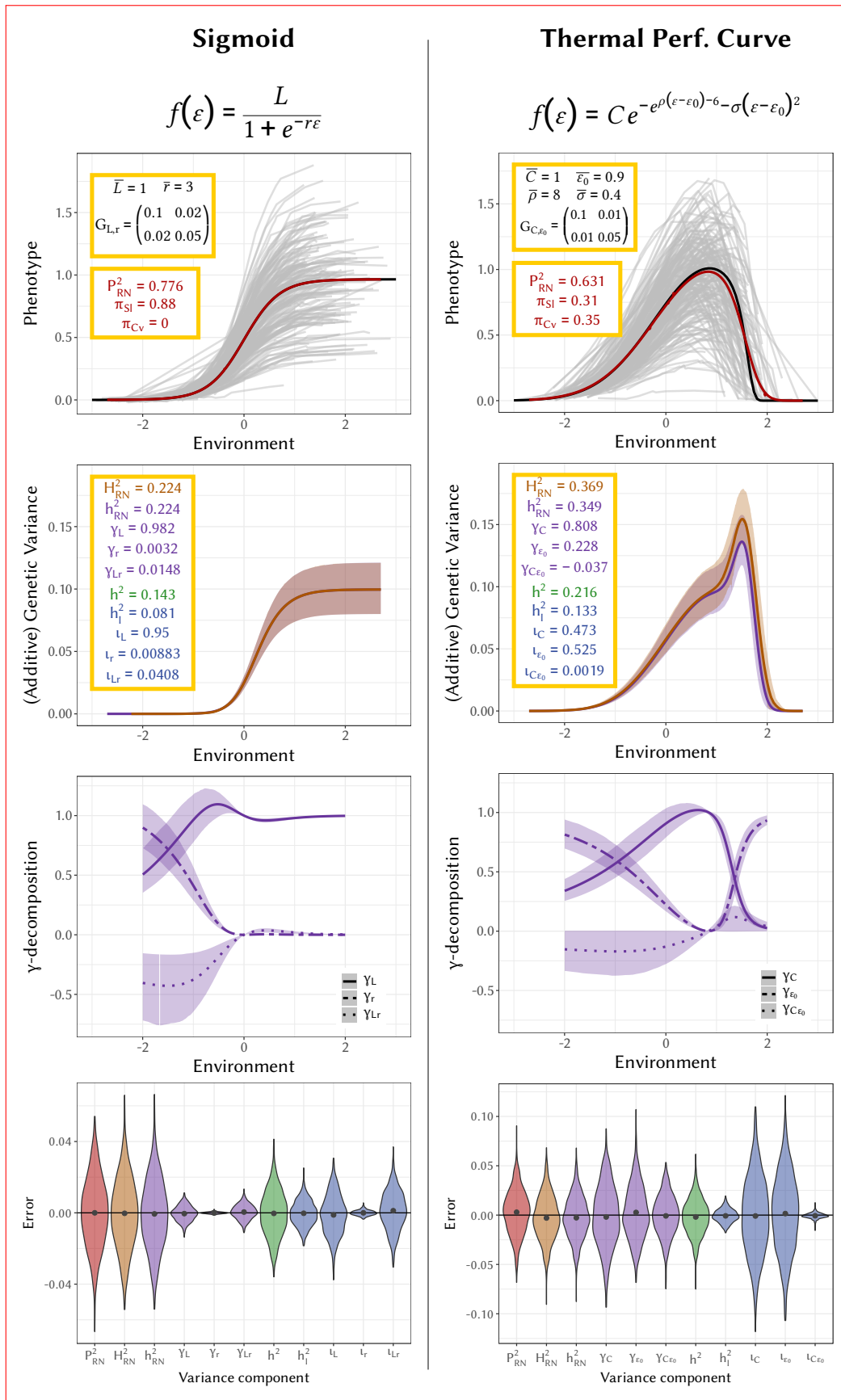


Figure 6: Scenarios and results of non-linear modelling of phenotypic plasticity in a continuous environment. On the left: results corresponding to a sigmoid curve scenario; on the right: results corresponding to a [..^a] TPC scenario. [..^b] First row: example of the individual curves (each curve corresponds to one individual) simulated in each scenario; yellow box: true parameters for the model and average shape; black curve : $f(\varepsilon, \theta)$; red curve : $E_{g|\varepsilon}(\hat{z})$. [..^c] Second row: distribution of the estimations of [..^d] $V_{G,\varepsilon}$ ([..^e] brown) and [..^f] $V_{A,\varepsilon}$ ([..^g] purple), [..^h] along the environment; [..ⁱ] solid line: average [..^j] value across simulations; [..^k] pale ribbon: 95% CI across simulations; yellow box: [..^l] true values for the genetic variance partition. [..^m] Third row: γ -decomposition of $V_{A,\varepsilon}$ along the environment, for each parameter and their covariation. Fourth row: distribution of the [..ⁿ] error [..^o] for each component of our variance partition [..^p] ("Variances") or for the [..^q] π - and γ -decomposition ("Components"), red dot is the average of estimates over all simulations.